



ARISTOTLE UNIVERSITY
OF THESSALONIKI



Conceptual Design of a Space Rover mission

Supervisor Efstratios Giannakis

Department of Mechanical Engineering

ARISTOTLE UNIVERSITY OF THESSALONIKI

December 15 2023

Abstract

This report is a technical documentation containing all the appropriate aspects and stages of the design of a space mission. More in particular, this reports covers the conceptual design of a MARS-rover vehicle. This project occurs during the academic course "*Mechanical Design and Product Development*" at Aristotle University of Thessaloniki. All of the technical work can be found in the below mentioned GitHub repository. The professor in charge of this project is Dr. Efstratios Giannakis of AUTh.

GitHub

Contents

1	Introduction	3
1.1	Project Overview	3
1.2	Operations	3
1.3	Mission Management	3
1.3.1	Team Information	3
1.3.2	Organizational	3
1.3.3	Time Plan	6
2	Project Information	9
2.1	Objective	9
2.2	Mission Information	9
2.2.1	Toolbox	10
2.3	Product Development	10
2.3.1	Development Process	10
2.3.2	First Steps	10
2.3.3	Quality Function Deployment	12
3	Subsystem Level Reports	13
3.1	Mobility Subsystem	13
3.1.1	Overview	13
3.1.2	Team Dependencies	13
3.1.3	Subsystem Management	14
3.1.4	Conceptual Design	14
3.1.5	References	34
3.2	Body and Differential Subsystem	35
3.2.1	Overview	35
3.2.2	Team dependencies	35
3.2.3	Design	35
3.2.4	Calculations	43
3.3	Robotic Arm Subsystem	46
3.3.1	Overview	46
3.3.2	Team Dependencies	46
3.3.3	Subsystem Management	46
3.3.4	Conceptual Design	47
3.3.5	References	57
3.4	Panel Deployment Mechanism and Energy Management Subsystem	58
3.4.1	Overview	58
3.4.2	Team dependencies	58
3.4.3	Subsystem management	58
3.4.4	Energy calculations and budgeting	58
3.4.5	Panel mechanism design	59
4	Rover Assembly	70
4.1	Design Overview	70
4.2	System Functionality	72
5	Conclusion	75
5.1	General Comments	75
5.2	Improvements	75
5.2.1	Mobility System	75
5.2.2	P.D.M.E.M.	75
5.2.3	Robotic Arm Subsystem	77
5.3	Manufacturing	78

5.3.1 Cost Budget	78
5.3.2 Manufacturing processes	78

Chapter 1

Introduction

1.1 Project Overview

The project at hand entails the preliminary design of a Mars Rover Mission, centered on the exploration and data collection from the Martian surface. Originating from the ingenuity of six undergraduate students enrolled in the Mechanical Engineering Department at Aristotle University of Thessaloniki (AUSTh), this initiative draws inspiration from NASA's Perseverance mission. Under the astute guidance of Dr. Efstratios Giannakis, who assumed the role of project overseer and provided mentorship, the team underwent monthly status updates in a presentation format throughout the academic period. These sessions, designed to ensure project progress and receive valuable feedback, served as a critical mechanism for aligning the project with established standards and objectives.

1.2 Operations

The team operates under a decentralized structure, fostering an all-equal hierarchy to optimize functionality. Sub-teams, aligned with specific subsystems, have been established to enhance information organization and facilitate seamless information flow. Notably, the absence of a designated team leader underscores the team's commitment to a collaborative and cooperative approach.

The equitable distribution of workload is a fundamental principle, with each sub-unit tasked to independently work on its designated subproject. Despite this autonomy, the team recognizes the importance of team-wide meetings and technical sessions throughout the project's course. These gatherings serve as valuable forums for addressing challenges collectively and ensuring a cohesive approach to problem-solving.

The interplay between sub-systems is crucial to the project's progression, and the intentional mixing of workloads among different sub-systems has proven to be instrumental. This dynamic approach enhances synergy, encourages cross-functional collaboration, and contributes to the overall advancement of the project.

1.3 Mission Management

1.3.1 Team Information

The team consists of 6 undergraduate students:

Name	ID	mail
Vasileios Papamichail	6920	vasilepi@meng.auth.gr
Vasileios Loukatos	6898	loukatos@meng.auth.gr
Orestis-Panagiotis Theotokoglou	6989	orestheo@meng.auth.gr
Anastasios Gousias	6865	agousias@meng.auth.gr
Zisis Tiliopoulos	6940	zisistili@meng.auth.gr
Christos Kotidis	6892	ckotidis@meng.auth.gr

Table 1.1: Team Members

1.3.2 Organizational

The project is split in four main subsystems in order to allow for better communication and collaboration of the team. The parts to be conceptually designed are:

- Wheels

- Mobility parts
- Body
- Differential
- Panel Deployment Mechanism
- Robotic Arm

Considering the above mentioned open design dependencies the project was split in the following four subsystems.

1. Mobility Subsystem
2. Body Subsystem
3. Robotic Arm Subsystem
4. Panel Deployment Mechanism and Energy Management Subsystem

Mobility Subsystem

The Mobility Subsystem assumes responsibility for both the directional control and suspension systems of the rover. In-depth analyses of various movement scenarios are conducted, aiming to design a robust and mission-capable mobility system. This subsystem plays a crucial role in determining movement constraints, such as the maximum achievable slope angle, ensuring the rover's adaptability to diverse terrains.

Body Subsystem

The Body Subsystem focuses on the design of the rover's main body, housing critical components such as the mobility system, robotic arm, and panels. Mechanical interfaces between the body and other subsystems are meticulously studied and designed. Additionally, this subsystem is tasked with the creation of housing structures for electronic components and the robotic arm's headset, ensuring seamless integration within the overall design. The differential mechanism is also one of this subsystem's responsibilities.

Robotic Arm Subsystem

The Robotic Arm Subsystem takes charge of designing and overseeing the rover's robotic arm, a pivotal component of the mission. Responsibilities encompass the mechanical intricacies of the arm, and establishing protocols for data and sample collection. This subsystem is instrumental in defining the operational capabilities of the robotic arm, optimizing its efficiency for mission success.

Panel Deployment Mechanism and Energy Management Subsystem (P.D.M.E.M.)

This subsystem plays a central role in designing and analyzing the mechanism for deploying solar panels. These panels serve as vital components for harnessing solar energy from the Sun, distributing it efficiently among various rover subsystems. The Energy Management Subsystem focuses on guaranteeing that the rover maintains sufficient energy levels to successfully fulfill its mission objectives. Thorough studies in energy management ensure the vehicle's autonomy and sustainability throughout its operational lifespan. The project's technical work can be divided into sections as can be seen in the organizational chart of Fig. 1.1.

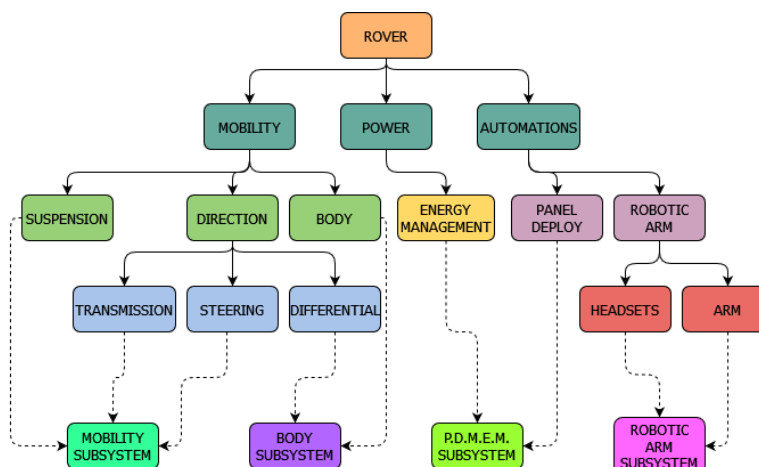


Figure 1.1: Organizational Chart

The allocated team members to each subsystem can be found in Tab. 1.2.

Name	Subsystems			
	Mobility	Body	Robotic Arm	P.D.M.E.M.
Vasileios Papamichail	✓			
Vasileios Loukatos	✓			
Zisis Tiliopoulos		✓		
Orestis Theotokoglou			✓	
Anastasios Gousias			✓	
Christos Kotidis				✓

Table 1.2: Subsystems Responsibles

Inherent to the project structure, which is compartmentalized into distinct subsystems, is a dynamic information exchange mechanism. A symphony of information flows seamlessly among all subsystems, fostering a collaborative environment that ensures each component aligns with the overarching mission objectives. To facilitate this holistic integration, both team-wide meetings and focused subsystem-level gatherings are scheduled throughout the project's life cycle. These forums serve as conduits for the dissemination of insights, updates, and critical developments, fostering a cohesive team synergy and enabling efficient problem-solving. Through these structured interactions, the project endeavors to maintain a synchronized trajectory, ensuring that the collective knowledge and progress of each subsystem contribute collaboratively to the success of the mission. A typical information flow diagram for the project can be seen in Fig. 1.2.

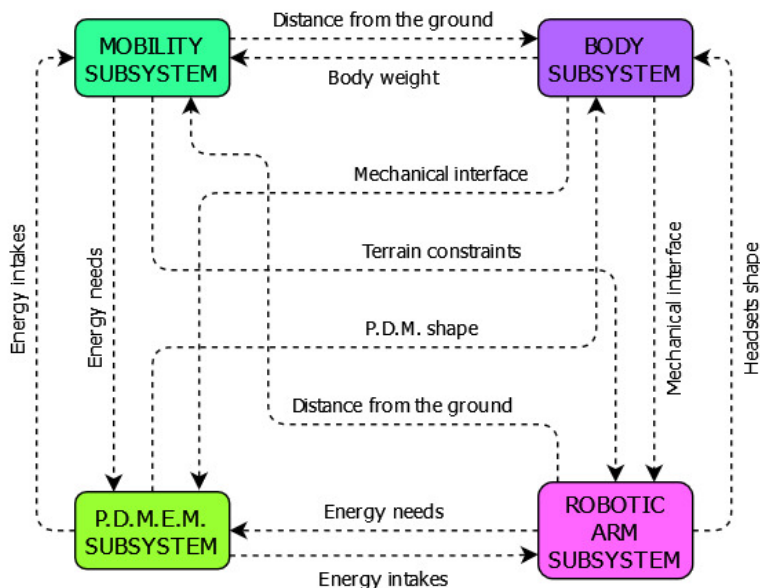


Figure 1.2: Information Flow Diagram

1.3.3 Time Plan

The Time Plan section is split in three parts. In total, three Gantt Charts are provided: the draft, the final (the outcome) and finally the ideal. Considering the final time plan and the workload throughout the course the ideal time plan can be concluded.

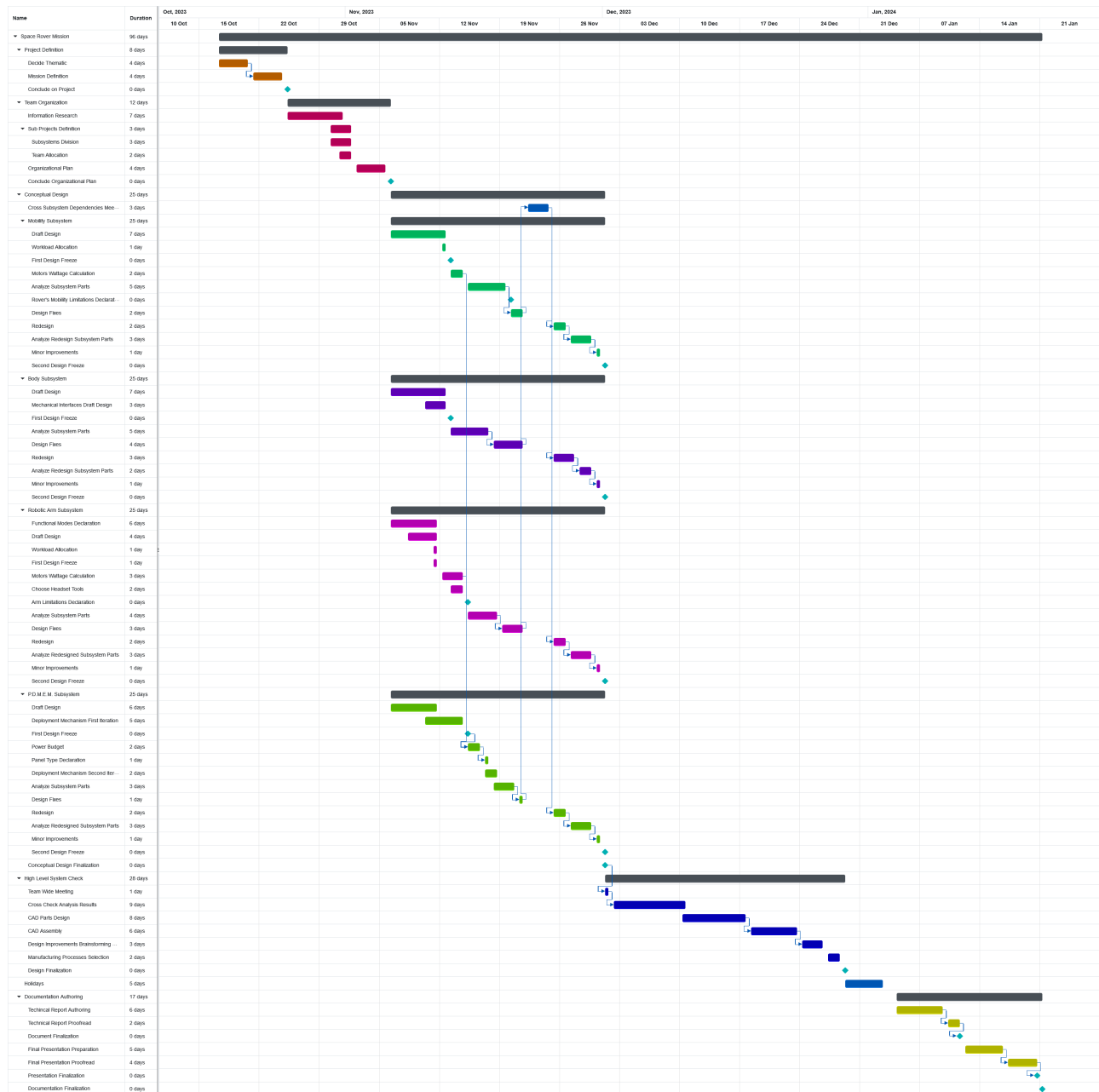


Figure 1.3: Ideal Project Time Plan

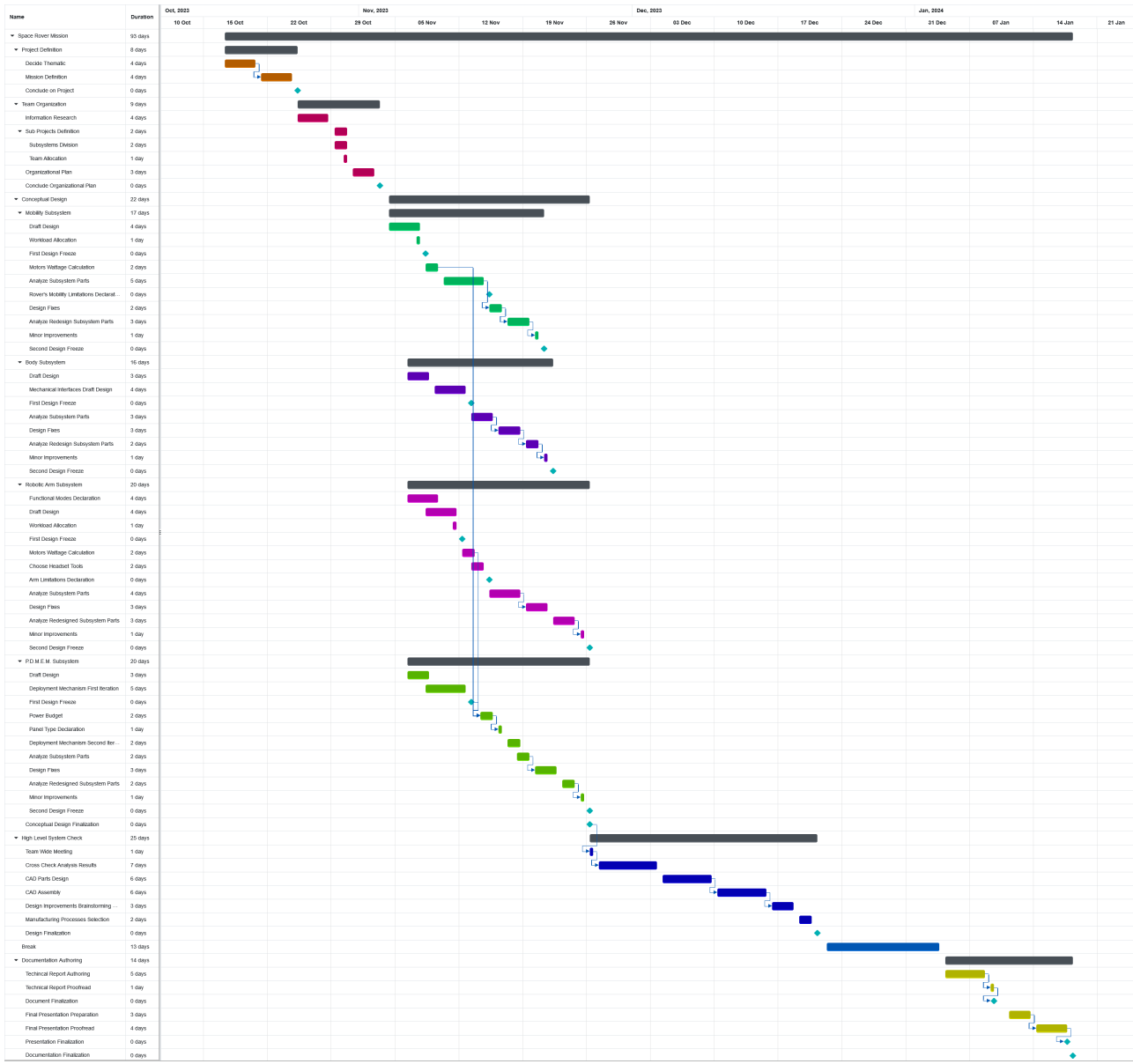


Figure 1.4: Draft Project Time Plan

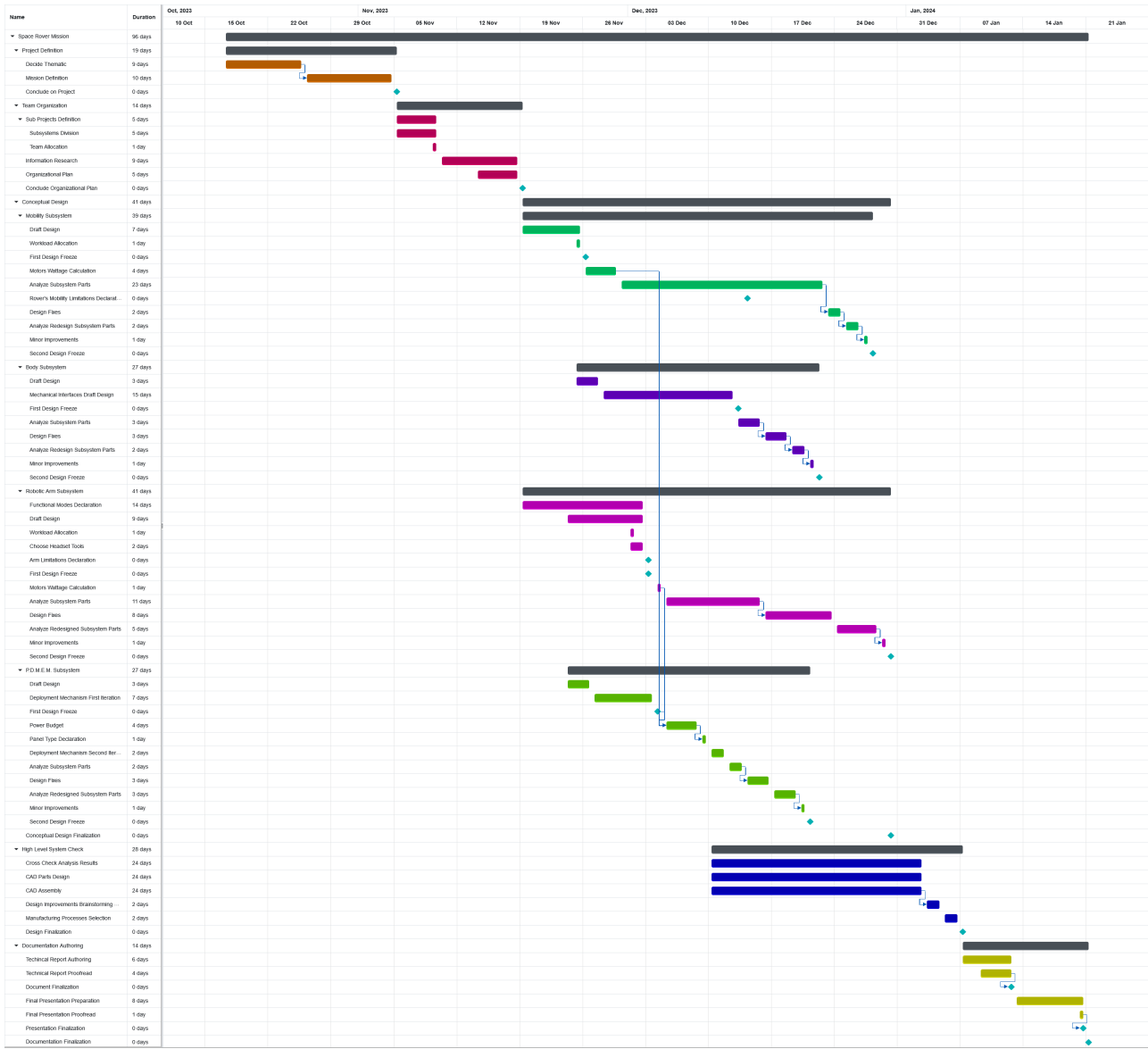


Figure 1.5: Final Project Time Plan

The observed outcome of time allocation did not align with the intended objectives. Additionally, the initial draft of the time plan closely approximated the ideal schedule, but the actual execution deviated significantly. The proposed time allocation for similar design challenges is the one in Fig. 1.3.

Chapter 2

Project Information

2.1 Objective

This design mission takes place on Mars, and represents a meticulous and interdisciplinary endeavor, aiming to create a robotic explorer tailored for the unique challenges presented by the Martian environment. The primary objective is to develop a cutting-edge rover capable of conducting scientific investigations, gathering data, and navigating the diverse and often rugged terrain of the Martian surface. The mission sets out to address key engineering challenges, such as designing a robust mobility system that can negotiate the planet's distinct topography, ranging from rocky outcrops to sandy plains.

The key objective of the rover vehicle to be designed, is the follow up mission of NASA's Perseverance Rover Mission. It launched in July 2020, and is a groundbreaking exploration initiative on Mars. Equipped with advanced scientific instruments, Perseverance aims to search for signs of past microbial life, collect Martian rock and soil samples, and pave the way for future human missions. Perseverance's key role in collecting ground data and depositing them in the Martian terrain is integral to advancing our understanding of Mars and its potential habitability, making significant strides in planetary exploration.

At last, this technical document delves into the design process of a Mars mission, aiming to collect the above mentioned sample data from the Perseverance mission. The rover's sole purpose is to gather these data into its main body and analyze them in order to pinpoint and unveil the secrets of Mars' terrain, making one step further to the planet's exploration.

2.2 Mission Information

In the initial phases of any design project, establishing clear and well-defined requirements is imperative. For the Mars mission, the selection of mission requirements is a crucial step to foster critical thinking and facilitate the unbridled flow of creativity. These chosen requirements serve as the foundation, guiding the design process with precision and ensuring that the mission objectives are systematically addressed. By carefully electing mission requirements, the project not only establishes a structured framework but also encourages innovative solutions that align with the overarching goals of the Mars mission. This meticulous approach at the outset is fundamental for the success of the mission, promoting a robust foundation for subsequent stages of design. The requirements that have been set are:

ID	Description
R-01	<i>The mission is to take place on planet Mars.</i>
R-02	<i>The life span of the vehicle is expected at least two months.</i>
R-03	<i>The robot vehicle is expected to be terminated on the Mars surface.</i>
R-04	<i>The vehicle is considered to survive the launch environment.</i>
R-05	<i>The robot vehicle is seamlessly deposited onto the Martian surface.</i>
R-06	<i>The vehicle is considered to fit as is into the spaceship.</i>
R-07	<i>The budgetary constraints for the mission shall meet NASA's Perseverance mission.</i>

Table 2.1: Mission Requirements

In the inaugural team meetings, a spectrum of objectives has been delineated to provide the team with a shared vision and foster collaborative efforts towards a unified goal. These objectives serve as guiding principles, shaping the trajectory of the team's endeavors and ensuring a collective understanding of the mission's overarching purpose. By establishing these objectives early on, the team gains a clear sense of direction and purpose, laying the groundwork for effective collaboration and synergistic contributions from each team

member. This deliberate approach in goal-setting during the initial team meetings not only enhances organizational cohesion but also cultivates a shared commitment to the success of the mission.

2.2.1 Toolbox

In order to design the mission there is the need of some computational tools and software assisting in overcoming the engineering obstacles along the way. Some of the tools the team used and the purpose of them can be seen in Tab. 2.2.

Software	Purpose
MATLAB	Computational engineering
Autodesk Inventor	3D Design of rover's parts
SOLIDWORKS	3D Design of rover's parts
Onshape	3D Assembly and Integration of rover system
Online Gantt	Make project Gantt charts
Draw.io	Make project diagrams
Excalidraw	Make diagrams and sketches
Overleaf	Author technical documents
Google Slides	Create presentations
GitHub	CAD storage, progress report, collaborative issue addressing

Table 2.2: Project's Toolset

2.3 Product Development

2.3.1 Development Process

The initial phases of the team's development proved pivotal for advancing the project and finalizing the design. The process employed during these early stages centered around team-wide meetings and brainstorming sessions. These gatherings played a crucial role in helping the team overcome various obstacles encountered along the way. The initial design emerged as a collective effort, considering aspects such as the rover's movements, mission objectives, and overall structure. Through collaborative brainstorming in team meetings, members explored ideas and design choices until an acceptable initial design step garnered unanimous approval.

After the completion of the initial design phase, the project team underwent a subdivision into specialized subsystems, with each subgroup dedicating efforts to address specific technical challenges. The chosen platform for collaborative communication and issue tracking was GitHub, providing a centralized and efficient means for the team to share technical insights, address challenges, and ensure a cohesive development process. This collaborative approach facilitated the seamless integration of various subsystems and streamlined the overall project workflow.

As illustrated in the time plan depicted in Figure 1.5, the primary objective of the team was to achieve the design freeze phase. This pivotal phase serves as a critical checkpoint in the mission design, marking a stage where the system's components are configured to function harmoniously. The design freeze phase provides a foundation from which subsequent iterations, tuning, and refinements can evolve, ultimately leading to an enhanced and finalized design.

2.3.2 First Steps

The commencement of the team's journey in this project marked the initiation of a challenging and protracted endeavor. From the embryonic conceptual drafts to the ultimate design, the team confronted numerous challenges, necessitating the consideration of multiple alternatives. The demanding nature of the field mandated improvisation across various facets of the rover, often with minimal references. Obtaining pertinent information proved to be more arduous than initially foreseen, resulting in delays at every juncture.

Following the commitment to the project, the initial step was to delineate which components of the rover would be designed. Primarily, the focus was on the mobility system and the rover body, tasks estimated to engage approximately three team members. Subsequently, a decision was made to incorporate a panel deployment mechanism, assigned to a fourth team member, and a mechanical arm, which required the workload to be allocated among two additional team members. This delineation formed the foundational structure of the team, streamlining responsibilities and tasks.

An early critical decision revolved around the selection of the suspension system. Rigorous research on existing suspension systems employed in space rovers was conducted to inform the choice. The initial design

exploration prominently featured the renowned rocker-bogie system, a well-established and proven choice celebrated for its efficacy in rover-type missions. Acknowledging its exceptional track record, the team initially considered adopting this system as the foundation for the rover's mobility subsystem. However, driven by a commitment to innovation and uniqueness, a pivotal decision was made to chart a distinctive path. Rather than adhering strictly to the conventional rocker-bogie system, the team opted for a creative reinterpretation. This decision reflects a deliberate departure from the familiar in favor of crafting a custom-designed mobility subsystem that draws inspiration from the principles of the rocker-bogie while introducing novel and optimized elements. The rough first design of the mobility subsystem was utilizing a spring like in most common suspension systems. Further consideration resulted in the removal of this part and the subsystem designed with no need for a conventional suspension spring assembly.

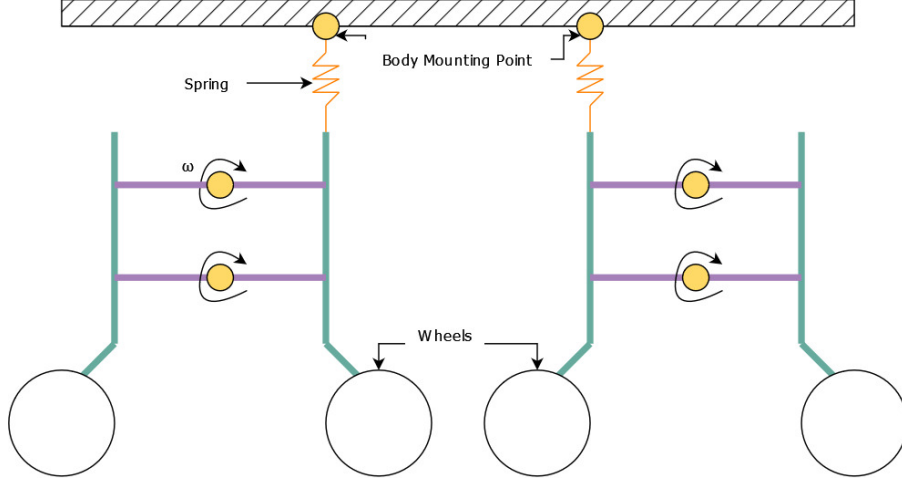


Figure 2.1: Initial Design Of The Mobility System

Another pivotal aspect of the rover that underwent substantial evolution from its initial conceptualization to the final design was the panel deployment mechanism. The preliminary design bore little resemblance to the finalized mechanism. The initial concept proposed a mechanism capable of accommodating a significantly larger panel area when deployed, with the ability to reduce to a much smaller size when retracted. However, this design was ultimately abandoned for several compelling reasons:

- The inclusion of an excessive number of moving parts posed an increased risk of multiple points of failure.
- The structural complexity of the initial design complicated the calculations for ensuring its integrity.
- The rover's operational requirements did not justify the inclusion of numerous panels, as per the energy allocation for each subsystem.

Subsequently, the P.D.M.E.M subsystem had to essentially start from scratch, leading to the conception of the final design, which alleviated these issues.

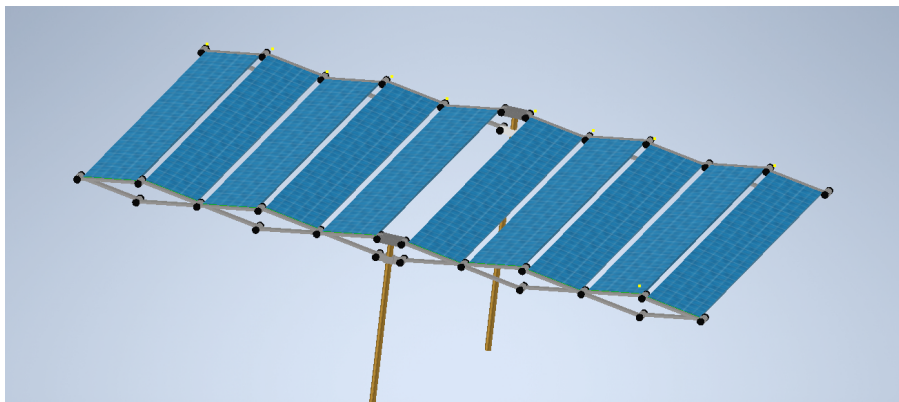


Figure 2.2: Initial Design Of The Panel Deployment Mechanism

The preliminary design of the robotic arm envisioned a magnetic head capable of seamlessly interchanging various specialized tools for diverse scientific purposes. The proposed toolkit included a drill, a sample collector, and a camera headset, each meticulously crafted to fulfill specific scientific objectives.

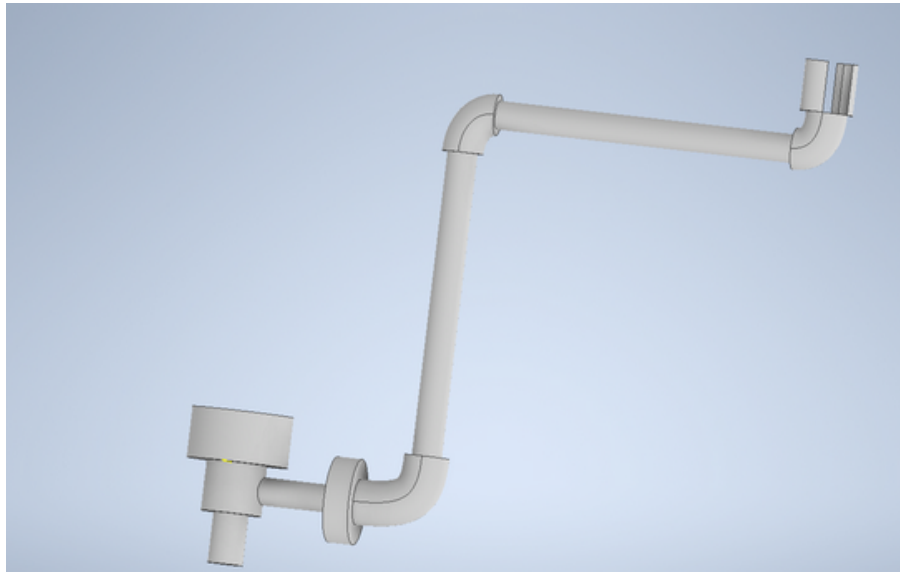


Figure 2.3: Initial Design Of The Robotic Arm

2.3.3 Quality Function Deployment

Quality Function Deployment involves the creation of a matrix that relates mission requirements to the engineering characteristics of the rover and it can be seen in 2.4. It is an important tool because it helps the team to understand the products features, and then translate them into specific design requirements. This ensures that the Rover will meet the initial needs and be of high quality. It also helps to prioritize features and characteristics, making sure that resources are focused on the most important aspects of the project. Furthermore, the QFD house promotes cross-functional collaboration within the development team. By involving different departments, everyone gets a better understanding of the project, reminding the goals and ensuring a successful outcome. 2.4.

Quality Function Deployment																							
Project title: Rover's QFD																							
Project leader: The Bubble King																							
Date: 10/1/2024																							
 Correlation: <table border="1" style="margin-left: auto; margin-right: auto;"> <tr> <td>+</td> <td>0</td> <td>-</td> </tr> <tr> <td>Positive</td> <td>No correlation</td> <td>Negative</td> </tr> </table> Relationships: <table border="1" style="margin-left: auto; margin-right: auto;"> <tr> <td>9</td> <td>3</td> <td>1</td> <td></td> </tr> <tr> <td>Strong</td> <td>Moderate</td> <td>Weak</td> <td>None</td> </tr> </table> Competitive evaluation (1: low, 5: high)										+	0	-	Positive	No correlation	Negative	9	3	1		Strong	Moderate	Weak	None
+	0	-																					
Positive	No correlation	Negative																					
9	3	1																					
Strong	Moderate	Weak	None																				
Customer importance rating 1: low, 5: high	Functional Requirements (How's)					Weighted Score	Satisfaction rating	Perseverance	Curiosity	Opportunity													
	Desired direction of improvement ($\uparrow, 0, \downarrow$)	Size-Shape	Strength	Control System	State of the Art Parts																		
Customer Requirements - (What's) ↓	→																						
1 Rover's Velocity	9	3	1	1	3	17	4	5	4	3													
2 Reliability	1	9	9	9	9	185	3	5	4	4													
3 Rover's Life Expectancy	1	9	3	3	9	75	2	4	3	3													
4 Maneuvrability	9	1	9	9	1	145	3	4	4	2													
5 Systems Collaboration	3	1	9	9	3	100	3	4	3	3													
6 Payload Innovative Design		1	1	9	3	42	2	5	4	3													
7 Weight	3	3	0	1	9	64	4	5	4	3													
8 Energy Consumption	3		3	9	3	54	3	4	4	3													
9 Versatility-Adaption	9		9	3	1	44	4	5	4	3													
Technical importance score					113	99	166	200	148	726													
Importance %					16%	14%	23%	28%	20%	100%													
Priorities rank					4	5	2	1	3														

Figure 2.4: Quality Function Deployment

Chapter 3

Subsystem Level Reports

3.1 Mobility Subsystem

3.1.1 Overview

The mobility system of a rover vehicle assumes a critical role in overcoming the unique challenges presented by the Martian surface. As can be seen in Fig. 1.1, the Mobility Subsystem of the examined rover encompasses both the directional control and suspension aspects of the vehicle. Notably, the design diverges from conventional suspension systems reliant on spring force. Instead, an innovative approach has been adopted, eliminating the need for a traditional suspension system. This groundbreaking design empowers the rover to traverse diverse terrains on Mars without the dependence on traditional suspension mechanisms. The rationale behind this design choice is further influenced by the rover's operational characteristics and a low amplitude of velocity, ultimately enhancing its adaptability and efficiency across varied Martian landscapes.

The Mobility Subsystem addresses every part responsible for the movement of the rover. The subsystem is mounted onto the main body. Core responsibilities of it are:

- Optimize Power Consumption for Enhanced Mobility - Prioritize the selection of a power consumption strategy that favors the mobility subsystem, ensuring an efficient allocation of energy resources to drive the rover across diverse Martian terrains.
- Wheel Geometry Design - Delve into the intricacies of wheel geometry design, considering factors such as size, shape, and tread pattern. Tailoring the wheel geometry to the specific demands of the Martian surface enhances traction and maneuverability.
- Engineering of Body-to-Wheel Connections - Calculate and meticulously design the components that facilitate the connection between the rover's body and its wheels. This involves ensuring structural integrity and mechanical efficiency in transmitting power from the mobility subsystem to the overall vehicle.
- Bearing Connections for Steering and Transmission - Develop robust bearing connections tailored for both steering and transmission systems. The design should prioritize durability, low friction, and precise control, contributing to the overall functionality and longevity of the rover's mobility subsystem.
- Selection of Permitted Movement Scenarios - Elect and define the range of permissible movement scenarios for the mission. This involves identifying and specifying the various modes of operation the rover will encounter during its exploration, ensuring the mobility subsystem is adept at navigating the diverse challenges posed by the Martian landscape.

3.1.2 Team Dependencies

There has been previously mentioned (Fig. 1.2) that the project is characterised by a dynamic information exchange mechanism. This means that each subsystem needs to address to all others to overcome various functionality blocking points. Thus, the mobility subsystem depends on every other subsystem of the rover and additionally every other subsystem depends on the Mobility.

Mobility - Body

Firstly, its collaboration with the main rover body subsystem is fundamental, as the mobility system is not only housed within the body but is also structurally integrated. The design and engineering decisions made in the main body subsystem significantly influence the performance and adaptability of the mobility system, ensuring seamless coordination between the rover's chassis and its ability to navigate diverse terrains on Mars.

Mobility - Robotic Arm

Secondly, the interaction with the robotic arm subsystem is essential for the rover's versatility. The mobility subsystem accommodates the robotic arm's reach and movement requirements, allowing the rover to position itself optimally for scientific experiments and sample collection. The synergy between mobility and the

robotic arm ensures a comprehensive approach to exploration, enabling the rover to access and analyze various points of interest with precision.

Mobility - P.D.M.E.M.

Lastly, the collaboration with the panel deployment mechanism and energy management subsystem is critical for sustaining the rover's mission. The mobility subsystem must align with the energy management strategy to ensure efficient power distribution across the rover. Additionally, the panel deployment mechanism, responsible for harnessing solar energy, influences the overall energy availability for the mobility subsystem.

3.1.3 Subsystem Management

The subsystem's main goal is to design an innovative but simple movement system for the rover. This is achieved through simple mechanical bearing connections between aluminum bars. The subsystem's design can be seen in Fig. 3.3.

Upon the draft design, the subsystem will undergo static analyses in order to ensure structural integrity of the vehicle. The whole subsystem's static analysis can be observed in Section 3.1.4. The analysis is conducted for specific movement scenarios. These scenarios are covering a wide spectrum of available rover maneuvers. The scenarios in question are:

- Linear movement on flat terrain
- Linear movement on sloped terrain (Hill Climb)
- Impact with infinite mass object

The Mobility subsystem shall be the one declaring the maximum slope angle the vehicle can undergo. It should also declare the maximum velocity. The values for these variables are thoroughly studied in 3.1.4. At last, the tools this subsystem used are all the tools mentioned in Tab. 2.2.

3.1.4 Conceptual Design

Mechanics

Motor Wattage Calculation

The motor wattage for the transmission and the steering of the vehicle are to be examined. In order to achieve that, a rough mass budget of the rover has been created. This can be seen in Tab. 3.1.

Parts	Mass (kg)	Quantity	Total (kg)
Battery Pack	50	1	50
Panel	2	1	2
Metallic Parts	20.8	-	20.8
Wheel	12	8	96
Robotic Arm	150	1	150
Body	300	1	300
Differential Mechanism	8	2	16
Electronics	5	1	5
Rover Weight (N)			2373.66

Table 3.1: Mass Budget

The maximum velocity of the rover was assumed:

$$V = 0.1 \text{ m/s}$$

The radius of the wheel was also assumed at this stage as:

$$R = 0.125 \text{ m}$$

The rotation per minute for each transmission motor can be calculated as:

$$RPM = \frac{d}{L}, \quad (3.1)$$

where d : the distance covered from the rover in one minute and L :the circumference of the wheel.

For the *flat terrain scenario* the free body diagram of the wheel can be seen in Fig. 3.1. The motor needs to

overcome the force that opposes to the motion and that is the friction force (rolling resistance). The vehicle is designed with eight in total wheels. Assuming even mass distribution on each wheel the rolling resistance is:

$$F_f = \mu \cdot \frac{W}{8} \quad (3.2)$$

According to [3] the coefficient of friction is estimated to be $\mu \approx 0.4$. Then,

$$M_o = F_f \cdot R \quad (3.3)$$

And thus,

$$P = M_o \cdot \frac{RPM}{9.55} \quad (3.4)$$

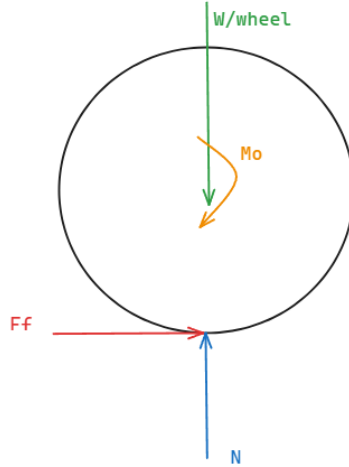


Figure 3.1: Wheel Free Body Diagram for Flat Terrain

For the *hill climb scenario* the free body diagram can be seen in Fig. 3.2. Here F_p is the required pull force all the motors need to produce. This needs to overcome the rolling resistance of all wheels and the total weight component on the slope tangent axis. The slope was considered to be the maximum elected $\theta = 30^\circ$. Thus the rolling resistance on each wheel is:

$$F_f = \mu \cdot \frac{W}{8} \cdot \cos 30^\circ \quad (3.5)$$

At last, the total pulling force should be:

$$F_p > W \cdot \sin 30^\circ + 8 \cdot F_f \quad (3.6)$$

Assuming that the pull force each motor shall produce would be evenly divided by the total pull force:

$$F_{p/wheel} > \frac{F_p}{8} \quad (3.7)$$

The torque of each motor is calculated this time as:

$$M_o = F_{p/wheel} \cdot R \quad (3.8)$$

The wattage can be calculated through Eq. 3.4.

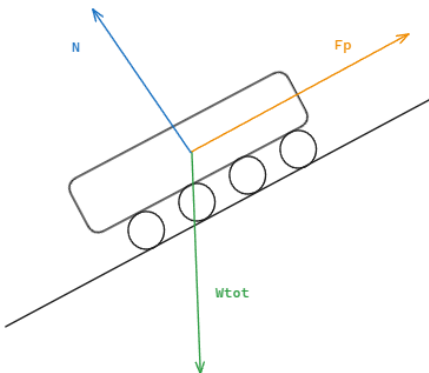


Figure 3.2: Rover Free Body Diagram On Slope

For the steering motor of the wheel, the desired angular acceleration needs to be considered. The value chosen was:

$$\alpha = \frac{\pi}{180} \text{ rad/s}^2$$

The wattage will be calculated for the worst case scenario of $0^\circ \rightarrow 90^\circ$ wheel steering. This maneuver is needed to complete in $\Delta t = 8 \text{ sec}$, as set by team requirements. Thus the wattage can be calculated through Eq. 3.9.

$$P = \tau \cdot \omega, \quad (3.9)$$

where:

$$\omega = \frac{\pi}{180} \cdot \Delta t \text{ rad/s} \quad (3.10)$$

The torque required is:

$$\tau = I \cdot \alpha + \tau_{\text{friction}}, \quad (3.11)$$

where τ_{friction} should be the torque transmitted through friction as described in Fig. 3.1. The moment of inertia can be calculated after a detailed design of the wheel is shaped in a CAD software. The results of the wattage calculations for each motor can be seen in Tab. 3.2.

Motor	Wattage
Transmission	> 24 Watt
Steering	> 2 Watt

Table 3.2: Motor Wattage Values

In accordance with these values, some commercial motors that can be used in this design are these motors.

Calculation of Subsystem Parts

In order to calculate the subsystem parts, the parts need to be designed so it is clear how the geometry is shaping. A draft iteration of the Mobility Subsystem can be seen in Fig. 3.3.

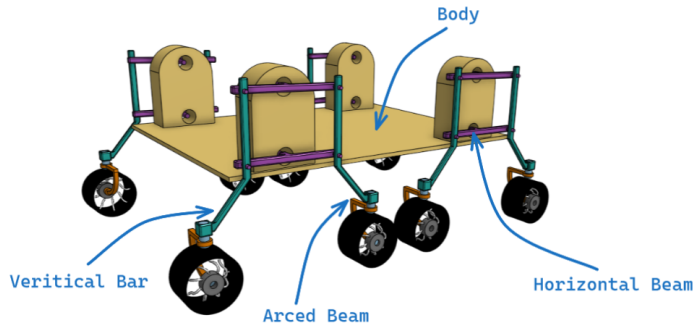


Figure 3.3: Mobility Subsystem Draft Iteration

Thus the parts to be calculated for various static scenarios are:

1. The Horizontal Beam
2. The Vertical Bar
3. The Arced Beam

The cross section of each bar/beam is of orthogonal shape as can be seen in Fig. 3.4.

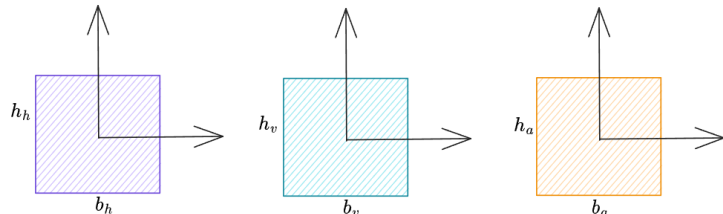


Figure 3.4: Cross Sections of Subsystem Parts

More detailed 3D views of the parts can also be seen in Fig. 3.5.

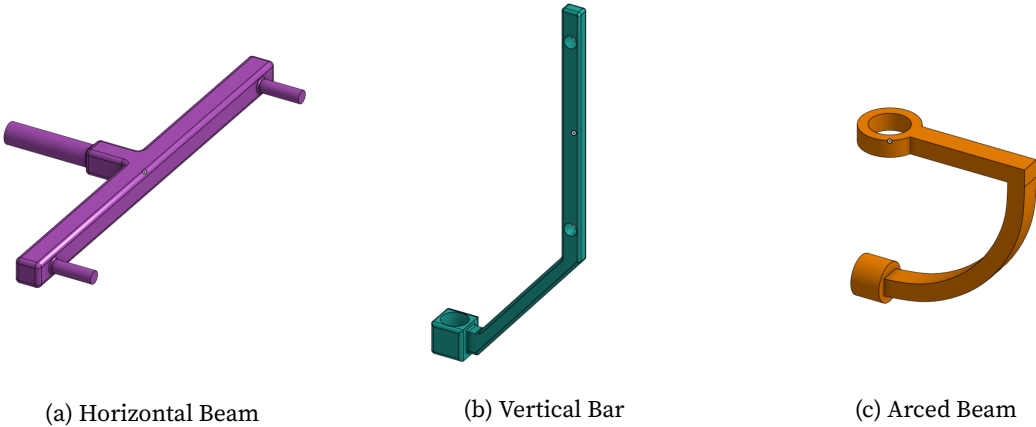


Figure 3.5: Subsystem Parts

The **Horizontal Beam** is to be calculated in bending and in tension/compression, the **Vertical Bar** is to be calculated in bending and on impact with infinite mass object and lastly the **Arched Beam** in bending. At last, deflections for both of the beams are to be calculated to ensure the robustness of the system. MATLAB script has been created in order to calculate all the above factors. For the safety factors it is:

$$SF = \frac{s_y}{\sigma_{applied}}, \quad (3.12)$$

where s_y is the yield strength of the chosen material. All the parts are to be calculated in a slope of angle f° .

The *Free Body Diagram* of the subsystem can be seen in Fig. 3.6. Here:

- N is the normal force from the ground
- T is friction force
- a_{ij}, b_{ij} are the reactions

For the parts, as well as the system it self it will be of course:

$$\sum F_x = 0, \sum F_y = 0, \sum M = 0,$$

where x would be the axis in parallel to the bar's center line and y would be the perpendicular to the bar's center line axis. For the high level system the axis can be seen in the figure.

For both the horizontal beams the moment equilibrium is taken at their left hand point (11 and 21 correspondingly). In total there is 3 equations for each horizontal bar. So 6 equations. Forces equilibrium produces another two equations for each of the vertical bars as well. In total 4 equations. For the last two equations, the mobility system is checked at a high level where only the weight forces as well as the ground normal forces and friction act. And thus forces equilibrium on each axis of the high level system produces another two equations. Here:

- $s = \sin f$
- $c = \cos f$
- $w = \frac{W}{8}$
- l is the horizontal beam's length

$$A = \begin{bmatrix} -s & -s & 0 & 0 & c & c & 0 & 0 & 0 & 0 & 0 & 0 \\ c & c & 0 & 0 & s & s & 0 & 0 & 0 & 0 & 0 & 0 \\ 0 & -sl & 0 & 0 & 0 & cl & 0 & 0 & 0 & 0 & 0 & 0 \\ 0 & 0 & -s & -s & 0 & 0 & c & c & 0 & 0 & 0 & 0 \\ 0 & 0 & c & c & 0 & 0 & s & s & 0 & 0 & 0 & 0 \\ 0 & 0 & 0 & -sl & 0 & 0 & 0 & cl & 0 & 0 & 0 & 0 \\ 0 & 0 & 0 & 0 & -1 & 0 & -1 & 0 & c & 0 & s & 0 \\ -1 & 0 & -1 & 0 & 0 & 0 & 0 & 0 & -s & 0 & c & 0 \\ 0 & 0 & 0 & 0 & 0 & 0 & 0 & 0 & 1 & 1 & 0 & 0 \\ 0 & 0 & 0 & 0 & 0 & -1 & 0 & -1 & 0 & c & 0 & s \\ 0 & -1 & 0 & -1 & 0 & 0 & 0 & 0 & 0 & -s & 0 & c \\ 0 & 0 & 0 & 0 & 0 & 0 & 0 & 0 & 0 & 0 & 1 & 1 \end{bmatrix}, Z = \begin{bmatrix} cw \\ ws \\ wc \frac{l}{2} \\ wc \\ ws \\ wc \frac{l}{2} \\ 0 \\ 0 \\ 2wc \\ 0 \\ 0 \\ 2ws \end{bmatrix}, x = \begin{bmatrix} a_{11} \\ a_{12} \\ a_{21} \\ a_{22} \\ b_{11} \\ b_{12} \\ b_{21} \\ b_{22} \\ N_1 \\ N_2 \\ T_1 \\ T_2 \end{bmatrix}$$

By solving for x the linear system $\mathbf{Ax} = \mathbf{Z}$ the forces are calculated.

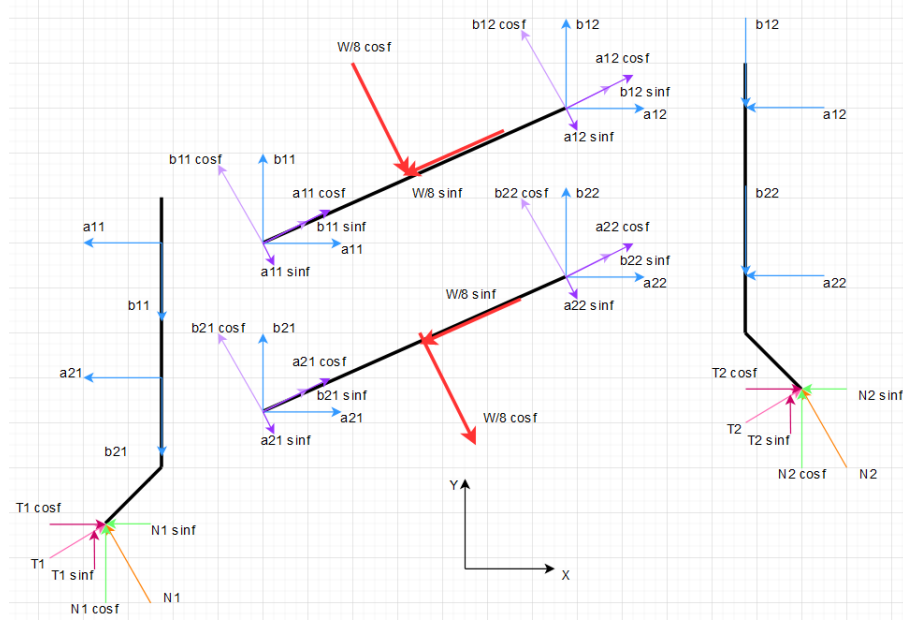


Figure 3.6: Free Body Diagram in slope angle f for the Mobility Subsystem

For the *Horizontal Beam*, safety factors for bending and tension are obtained using MNQ method. Considering a rectangular cross section with b_h : base, h_h : height the applied stresses are calculated as:

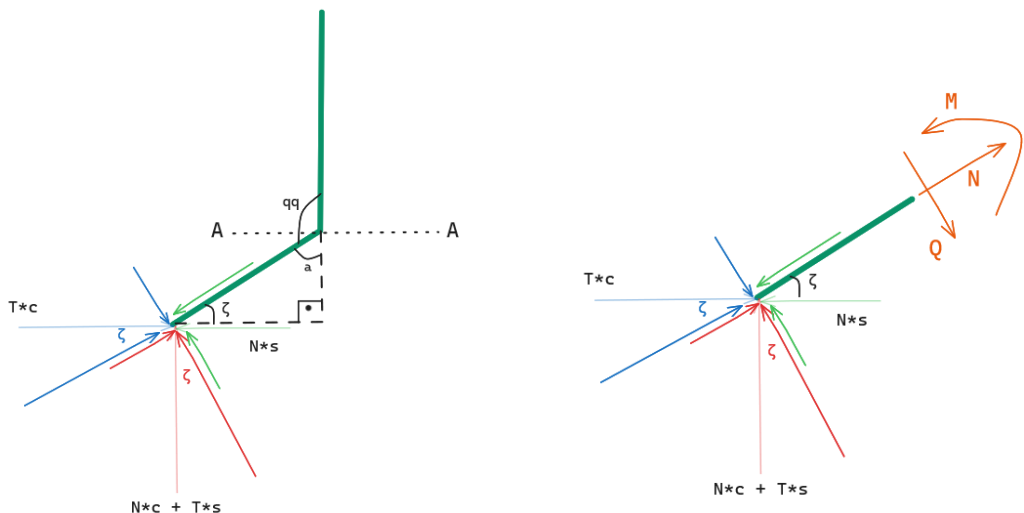
$$\sigma_z^{hor} = \frac{N}{h_h \cdot b_h} \quad (3.13)$$

$$\sigma_b^{hor} = \frac{N}{h_h \cdot b_h} + \frac{M}{I_h} \cdot z_h \quad (3.14)$$

The critical cross section for the bending load would be in the middle of the beam, while for the tension it is calculated through MNQ arrays from MATLAB. Lastly, the deflection across the vertical axis from a load at the center of a beam P , is calculated as [12][13]:

$$\delta_{hor} = \frac{P \cdot l^3}{48 \cdot E \cdot I_h} \quad (3.15)$$

In order to analyze the *Vertical Bar* the free body diagram of it has been created in Fig. 3.7.



(a) Vertical Bar Free Body Diagram

(b) Vertical Bar MNQ Diagram

Figure 3.7: Vertical Bar

Given the qq angle the rest of the angles can be calculated. The critical cross section is AA . Finally:

$$N_{max} = -T \cdot c \cdot \cos\zeta - (N \cdot c + T \cdot s) \cdot \sin\zeta + N \cdot s \cdot \cos\zeta \quad (3.16)$$

$$M_{max} = -T \cdot c \cdot \sin\zeta \cdot x_{max} + (N \cdot c + T \cdot s) \cdot \cos\zeta \cdot x_{max} + N \cdot s \cdot \sin\zeta \cdot x_{max}, \quad (3.17)$$

where:

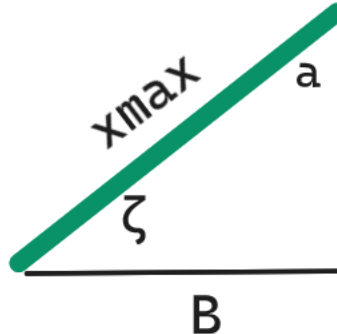


Figure 3.8: x_{max} of Eq. 3.17

Of course:

$$\sigma_b^{ver} = \frac{N_{max}}{A_v} + \frac{M_{max}}{I_v} z_v \quad (3.18)$$

In the conceptual design stages, in order to calculate for an impact, the impact dynamic load can be approximated with a static one. This can be done with an impact load factor. For a mass moving horizontally with velocity of V this is [1]:

$$n = \sqrt{\frac{\eta \cdot V^2}{g \cdot \delta_{static}}} \quad (3.19)$$

In the provided expression, where η represents the efficiency, indicating the proportion of kinetic energy converted, a value of $\eta = 1$ signifies perfect elasticity, with all kinetic energy effectively converted. The efficiency parameter becomes particularly relevant when considering the mechanical behavior of materials and components within a system. By consulting datasheets [15] specific to the materials employed in the design, one can glean information about their inherent efficiency, facilitating a precise estimation of energy conversion and absorption characteristics. The term δ_{static} represents the equivalent static deflection in the direction of the impact load, as if the applied load were static rather than dynamic. The impact load would be equal to the momentum difference according to Newton's law:

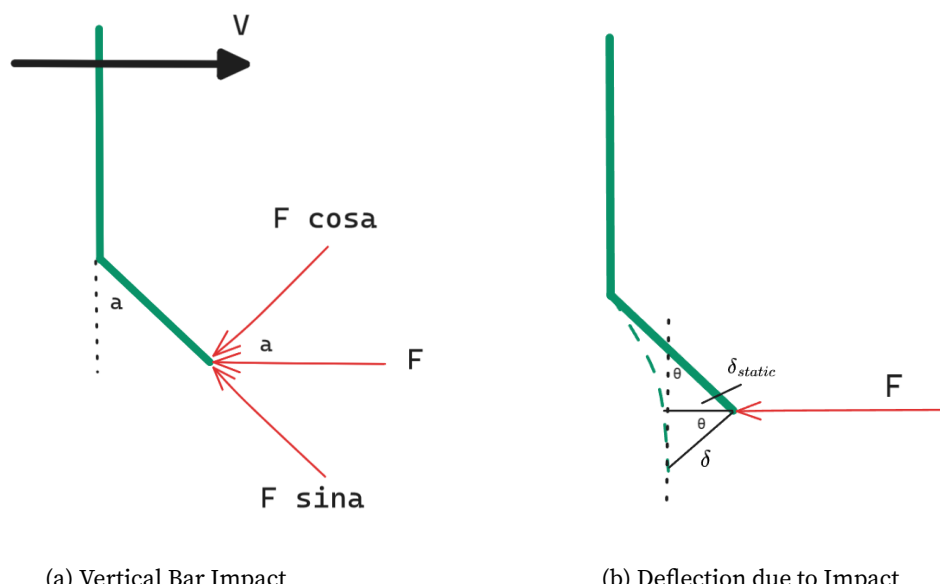


Figure 3.9: Vertical Bar

$$F = m_{rover} \cdot V \quad (3.20)$$

From Mechanics it is derived that:

$$\delta = \frac{F \cdot \cos a \cdot x_{max}^3}{3 \cdot E \cdot I_v} \quad (3.21)$$

$$\theta = \frac{F \cdot \cos a \cdot x_{max}^2}{2 \cdot E \cdot I_v} \quad (3.22)$$

Finally, the equivalent static loading will be:

$$\vec{F}_{se} = \vec{F} \cdot n \quad (3.23)$$

The stress can be derived from Eq. 3.18, where:

$$N_{max} = -F_{se} \cdot \sin a \quad (3.24)$$

$$M_{max} = -F_{se} \cdot \cos a \cdot x_{max} \quad (3.25)$$

The *Arced Beam* consists of a linear half and a quarter of circle (arced) half with radius of R . For the beam the diagrams can be seen in Fig. 3.10.

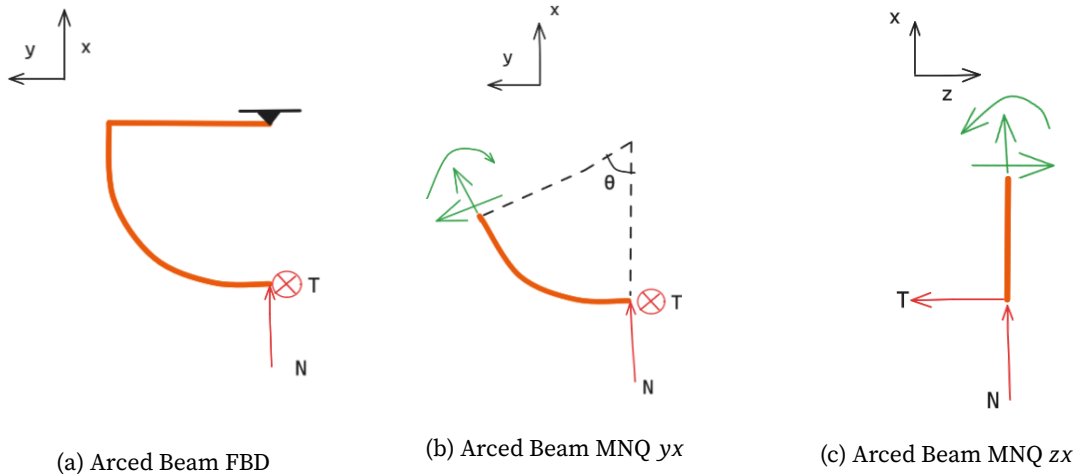


Figure 3.10: Arced Beam

At last:

$$\sigma_b^{arc} = \frac{M_{zy}}{I_{zy}} \cdot z_{zy} + \frac{M_{yx}}{I_{yx}} \cdot z_{yx} \quad (3.26)$$

It is important to calculate the deflection of the linear half of the beam. Instead of that the deflection of the arced half will be calculated, making the assumption that these are equal. Therefore [17]:

$$\delta_{arc} = \frac{\frac{\pi}{4} \cdot N \cdot R^3}{E \cdot I_a} \quad (3.27)$$

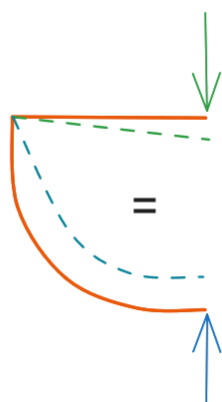


Figure 3.11: Deflection of Arced Beam

Finally, the subsystem is designed and tested with the following characteristics:

Description	Variable	Value
Maximum slope angle	f	30°
Vertical Bar geometric angle	qq	140°
Horizontal Beam base	b_h	30 mm
Horizontal Beam height	h_h	30 mm
Arched Beam base	b_a	18 mm
Arched Beam height	h_a	22 mm
Arched Beam radius	R	150 mm
Vertical Bar base	b_v	20 mm
Vertical Bar height	h_v	30 mm
Vertical Bar width	B	151.26 mm
Horizontal Beam length	l	440 mm

Table 3.3: Mobility Subsystem Geometric Values

The safety factors and the deflections occurred can be seen in Tab. 3.4. The maximum velocity was the one used. Also, the material that has been assumed is Aluminum 6061-T6 for all parts.

Description	Variable	Value
Tension of Horizontal Beam	SF_z^{hor}	1.1163×10^3
Bending of Horizontal Beam	SF_b^{hor}	42.2768
Deflection of Horizontal Beam	δ_{hor}	0.0979 mm
Bending of Arched Beam	SF_b^{arc}	10.3487
Deflection of Arched Beam	δ_{arc}	0.618 mm
Bending of Vertical Bar	SF_b^{ver}	22.6711
Impact of Vertical Bar	SF_i^{ver}	347.1974

Table 3.4: Mobility Subsystem Calculation Results

The joints of the suspension system

The term "joints" refers to the mechanical mechanisms inherited in the suspension system, which empower it to execute its intended movements. There are two types of joints in the suspension system and each one of them is going to be presented in the following paragraphs. In all loading cases, the use of Fig. 3.6 proved fundamental.

First Joint

The purpose of the first joint is to allow the vertical bar to move vertically and simultaneously withstand the forces that this point of the suspension system deals with. Lastly, it must be fully sealed from the atmosphere of Mars. Below is portrayed the main idea of the desired movement:

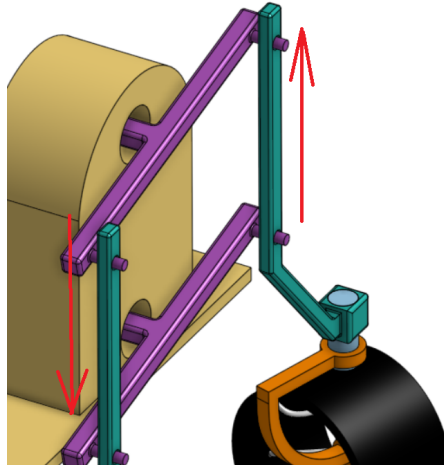


Figure 3.12: First Joint Desired Movement

The solution to this problem consists of basically two deep groove bearings, two spacers, two retaining rings, two connectors and finally 8 bolts. With this configuration, the vertical bar has a stationary-mobile mount that with the combination of four of these joints the desired high level system movement is accomplished. In addition, to seal this joint one radial shaft seal and the connectors are used. The design of the joint is illustrated in Fig. 3.13.

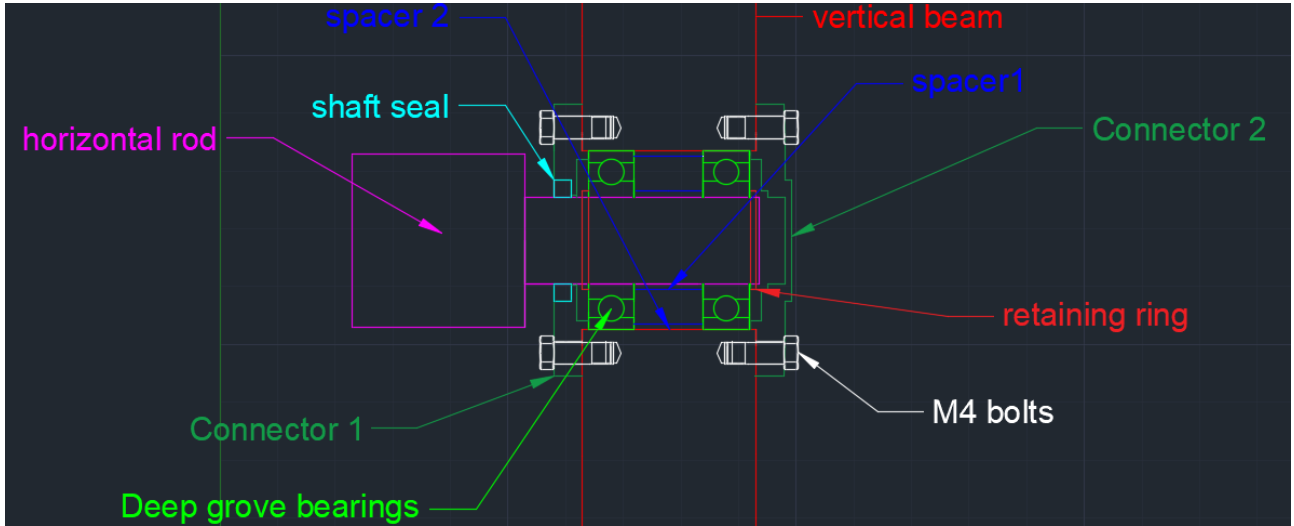


Figure 3.13: 2D Sketch Of The First Joint

The credibility of this concept is depended only by the durability of the bearings which is measured by the static load they accept in this scenario. That is equal to P . Furthermore, P is equal to the radial forces F_r , since there are no axial forces in this loading case. Fig. 3.14 portrays the Free Body diagram of the joints with A being the point of the placement of the first bearing and B of the second bearing respectively. Assuming the connection load point is equally distanced from points A and B then:

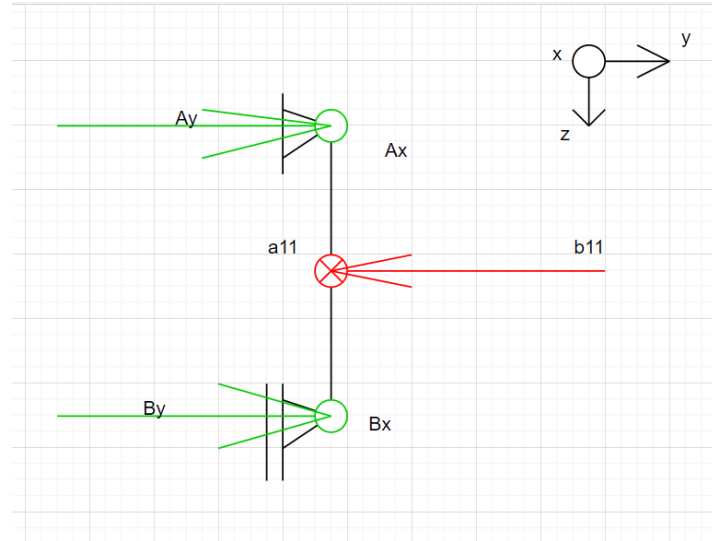


Figure 3.14: Free Body Diagram Of The First Joint

$$\sum F_x = 0, \sum M_{Ax} = 0$$

Consequently,

$$A_x = B_x = \frac{a_{11}}{2} \quad (3.28)$$

Like wise,

$$A_y = B_y = \frac{b_{11}}{2} \quad (3.29)$$

In conclusion the equivalent connection load is as follows in Eq. 3.30.

$$P = \sqrt{\left(\frac{a_{11}}{2}\right)^2 + \left(\frac{b_{11}}{2}\right)^2} \quad (3.30)$$

At last, P even in the worst case scenario, is much lower than the static load that the chosen bearing (*SKF 16002 Deep Groove Ball Bearing*) can withstand. Results can be seen in Tab. 3.5.

Variable	Value
c	2.85 kN
P	74 N

Table 3.5: First Bearing Joint Calculation Results

Thus, the validness of this design is ensured. The next step is the construction of the CADs of each component of the Bearing Connection.

Second Joint

Firstly, the purpose of this joint is to allow the arced beam to rotate and simultaneously withstand the forces that this point of the suspension system deals with. Lastly, it must also be sealed from the atmosphere of Mars. The desired movement is portrayed in Fig. 3.15.

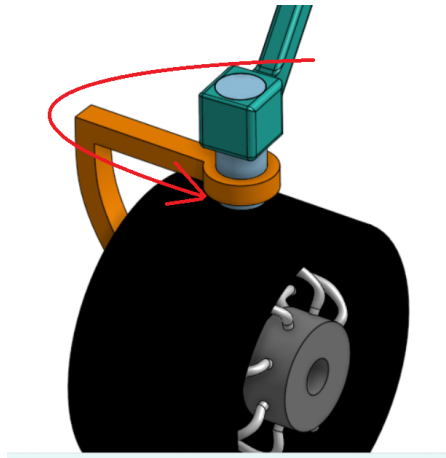


Figure 3.15: Second Joint Desired movement

This problem is solved by making use of two different types of bearings. Firstly, with the use of a thrust bearing, the arced beam can freely rotate along the vertical bar's axis. Simultaneously, it can accept the vertical forces that act on it. Secondly, with the use of two deep groove bearings and two spacers, vertically arranged, and a retaining ring, the arced beam is able to rotate while accepting the horizontal forces that act on it. Finally, this mechanism is facilitated in two cylinder shaped cases. At last, *the first casing* also makes use of a lip seal as demonstrated in Fig. 3.16.

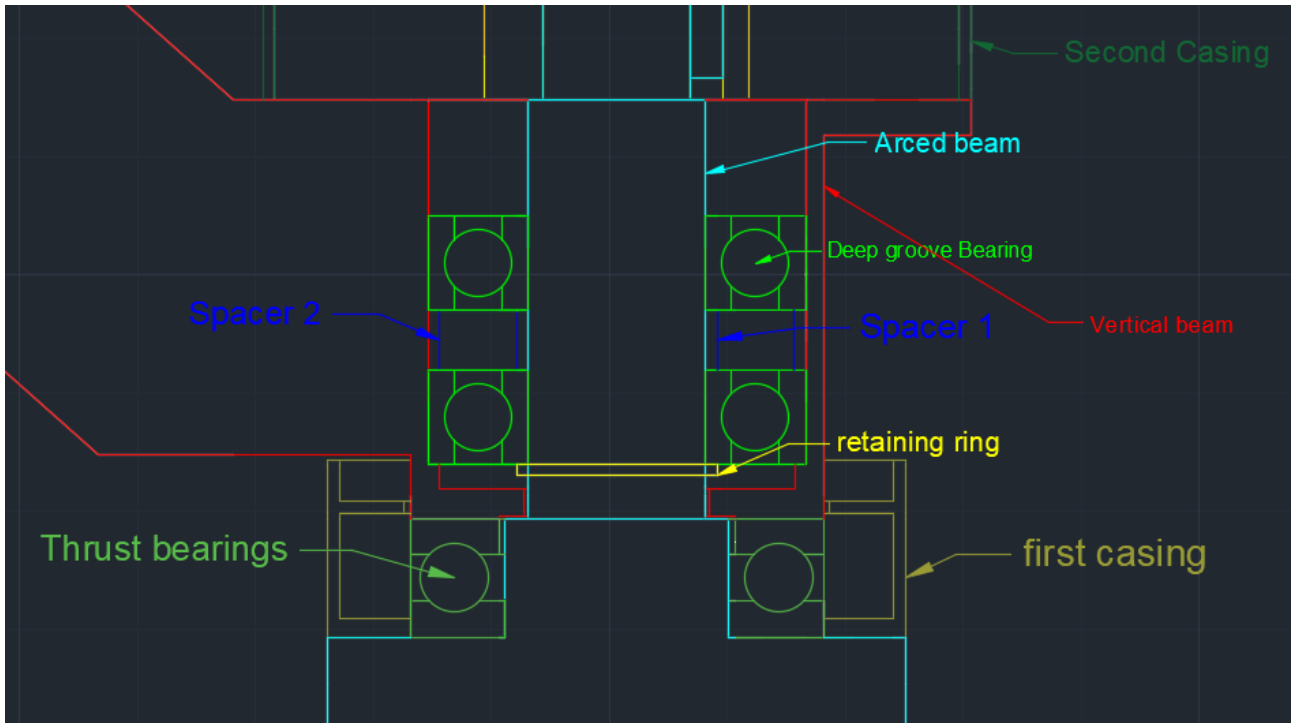


Figure 3.16: 2D Sketch Of The Second Joint

Again the credibility of this concept is depended only by the durability of the bearings which is measured by the static load that they accept. The only factor that must be calculated is the equivalent force that the bearings are dealt with. Each of them needs to be examined separately. Regarding the *thrust bearing*, P is equal to the axial force F_a that it accepts. That is because there are no radial forces in this loading case. Fig. 3.17 portrays the Free Body diagram of the thrust bearing.

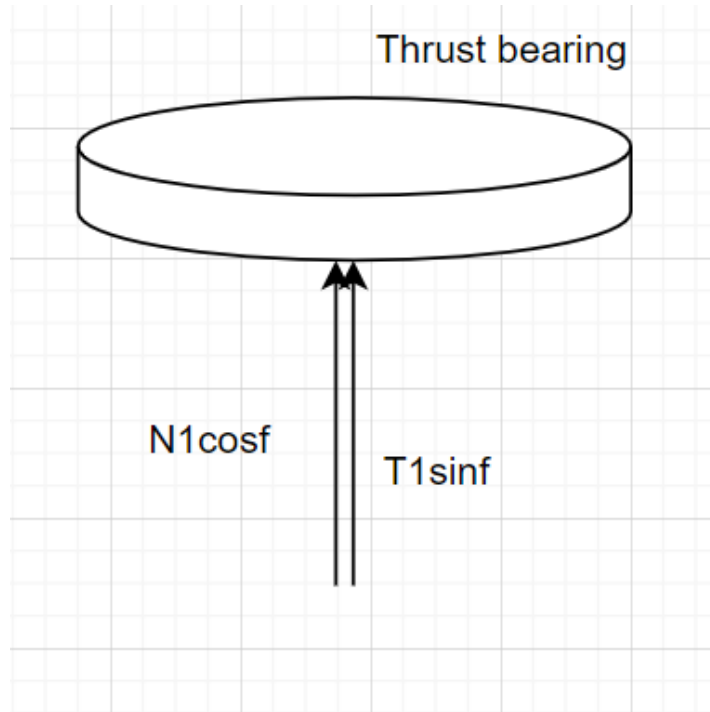


Figure 3.17: Second Joint Thrust Bearing Free Body Diagram

In conclusion:

$$P = N_1 \cdot \cos f + T_1 \cdot \sin f, \quad (3.31)$$

where $f = 0^\circ$ is the worst case scenario for the above mentioned loading case (f : slope angle). Thus, P , even in the worst case scenario is much lower than the static load that the chosen thrust bearing (*SKF 51104 Single Direction Thrust Ball Bearing*) can withstand. The above assumptions are approved by Tab. 3.6.

Variable	Value
c	15.1 kN
P	148 N

Table 3.6: Second Joint Thrust Bearing Calculation Results

Furthermore, as for the *deep groove bearings*, P is equal to the radial forces F_r that the deep groove bearing accepts, since there are no axial forces in this case. In Fig. 3.18 someone can observe the Free Body diagram of the deep groove bearing of the second joint. Here, A is the point of the placement of the first bearing and B of the second respectively.

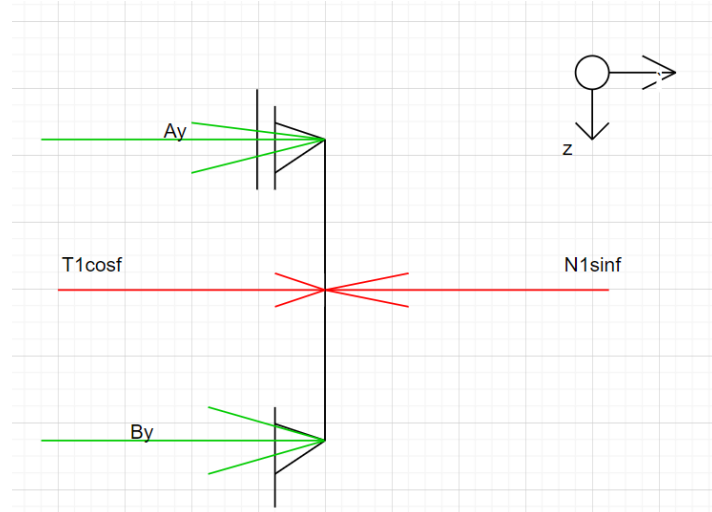


Figure 3.18: Second Joint Deep Groove Bearings Free Body Diagram

Hence,

$$\sum F_y = 0, \sum M_{Ay} = 0$$

Furthermore,

$$A_y = B_y = \frac{T_1 \cdot \cos f + N_1 \cdot \sin f}{2} \quad (3.32)$$

In conclusion, assuming the loading point is equally distanced from the two bearings, the equivalent connection load is as follows:

$$P = \frac{T_1 \cdot \cos f + N_1 \cdot \sin f}{2} \quad (3.33)$$

As a result, both the deep groove bearings accept the same equivalent P force. In addition, f is chosen to be 30° since at this angle $P = P_{max}$. Furthermore, as Tab. 3.7 illustrates the static load that the chosen bearings can accept is far greater than the load that is acted upon them. Therefore, the bearings (*16002 Deep Groove Ball Bearing*) are rightfully chosen.

Variable	Value
c	5.85 kN
P	148 N

Table 3.7: Second Joint Deep Groove Bearing Calculation Results

At last, the next step is the construction of the CADs of each component of this joint and finally the assembly of them.

Electrical Motors Mounting And Connection

The rover is chosen to have a configuration of motors at each wheel to achieve high maneuverability. As a result, it is able to navigate itself through the Mars hazardous terrain with ease. This part of the report, addresses the mounting and the connection of the two electrical motors that are required in order to steer and transport the rover. The desired mechanism can be observed in Fig. 3.19.

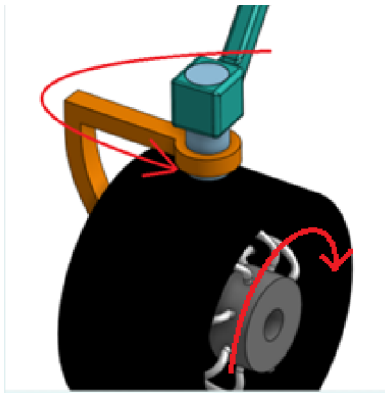


Figure 3.19: Mobility System's Motors Degrees Of Freedom

The *mount of the steering motor* consists of a cylinder shaped case. The case is locked in place with six bolts that connect it with the frame of the motor as instructed by the motor provider. In addition, the casing itself is also locked in place with the vertical bar with six bolts. This configuration is presented in Fig. 3.20.

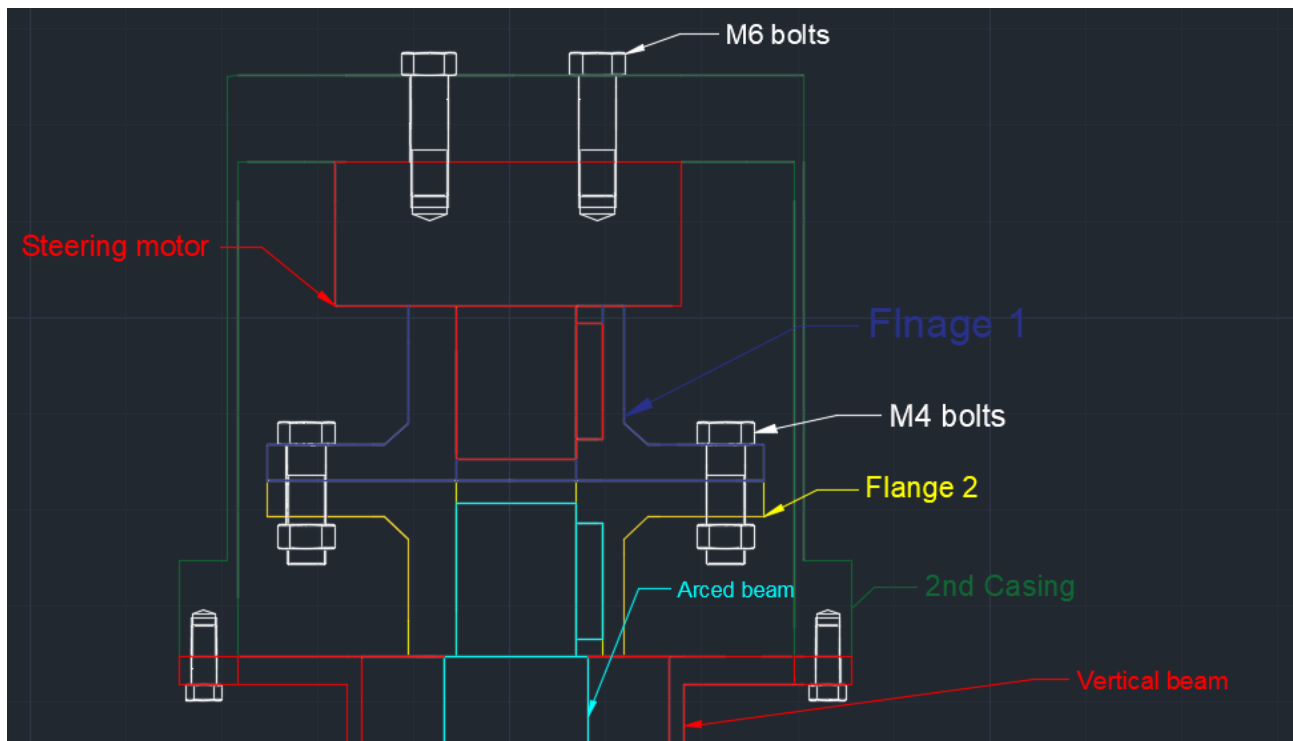


Figure 3.20: 2D Sketch Of Steering Motor Mounting

The validness of this design depends on the durability of the bolts connection. This is determined by their safety factor on shear stress. The method that is going to be used is calculated as in [4]. In the bellow tables, calculation information as well as the safety factors are presented.

Description	Variable	Value
M6 Bolt Type		
Number of bolts	n	4
Force Of Shear Stress	F_p	515 N
Safety Factor	S	2

Table 3.8: Case-Steering Motor Bolt Connection

Description	Variable	Value
M4 Bolt Type		
Number of bolts	n	6
Force Of Shear Stress	F_p	349 N
Safety Factor	S	2.46

Table 3.9: Case-Vertical Bar Bolt Connection

As can be observed above, the mount is rightfully design. Considering *the connection of the motor to the arced beam*, the configuration is as follows. The shaft of the motor has an integrated key that will be connected with a flange (Flange 1). Additionally, that flange is connected with another flange (Flange 2) by $6 \times M4$ bolts. Flange 2, is connected with an integrated key to the upper end of the steering system. Lastly, this connection is sealed from the atmosphere of Mars along with the second joint (see Section 3.1.4) in a cylinder metal casing connected with the vertical bar and sealed with the combination of bolts and gaskets. This configuration is presented in Fig. 3.21:

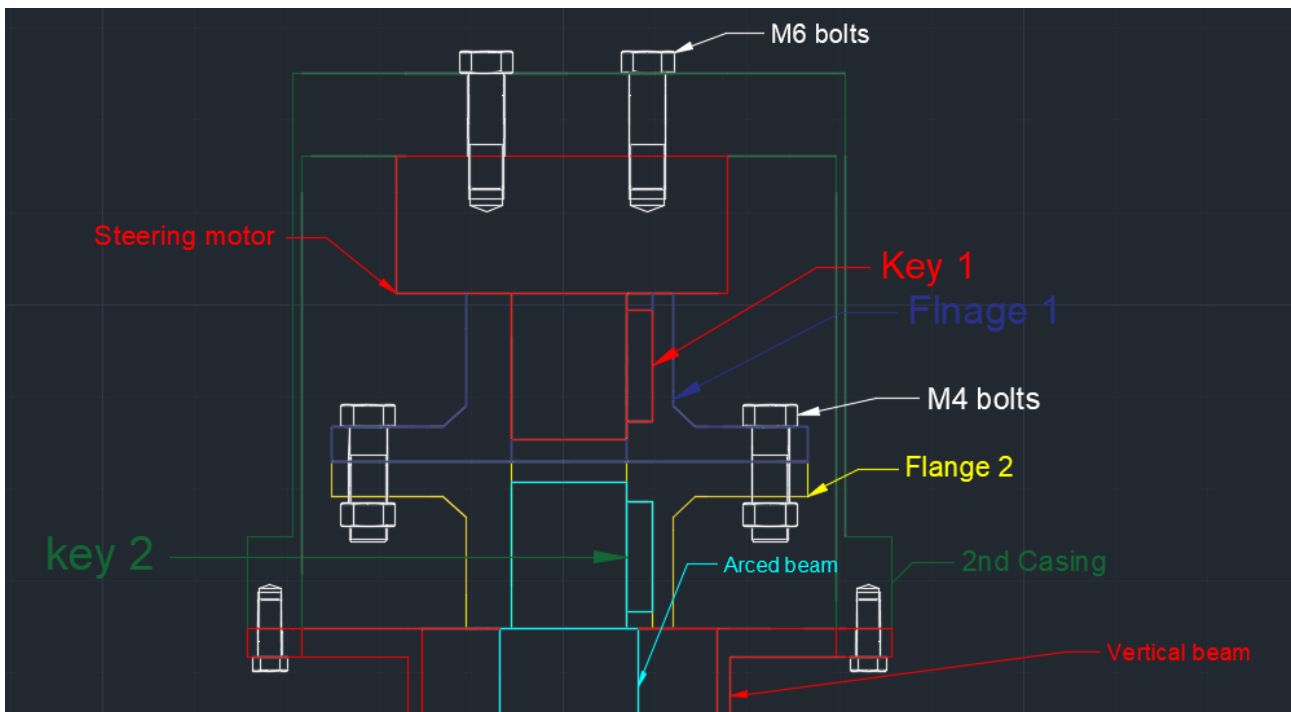


Figure 3.21: Steering Motor And Arced Beam Configuration

The durability of this connection is valid if two conditions are met. (The key-flange configuration that is used in both flange-shaft connections has to be examined only one time since they both receive the same pressure as they are identical). Firstly, the surface pressure acting on the key has to be lower than the material permitted surface pressure. Secondly, the safety factor of the flange-to-flange connection needs to be appropriate. This safety factors depends on the bolts connection only. All the above, are calculated as mentioned in [4]. Below, in Tab. 3.10 the surface pressure is calculated and in Tab. 3.11 the bolt connection is calculated also.

Description	Variable	Value
Shaft Diameter	d	12.5
Shaft Torque	T	18 Nm
Surface Pressure	p_m	12 kp/mm ²
Permitted Pressure	p_{max}	15 kp/mm ²

Table 3.10: Steering System Key-Flange Configuration

Hence, it is:

$$p_m \leq p_{max} \quad (3.34)$$

Description	Variable	Value
<i>M4 Bolt Type</i>		
Number of bolts	n	6
Force Of Shear Stress	F_p	515 N
Safety Factor	S	1.69

Table 3.11: Steering System Flange-Flange Connection

Since $S \geq 1.1$ the connection is rightfully designed. In conclusion, the design of first motor mounting and connection is finished and thus the next step is the construction of the CAD of the design which is demonstrated in Section 3.1.4.

Onto *the transmission motor mounting*, the same method is applied, facilitating it again in a cylinder casing that is connected with the arced beam while the casing is connected with the frame of the motor as instructed by the producer of the motor with the arrangement of six M4 bolts, as the two-dimensional design in Fig. 3.22 illustrates. The credibility of this design is dependant on the bolts connection which will be again associated with the safety factor on shear stress using the same methodology as before.

Description	Variable	Value
<i>M4 Bolt Type</i>		
Number of bolts	n	6
Force Of Shear Stress	F_p	833 N
Safety Factor	S_1	1.15

Table 3.12: Steering System-Wheel Motor Bolt Connection

As far as *the connection of the shaft motor with the wheel of the rover* a similar like configuration is going to be used. In more detail, this motor has an integrated flange attached on its shaft. Furthermore, this flange is connected at the frame of the wheels with $6 \times M4$ bolts. Fig. 3.22 presents this configuration.

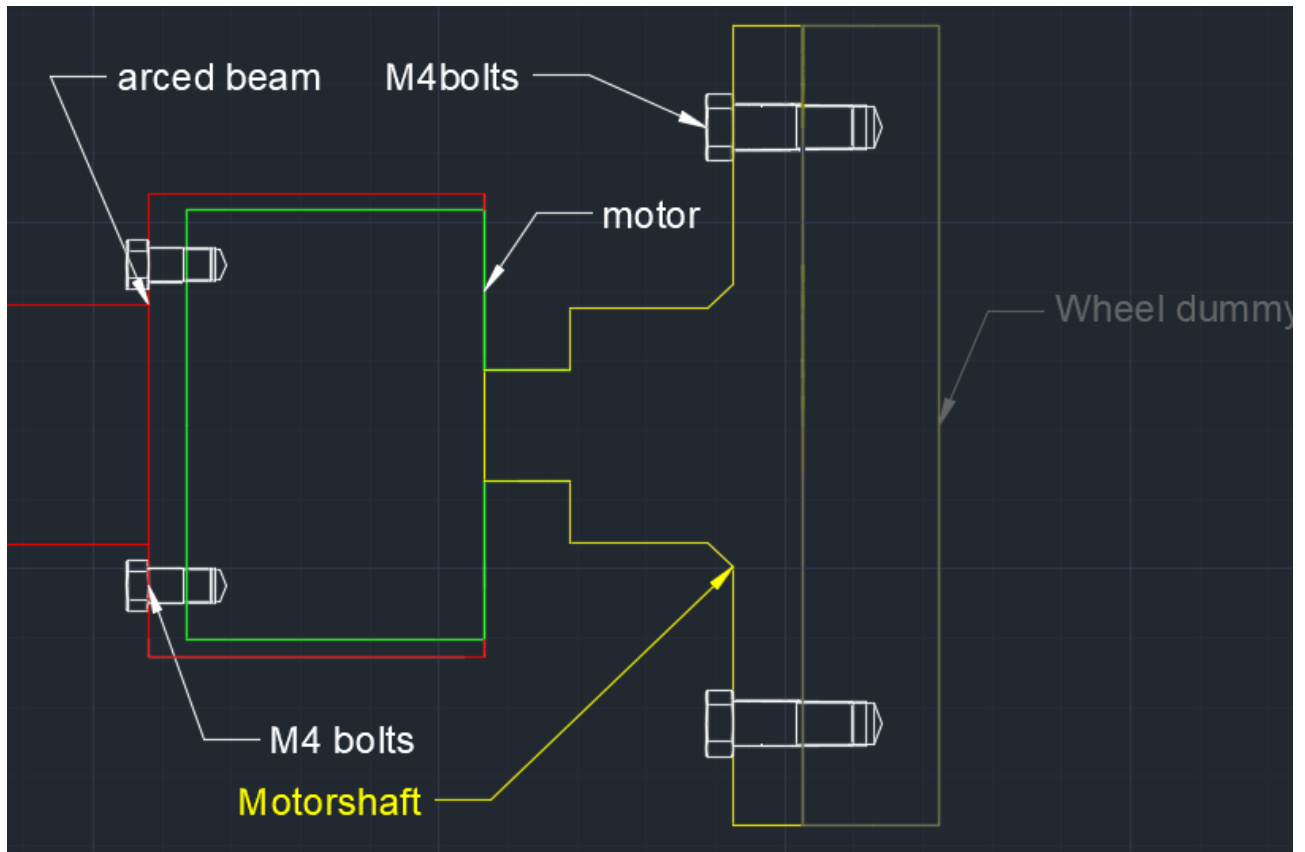


Figure 3.22: Wheel-Wheel Motor Configuration

The durability of this connection is valid if the safety factor of the flange-to-wheel connection is appropriate. This is going to be calculated with the same method as before. Thus, the results of this calculation are presented in Tab. 3.13.

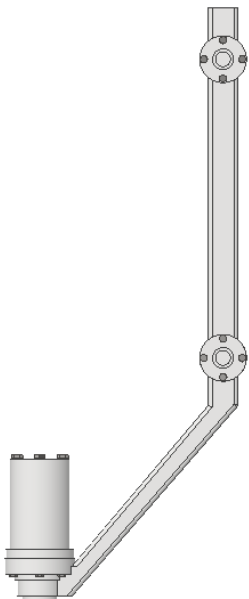
Description	Variable	Value
<i>M4 Bolt Type</i>		
Number of bolts	n	6
Force Of Shear Stress	F_p	793 N
Safety Factor	S_2	1.2

Table 3.13: Transmission Motor-Wheel Hub Bolt Connection

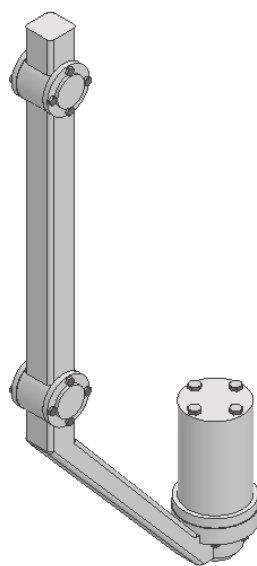
Hence, since $S_1, S_2 \geq 1.1$ both connections are rightfully designed. In conclusion, the design of the motor-to-wheel connection is successful and the next step is the construction of the CADs. Note that, the dimension depicted in the above images are not model representative and are used purely for reference.

Design Overview

The design can be seen in the following figures.

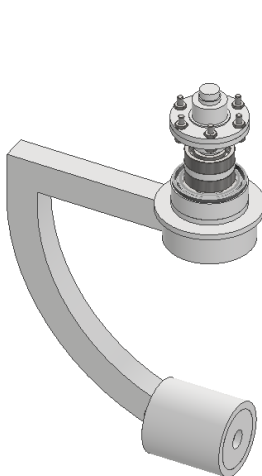


(a) Mobility Vertical Bar Final Design Isometric View

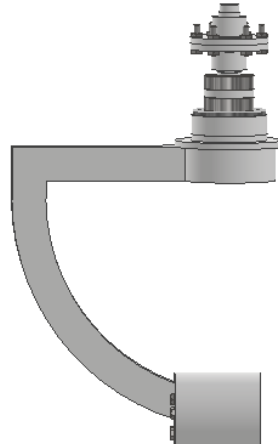


(b) Mobility Vertical Bar Final Design Front View

Figure 3.23: Mobility Vertical Bar Final Design

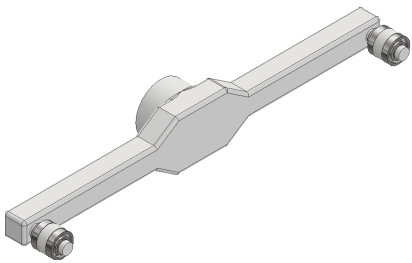


(a) Mobility Arced Beam Final Design Isometric View

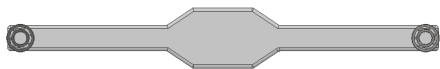


(b) Mobility Arced Beam Final Design Front View

Figure 3.24: Mobility Arced Beam Final Design

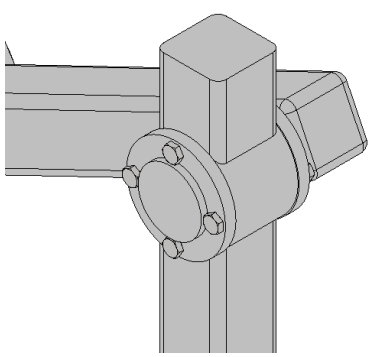


(a) Mobility Horizontal Beam Final Design Isometric View

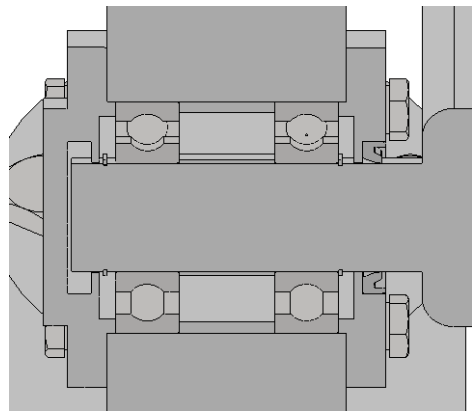


(b) Mobility Horizontal Beam Final Design Front View

Figure 3.25: Mobility Horizontal Beam Final Design

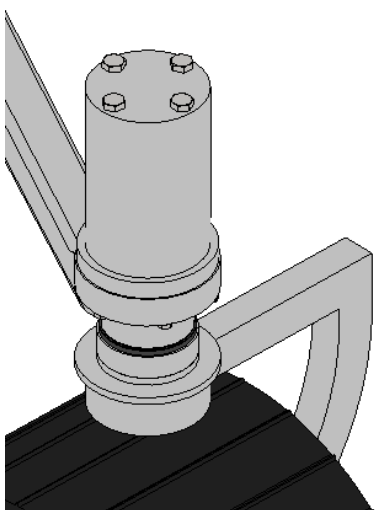


(a) First Joint Overview

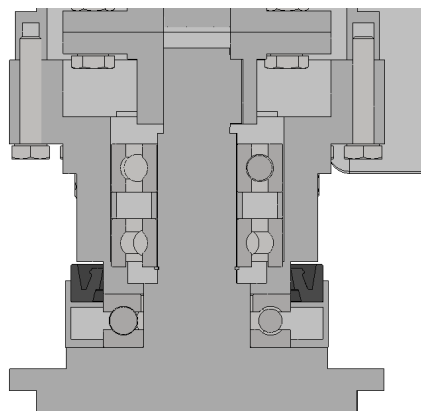


(b) First Joint Cross Section

Figure 3.26: Mobility First Joint

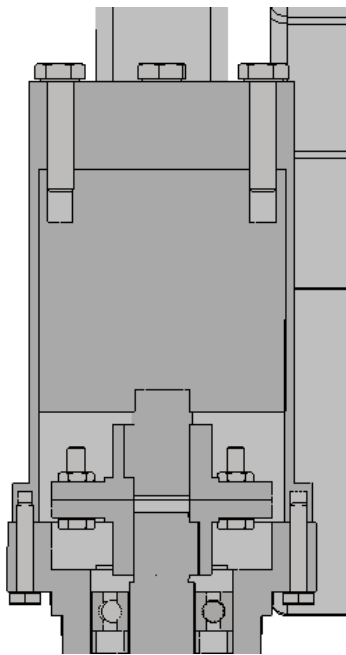


(a) Second Joint Overview

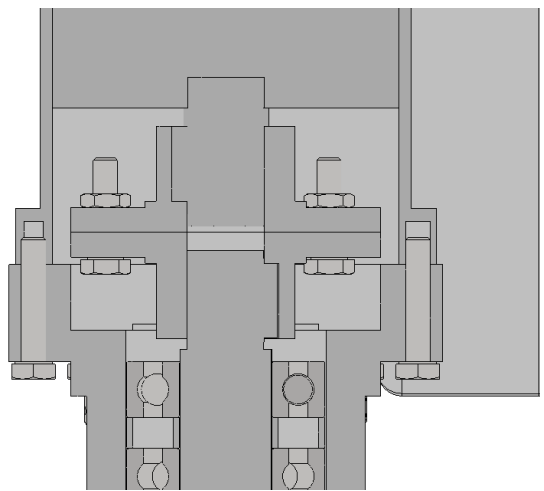


(b) Second Joint Cross Section

Figure 3.27: Mobility Second Joint



(a) Steering Motor Mounting



(b) Steering Motor Connection

Figure 3.28: Mobility Second Joint Steering Motor Configuration

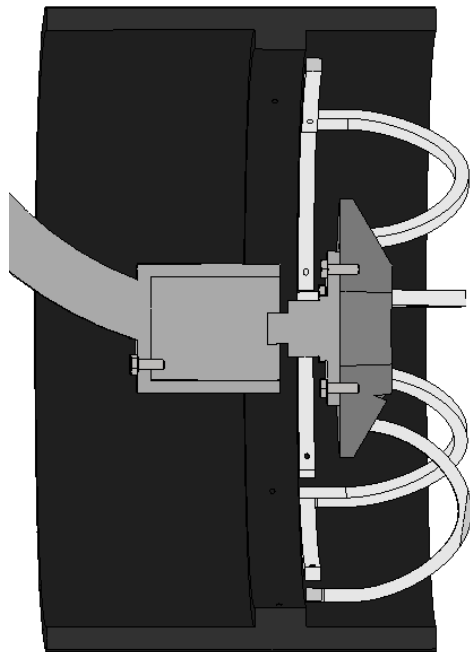
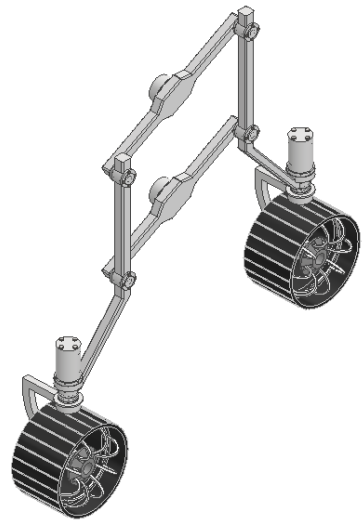
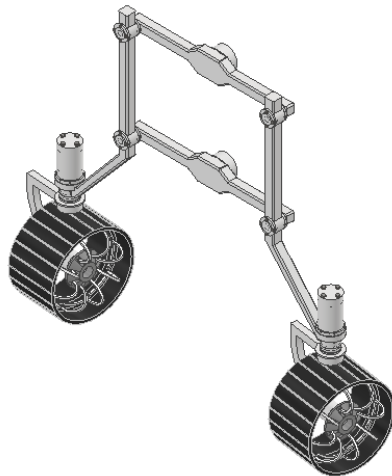


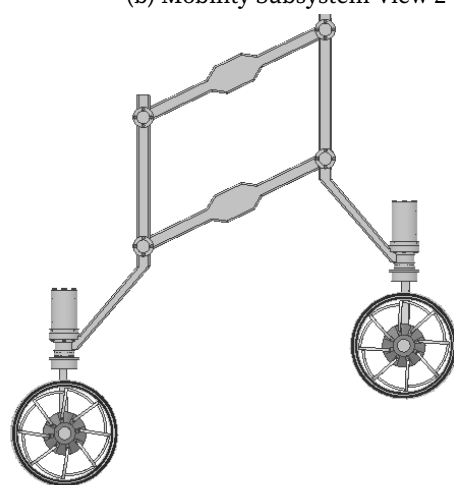
Figure 3.29: Wheel Motor Configuration



(a) Mobility Subsystem View 1

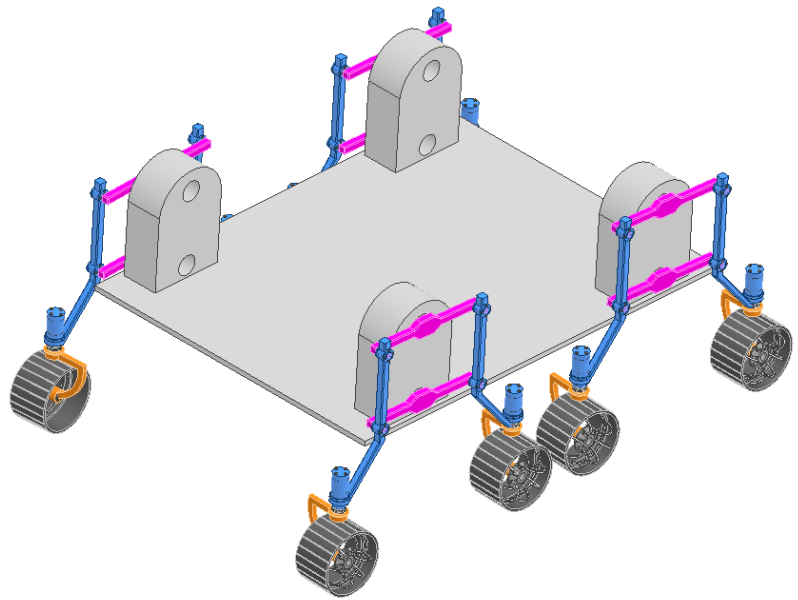


(b) Mobility Subsystem View 2

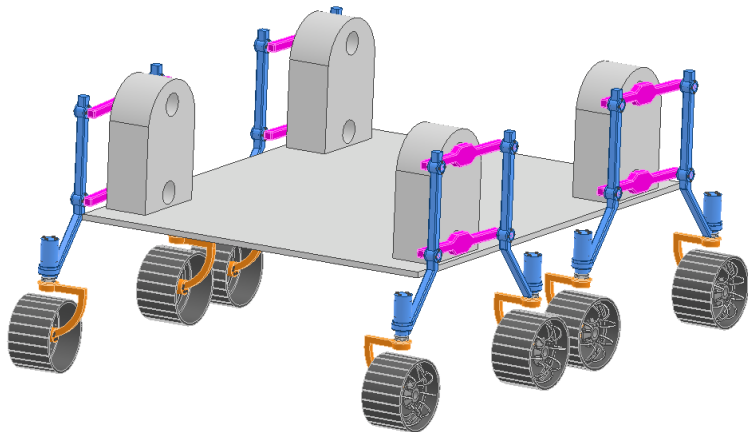


(c) Mobility Subsystem View 3

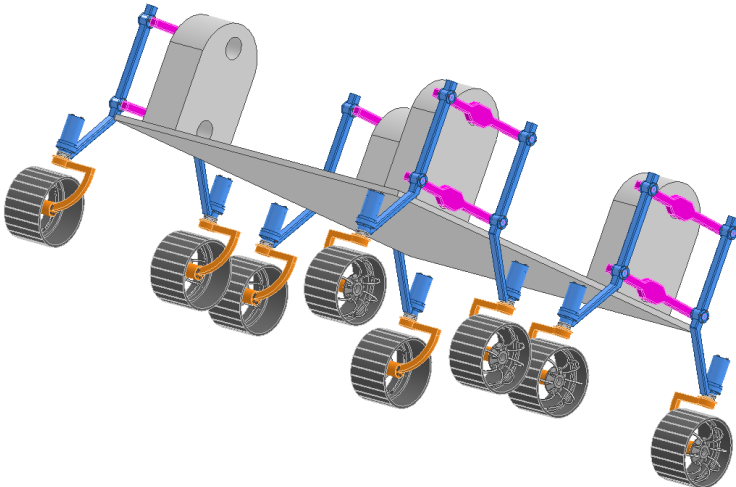
Figure 3.30: Mobility Subsystem Assembly



(a) Mobility Assembly View 1



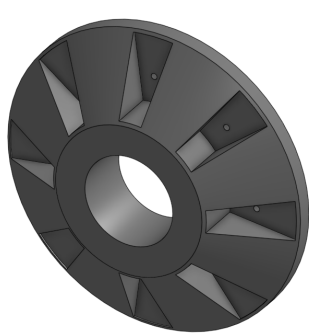
(b) Mobility Assembly View 2



(c) Mobility Assembly View 3

Figure 3.31: Mobility Assembly With Dummy Body

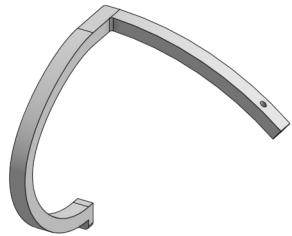
The *wheel design* was greatly inspired by the Perseverance Mission. The three dimensional wheel spokes allow the configuration to be almost fully rigid. The aluminum wheel tire is not hence able to deform due to the weight of the vehicle acting upon it. The wheel parts can be observed separately in Fig. 3.32 while the assembly in Fig. 3.33.



(a) Wheel Hub



(b) Wheel Tire

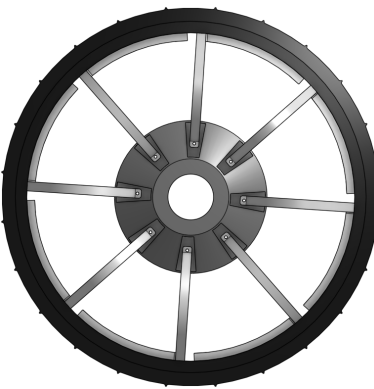


(c) Wheel Spokes

Figure 3.32: Wheel Parts



(a) Wheel Assembly Isometric View



(b) Wheel Assembly Front View



(c) Wheel Assembly Side View

Figure 3.33: Wheel Assembly

3.1.5 References

In the course of this project, several key references have been consulted to inform and substantiate our design decisions. The study on impact dynamics [1] has been instrumental in understanding the structural response to dynamic loads, shaping the approach to impact-resistant design. Additionally, insights from the work on vehicle design principles [3] have played a crucial role in guiding the conceptualization and development of this Mars rover's subsystems. Dr. Vouthounis' research [12] and its subsequent extension [13] have provided valuable perspectives on static analysis, enriching the understanding and influencing certain design considerations. Moreover, the efficiency calculations based on material data-sheets [15] have contributed to the impact loading analysis. Furthermore, Mr. Grekousis studies on Machine Elements and Machine Design in [4] proved instrumental for the calculation of the vehicle's mechanical connections. Lastly, the foundational principles outlined in Young's work on structural analysis [17] have been pivotal in ensuring the structural integrity and resilience of rover's Mobility Subsystem.

These references collectively form the knowledge backbone of our project, allowing us to draw upon established theories, methodologies, and empirical data to bolster the robustness and reliability of the current Mars rover mission design.

3.2 Body and Differential Subsystem

3.2.1 Overview

The function of this subsystem is the housing and connection of all of the other subsystems as well as the inclusion of a differential mechanism.

These roles are accomplished by the design of:

- A main body part, where all the other systems as well as any other necessary parts and equipment can be mounted on.
- A housing assembly, where the shafts of the horizontal rods of the suspension subsystems can be connected.
- The connecting parts where the aforementioned housing assembly can be mounted.
- A differential mechanism that accomplishes a specific relative motion between the front two sets of wheels, which will be explained further on.

The above objectives must be achieved in a way that complies with the conditions of the mission for which the project is destined, wherever that is feasible within our limitations considering industrial parts availability. The selected execution of these objectives will be checked through the use of the appropriate calculations.

3.2.2 Team dependencies

The body subsystem is the one with the highest need of communication and cooperation between the different teams since it is the only one that is directly attached with every other subsystem. Some of the specific relationships between each subsystem are listed below:

- The connection of the robotic arm on the surface of the main body part.
- The proper connection of the suspension system and the coordination of movement between this system and the differential mechanism, including the exact matching dimensions between the sets of wheels as calculated first in cooperation with the corresponding team.
- The appropriate mounting of the panel mechanism on top of the rover body in a way that conveniences both subsystems and doesn't cause any interference between other parts of the assemblies.

In addition to all of the aforementioned objectives, it was necessary to communicate properly about the proper distribution of forces and the equivalent calculations, which was rather challenging because the accumulated force applied on the parts of the body subsystem is depended on all of the other systems and is applied to every point of contact with each one of them.

3.2.3 Design

Main body

The main body of the rover is made by a single plate of machined aluminium. The dimensions of the solid aluminium plate are $2000 \times 1300 \times 5$ mm and the material is specifically aluminium alloy 6061 t6. This part went through a few revisions like, for example, a closed box design, where all the electronics and other important components would be housed, or open top box design. However, eventually it was decided that the simple plate was optimal as it was simpler, easier to construct and overall more efficient as a design choice. On the part of the main body have been made all the necessary configurations (holes etc.) to allow for the mounting of every other part, mainly with the use of bolt connections, and any additional sensitive components have been placed in housings on top of the main body's surface, in order to be protected by the martian environment, if that is deemed necessary.

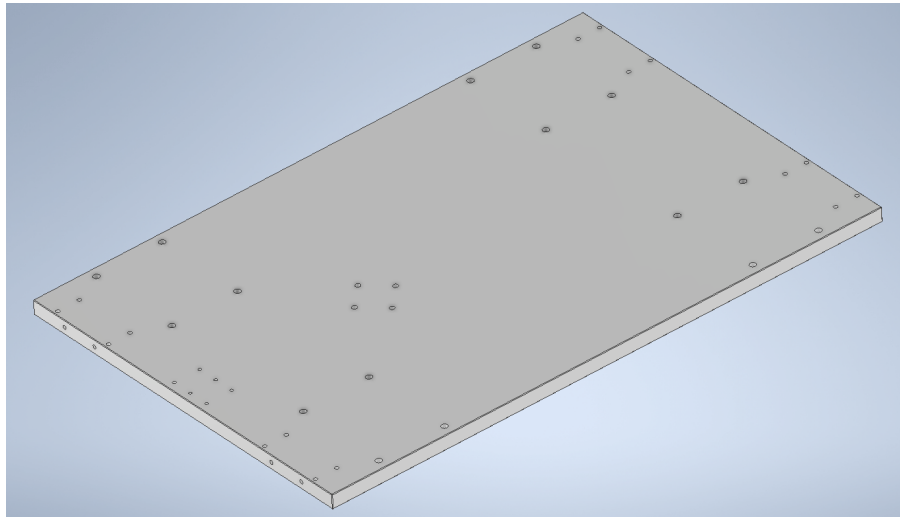


Figure 3.34: Main body plate

Suspension system connection

The suspension system is connected to the body of the rover through the horizontal rods, the ends of which connect to the vertical beams that eventually connect to the wheels. The design that was chosen houses the shafts that protrude through the middle of those rods. The housing is comprised by two tapered roller bearings, a lock nut, a seal and the custom designed housing for these parts. The specific choice and design of these parts is explained below.

- **Bearings**

Firstly, the inclusion of bearings is necessary as, in order for it to function at all, the horizontal rods of the suspension system need to rotate freely on the axis parallel to that system. The selection of the tapered roller bearings was based on the need for both axial and radial support of the suspension system. The rover is supposed to be able to move while tilting up to 30 degrees, which would apply a non negligible axial load to the bearings. The need to withstand a radial load is self-explanatory as they support the weight of the whole assembly. However, they are not put through any dynamic load as the rods are not meant to rotate constantly or in any notable speeds, so the load applied on them is considered static and the weight of the assembly is distributed across 16 of them so the choice may have been a bit overkill. The choice of the size was mainly based on the necessary diameter of the shaft ending which turned out to also be exaggerated so the size of the whole assembly should definitely be a lot smaller.

The specific bearings that were selected are the SKF 30310 and were picked through the catalogs in the website of SKF.



Figure 3.35: SKF 30310

- **Lock nut and seal**

The lock nut was the SKF KM10 and the seal was the SKF MS5 V. They were selected simply based on the dimension of the shaft and the bearings.



(a) SKF 30310



(b) MS5 V

- **Housing**

The housing of the aforementioned components was specifically designed for this assembly. The dimensions were calculated to secure the bearings properly and in the right distance for the correct function of the suspension system, where the shafts of the two horizontal rods are meant to seat right on top of each other and the right distance apart. In addition, configurations and holes were made to allow for the connection of the two parts of the housing as well as the mounting of the housing on the leg of the body, which eventually connects with the main part. The whole design of this housing was inspired by existing bearing housing designs with many changes to accommodate our special requirements, however eventually it was shown that an even more unusual concept could better suit our project.

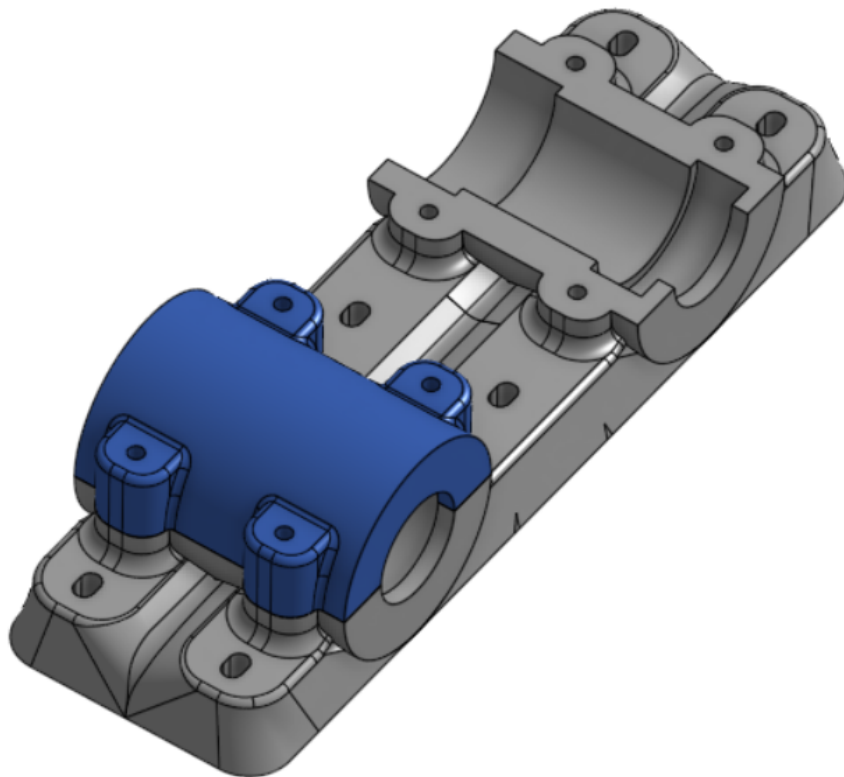
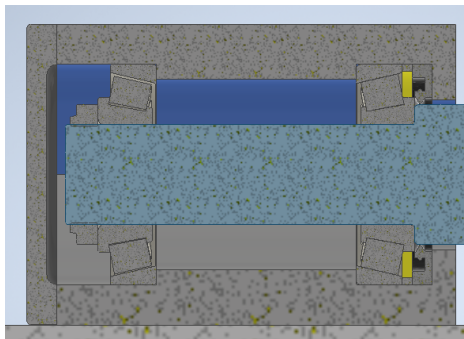


Figure 3.37: Housing design

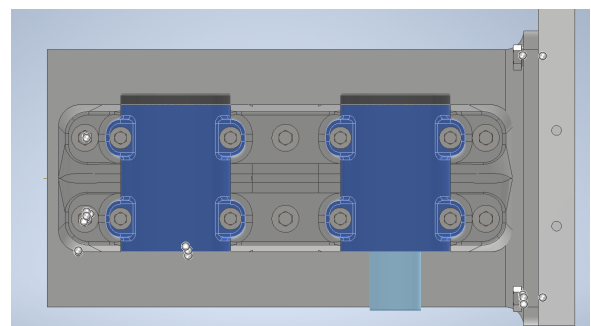
- **Assembly**

Firstly, the bottom part of the housing is bolted to the leg through the 6 holes shown above (Figure:3.37). The seal, spacer and bearings are inserted to the shaft with a loose fit as the inner ring of the bearing receives a force with standard direction. The assembly is placed in the bottom part of the housing, attempting a more tight fit as this part will be receiving forces with changing directions, although not that crucial since there is no constant rotation or dynamic loads applied. Finally, the top parts of the housing are placed and bolted on the bottom part through the four holes that exist for each cap, as shown above (Figure:3.37).

The screws used for the connection were DIN EN 24017 M12×90 and the washers were DIN EN ISO 7093-2 12.



(a) Housing assembly



(b) Bottom part connection

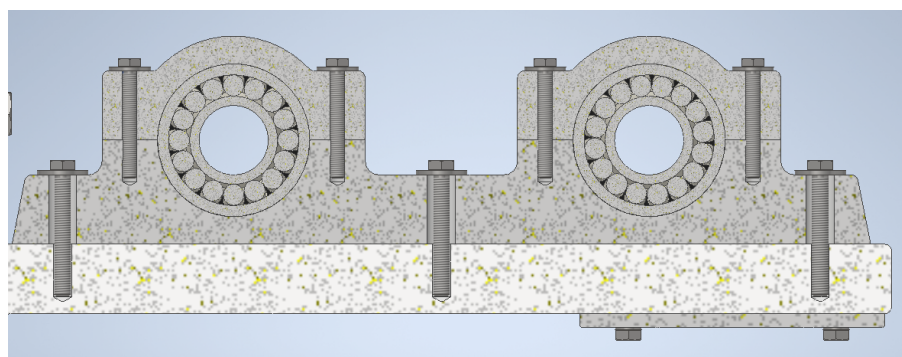


Figure 3.39: Full housing assembly and connection

Legs

The "legs" of the body are essentially four 50 mm thick solid aluminium plates designed to connect the main body and each of the housing assemblies. The bottom of the plates feature a base with four holes through which the legs are connected to the main body. On the side of the plate are six holes where the bottom part of the housing is mounted on, as explained above. The screws used for the mounting of each leg are four DIN EN 24017 M20×40 and the washers are four DIN 988 S22×30.

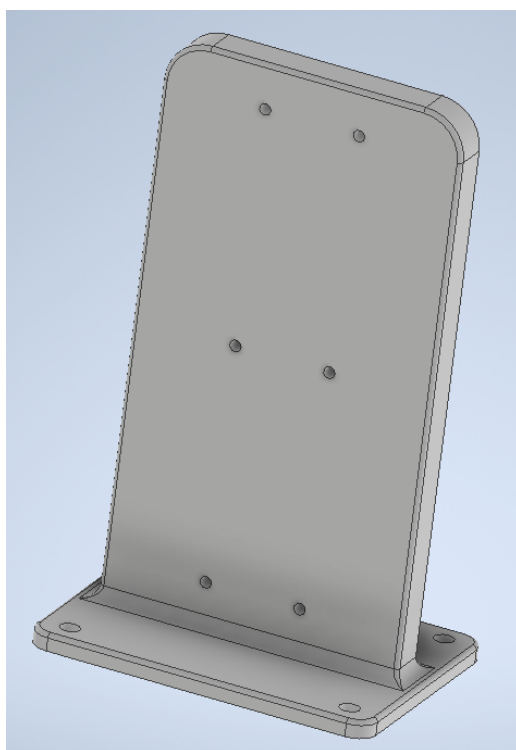


Figure 3.40: Leg

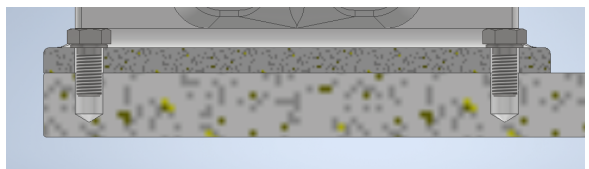
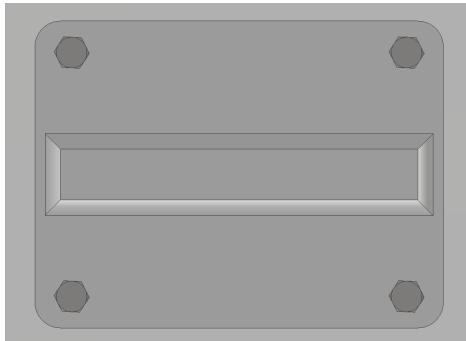


Figure 3.41: Leg connection

Leg support

The "leg support" is a part designed to provide additional support to the leg connection as it is the part connecting the whole assembly to the suspension system. The part consists of two 10 mm plates, each connecting to the main body and the leg respectively, and a hollow 5 mm thick tube that connects the two plates. The screws used for the connection are DIN EN 24017 M12×25 and the washers are DIN 988 S13×19 and there are four of them between the support piece and the leg and six of them between the support and the main body.

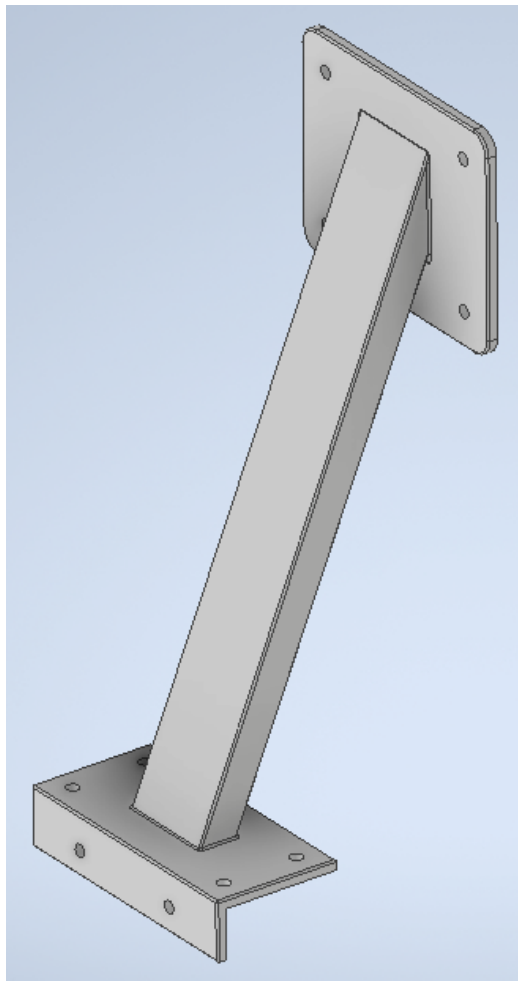
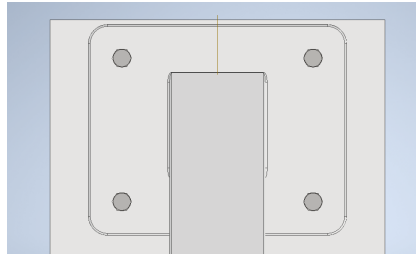
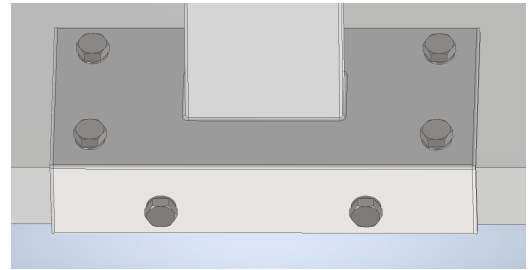


Figure 3.42: Leg support



(a) Support-leg connection



(b) Support-body connection

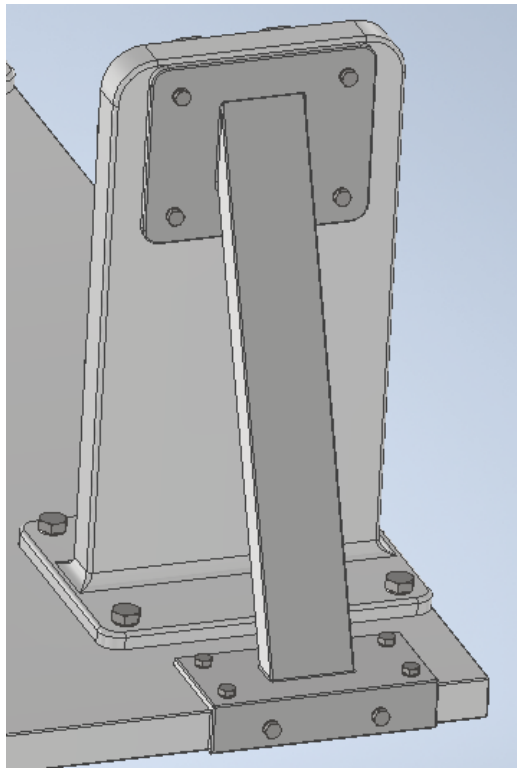


Figure 3.44: Support connection

Panel system connection

The panel deployment mechanism is simply mounted to the main body through a bolted connection with four screws in each "leg" of that assembly, as shown below. The screws used are 32 DIN EN 24017 M10×25.

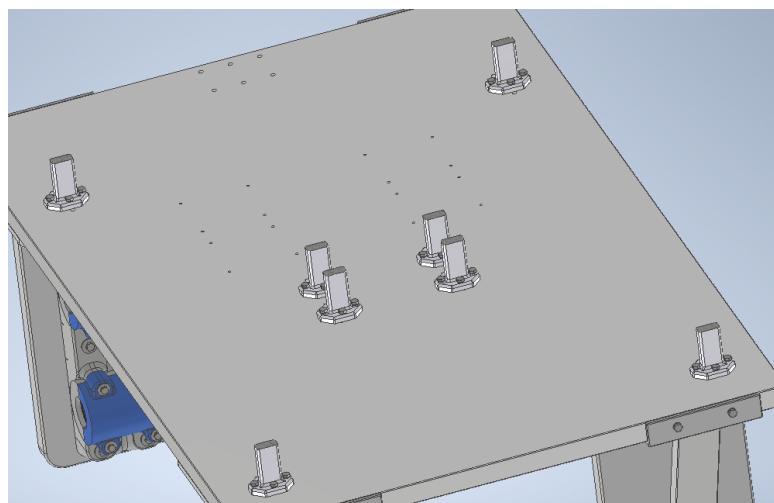


Figure 3.45: Panel connection

Arm system connection

The mounting of the robotic arm assembly is accomplished through another bolted connection at the front of the main body. The first part of the arm assembly slides onto the main body and is then screwed on by four M12 bolts.

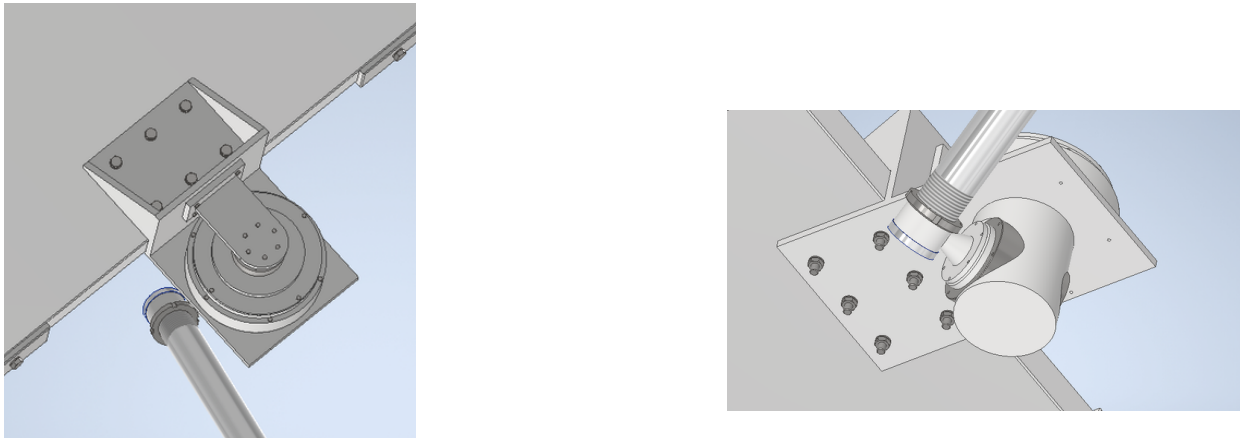
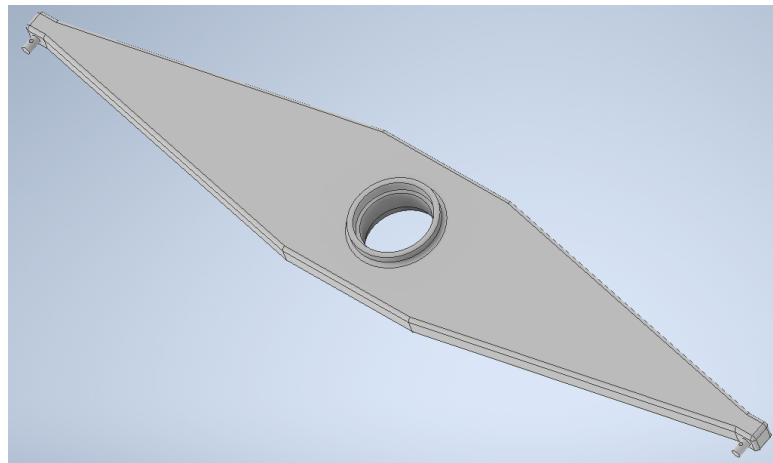


Figure 3.46: Arm connection

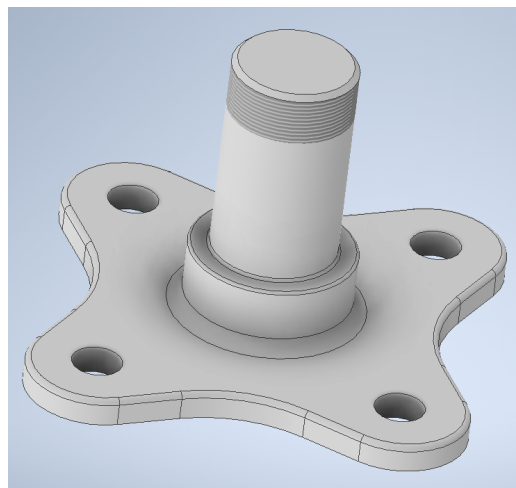
Differential mechanism

The differential mechanism is meant to accommodate the function of the suspension system. The design is inspired by the function of the rocker bogie mechanism, used in rovers designed by NASA ever since 1975 as well as other applications including railway tracks. However, there was an attempt to make a few modifications in order for the final design to differentiate from existing mechanisms. The differential system is comprised by the following parts:

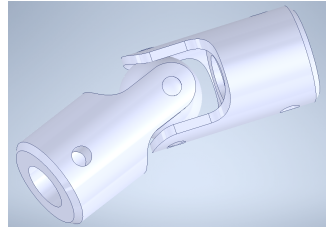
- The differential centre piece



- The shaft through which the differential system is mounted on the body



- Two deep groove sealed roller bearings (6309-RS1 SKF)
- A spacer
- A lock nut
- Two universal ball joint



- Two rods
- Two pins
- Two screws for the pins and four screws for the ball joint connections
- A configuration at the end of the suspension system shafts

Purpose

The purpose of the differential mechanism is to assist the mobility of the rover. It ensures that the two front sides of the mobility system move inversely, which means that when one of the two wheels of the right side of the rover moves up, the equivalent wheel of the left side moves down proportionally. The reason this is of assistance to the mobility of the system is that if, for example, one of the front wheels of the rover tries to overcome an obstacle that meets its path, then the opposite wheel will move down lifting the whole front up, thus assisting the rover to climb over the obstacle while keeping the body relatively level, contrary to tilting the whole body to the side. Therefore, it is able to move through rough and rocky terrains, like the martian surface, with ease and a low chance of turning on its side, which would be catastrophic for the mission.

Assemblies

- Below is shown how the centre piece connects with all the other parts that eventually end to the suspension system shaft

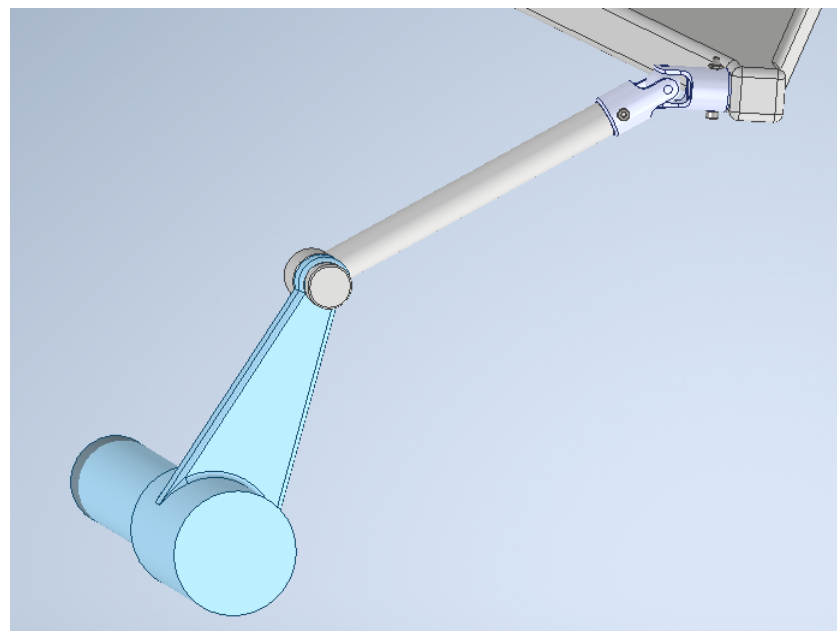


Figure 3.47: Centre piece - ball joint - rod - shaft assembly

-

- The two bearings are inserted onto the shaft and held in place by the configurations of the centre piece as well as the lock nut and the spacer. The centre piece is inserted between the two bearings in order for it to be able to rotate freely and receive radial loads by the connected suspension system. The shaft is mounted on the main body through a four screw connection.

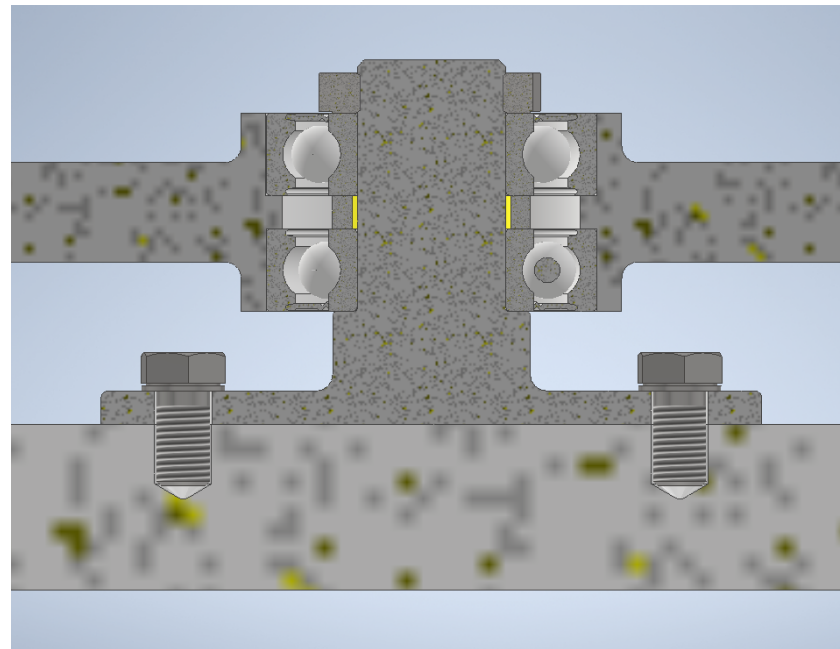


Figure 3.48: Shaft assembly

- This is how the whole differential system looks like when fully assembled

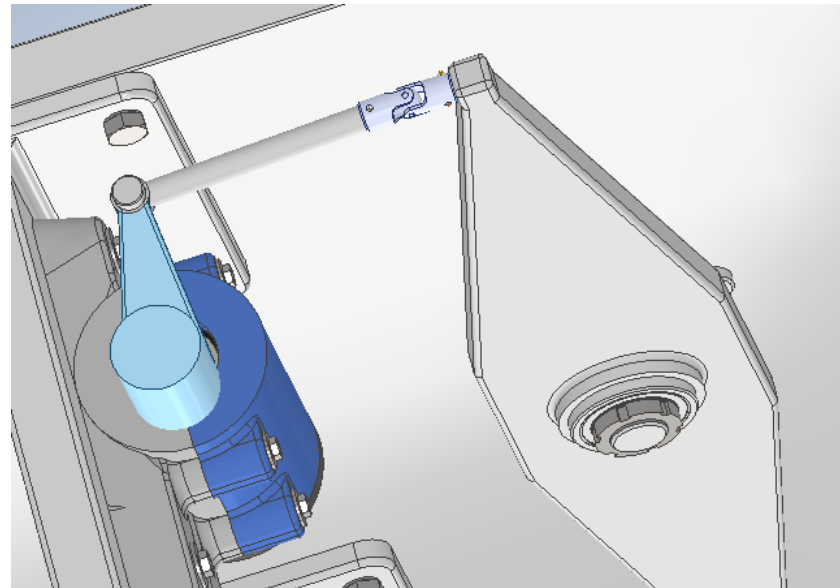


Figure 3.49: Differential assembly

3.2.4 Calculations

Housing connection screw calculation

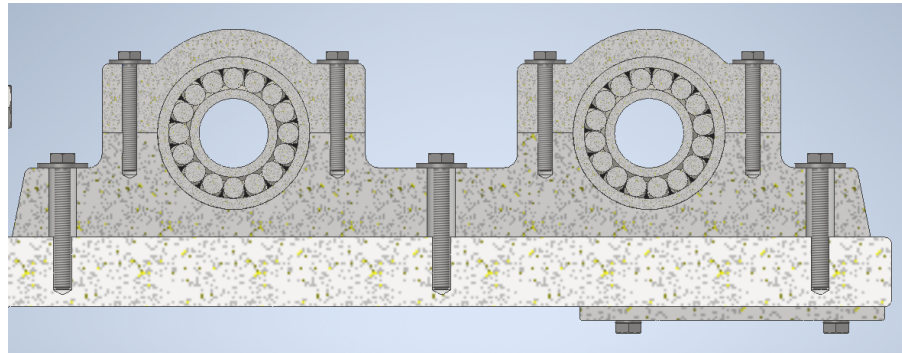


Figure 3.50: Full housing assembly and connection

The bolt connection pictured above is the one with the highest amount of tension applied on it as it holds the weight of every assembly apart from the suspension system which the rover sits on and it is, therefore, subject to a high amount of sheer force. For this reason, the endurance of the connection needs to be calculated.

The method used, similarly to earlier calculations, is calculating the safety factor of the connection as mentioned in [4]. As the bellow table illustrates the safety factor is found to be much bigger than the needed thus the given connection durability is certain.

Description	Variable	Value
<i>M12 Bolt Type</i>		
Number of bolts	n	6
Force Of Shear Stress	F_p	272 N
Safety Factor	S	14.7

Table 3.14: Housing bolts connection

Main body endurance calculation

The endurance of the main body plate needs to be calculated as the highest amount of force is applied on it due to the weight of the assembly. Firstly, the 3d problem is split into two 2d problems, in relation to each axis. The forces for each 2d problem are calculated using a free body diagram and then the method used for the final calculation is that of the MNQ diagrams.

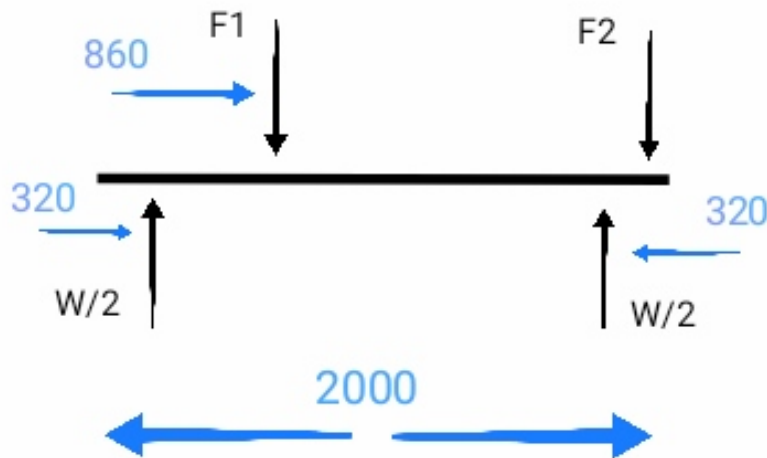


Figure 3.51: Free body diagram xz

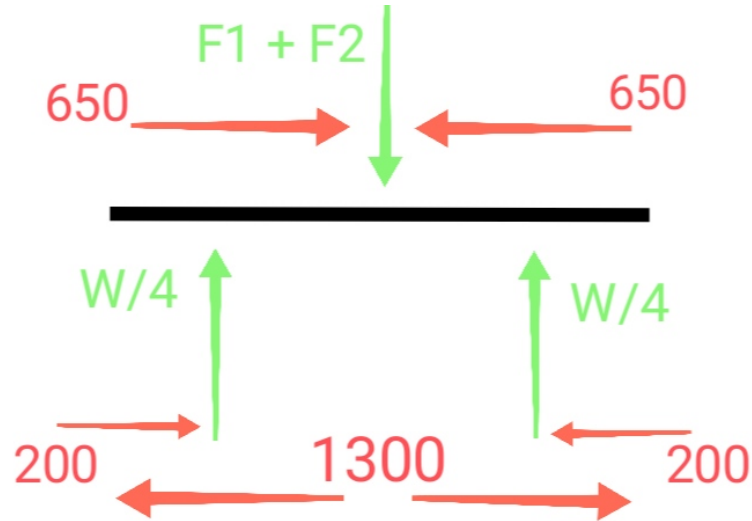


Figure 3.52: Free body diagram yz

- F1: The accumulated force applied by the panel system, which is approximated to be applied on only one point in the centre of the mount.
- F2: The force applied by the arm connection on the front of the body.

The result is the tension in the y axis being 0.66 N/mm^2 and in the x axis being 0.72 N/mm^2 , which concludes in the highest amount of resultant stress to be 1.3 N/mm^2 which is a lot lower than the limit of the chosen material. This result means that the selected thickness of the main plate was a lot higher than necessary and a lot of cost and weight could have been saved.

3.3 Robotic Arm Subsystem

3.3.1 Overview

The robotic arm is one of the most prominent features of the rover that allows the rover to explore the alien planet with much ease. It plays a critical role in discovering the martian environment because the various number of experiments and sampling that it can execute. As space exploration continues, robotic arms are expected to play an increasingly significant role. Future missions may involve more advanced robotic systems with enhanced capabilities. Being autonomous, it is a highly reliable and robust main subsystem. Its architecture mimics a human arm with a shoulder, elbow and wrist. The robot can perform a large range of movements with five degrees of freedom. Its elbow, wrist, and shoulder "joints" allow for optimal flexibility. The arm enables the rover to operate similarly to a human geologist by gripping and utilizing scientific instruments. The rover's tools are used to collect rock cores, capture microscopical photographs, and examine the mineral and elemental composition of Martian soil.

3.3.2 Team Dependencies

Teams are interconnected systems that work together to achieve a fully high quality Rover. These subsystems have dependencies on each other, as changes in one subsystem can have an impact on the functioning of other subsystem. The subsystems integration is crucial for the successful operation of the whole complex system. By understanding and integrating the individual subsystems, the larger system can function efficiently and effectively, meeting its intended purpose.

- *Robotic arm- Mobility System*

The rover's arm versatility is dependent on its interaction with the mobility subsystem. Its ability to traverse vast distances and explore diverse terrains allows scientists and researchers to gather data from different regions, as intended. The System is designed to provide traction and stability while navigating through the loose soil and rocks. This robust system allows the rover to traverse rough terrain by absorbing shocks and vibrations, ensuring that its delicate scientific instruments remain undamaged.

- *Robotic Arm- P.D.M.E.M.*

Without solar panels, the robotic arm would not have a reliable source of power, and without the robotic arm, the solar panels would not serve the purpose needs effectively. Therefore, both components must be designed and integrated carefully to ensure a successful operation. The solar panels need to be strategically placed to capture the maximum amount of sunlight, while also allowing enough space for the robotic arm to move and perform its tasks without obstruction under strict control.

- *Robotic Arm- Body* Because the robotic arm system is linked to the body, its collaboration with the main rover body subsystem is essential. The design and engineering features made in the robotic arm subsystem have a significant impact on the design of the body's front face. The robotic arm relies on the sturdy and stable chassis to provide a solid platform for its movements. The chassis plays a crucial role in maintaining balance and stability while the robotic arm is extended and performs various tasks.

3.3.3 Subsystem Management

However, to maintain its versatility and efficiency, the robotic arm have certain constraints that limit their capabilities, which have to been overcame, such as:

- Limited range of motion. The robotic arm is designed with specific joints and degrees of freedom, which restrict its movements. This can make it challenging for them to perform tasks that require complex and precise movements.
- A power source to operate. Its requirements can be a constraint in the harsh conditions of the Mars.
- Physical constraint of payload weight. This refers to the maximum weight that the arm can lift and manipulate without compromising its stability or performance. The size and strength of the arm's motors and joints will determine its payload capacity.

All of these constraints must be taken into consideration, from the team, when designing the robotic arm to ensure its efficient and safe performance. Other than that, static analysis will be performed on the subsystem after design to verify the structural safety factor of the robotic arm. A static analysis of the entire subsystem can be found in Section 3.3.4. The analysis is carried out for the scenario in which the hand is constructed on the rover's body under the influence of Mars gravity.

3.3.4 Conceptual Design

Background Study

Robotic arm is charged with the handling of the payload, which means that they are employed for precise and highly valuable missions. The five motors configuration achieves a wide area of physically interaction with Mars terrain. They enable a high maneuverability, despite that the rover remains stable, ensuring its safety and low energy consumption. Moreover the sensors of the payload are favored by the precise reorientation and reposition, giving them the chance to do immediately multipurpose sampling tests.

Motor Torque Calculation

The motors torques for the moving parts of the robotic arm has to be calculated. In order to achieve that, a mass budget of the robotic arm parts has been constructed. This can be seen in the following figure.

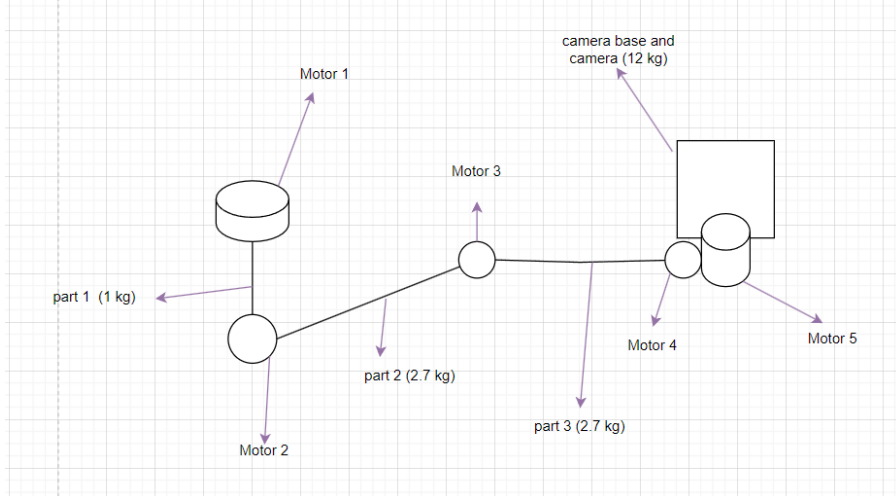


Figure 3.53: Robotic Arm Mass Budget

Below the Free Body Diagrams of each part along the robotic arm are simply portrayed, starting with the payload base.

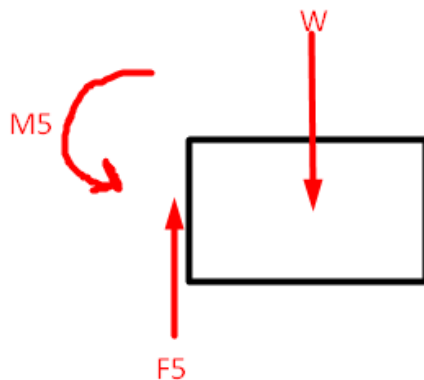


Figure 3.54: Free Body Diagram Of Payload

$$g_{mars} = \frac{9.81}{3} m/s^2$$

$$W_{payload} = m_{payload} \cdot g_{mars} = 12 \cdot \frac{9.81}{3} = 39 N$$

Thus, the applied force at the tip of the arm is:

$$F_5 = 39 N$$

Furthermore, assuming that the length of the base is 0.2 m, the torque of Motor 4:

$$M_5 = 39 \cdot 0.1 = 3.9 Nm$$

Besides that assuming, the length of part 3 and part 2 (see Fig. 3.53) is 0.5 m, and the weight of part 3 is $w_{lower} = 2.7 \text{ kg}$ respectively, the worst case scenario is for the parts to be horizontal. The Free Body diagram of part 3 can be seen in Fig. 3.55

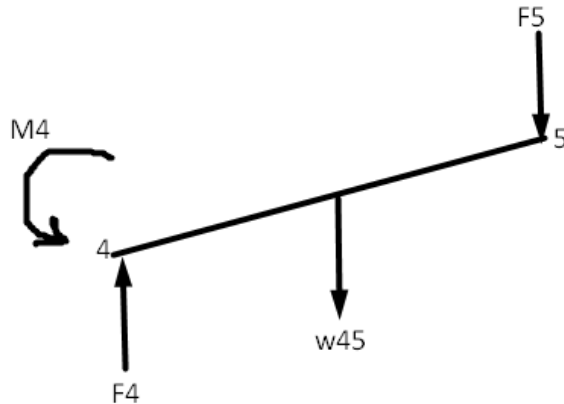


Figure 3.55: Free Body Diagram of Lower Arm

$$F_4 = F_5 + w_{45} = 47.829 \text{ N}$$

So, the torque calculation for Motor 3:

$$M_4 = w_{45} \cdot \frac{l_3}{2} + l_3 \cdot F_5 = 20.5 \text{ Nm}$$

Similarly, the Free Body Diagram for Part 2(Lower Arm) is seen below:

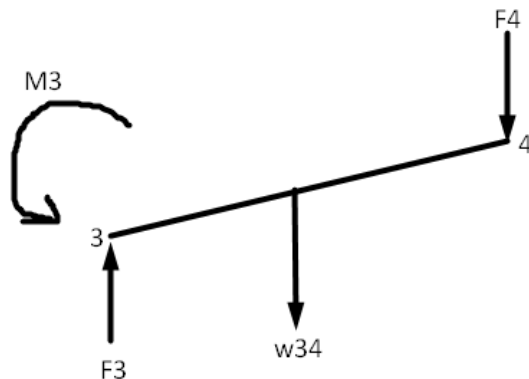


Figure 3.56: Free Body Diagram of Lower Arm

$$F_3 = w_{34} + F_4 = 56.658 \text{ N}$$

Consequently, the torque of Motor 2:

$$M_3 = w_{34} \cdot \frac{l_{34}}{2} + F_4 \cdot l_{34} = 26.1 \text{ Nm}$$

The Free Body Diagram of part 1 is the following figure:



Figure 3.57: Free Body Diagram Of Part 1

$$F_2 = F_3 + w_{23} = 60 \text{ N}$$

Continuing the static analysis, in order to calculate the torque of the motor in point 2, the angular acceleration $a = 1 \text{ m/s}^2$ is assumed. The diameter of part one is $d = 50 \text{ mm}$. The torsional moment that the motor should will be calculated by:

$$M_t = I \cdot a$$

$$I = \frac{1}{2} \cdot m \cdot \frac{d^2}{4} + \frac{1}{12} \cdot m \cdot l_{34}^2 + \frac{1}{12} \cdot m \cdot l_{45}^2 + m_{camera} \cdot (l_{34} + l_{45} + l_{base})^2 = 17.73 \text{ kgm}^2$$

Finally the torque of Motor 1:

$$M_t = 17.73 \text{ Nm}$$

Nevertheless a motor could be damaged or blocked by the control system for various reasons. Assuming that motor 3 and motor 4 do not function, then torque of motor 2 needs to be:

$$M \geq 26 \text{ Nm}$$

$$M_3 = w_{35} \cdot \frac{l_{35}}{2} + w_{camera} \cdot (l_{35} + \frac{l_{base}}{2}) = 52 \text{ Nm}$$

This means that the motor that will be chosen should overcome the 52 Nm torque barrier.

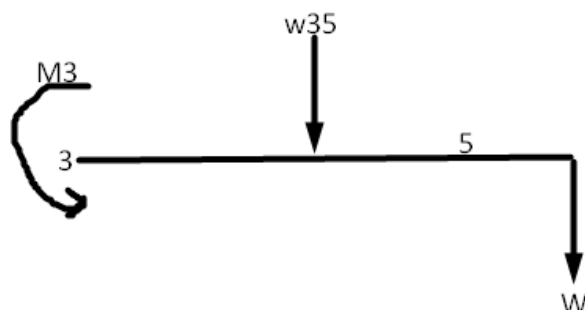


Figure 3.58: Free Body Diagram of Motor 3 to the Tip

Assuming that Motor 4 does not function. In that scenario, Motor 3 should apply greater torque than.

$$M_2 = w_{45} \cdot \frac{l_{45}}{2} + w_{payload} \cdot (l_{45} + \frac{l_{base}}{2}) = 26 \text{ Nm}$$

Hence, the motor that will be chosen should overcome the 26 Nm torque barrier.

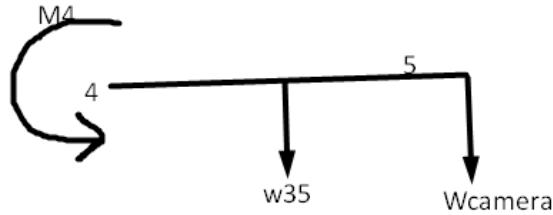
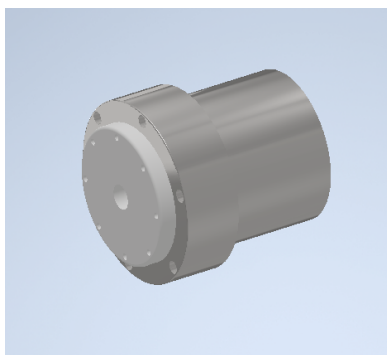


Figure 3.59: Free Body Diagram of Assembled Payload and Lower Arm

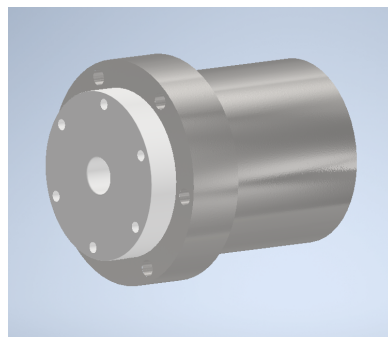
Choosing the Proper Rotary Actuators

Object of this design is to simulate a fully working human hand to carry out the desired scientific goals on Mars with a five degrees of freedom robotic arm. The five motors design allows the arm to move in numerous axes and planes. As shown in Fig. 3.53 above, Motor1 provides movement in the horizontal plane, Motor 2 and Motor 3 enable the upwards and downwards movement of the two arm parts and finally the dual link at the tip of the arm can combine both the vertical and horizontal transition.

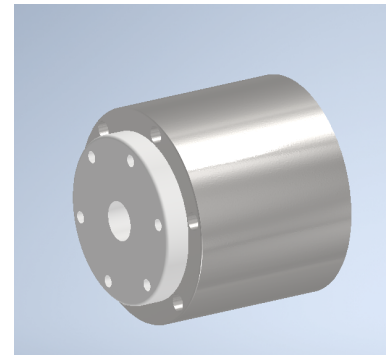
The five in total motors implies a sufficient energy demands. Assuming that the rotary speed is 4 RPM and their minimum torque is analyzed in 3.54 each motor wattage is calculated by the below formula: The rotary actuators must combine high torque output, low RPM speed, and low energy consumption, mass and volume as well. From the top of the arm to the tip the torque requires for decrease, so the sizing do. Each motor complies with the best industrial standards for robotic applications.



(a) 110mm Actuator



(b) 80mm Actuator



(c) 70mm Actuator

Figure 3.60: Robotic Arm Actuators

Data and more information about the above actuators are [here](#):

Model	eRobot1000 (V4)				
Strain wave gear-ratio	25-50	25-60	25-100	25-120	25-160
Peak torque for start and stop(Nm)	127	178	204	217	229
Permissible max.value at average load torque(Nm)	72	113	140	140	140
Rated torque(Nm)	51	62	87	87	87
Permissible maximum momentary torque(Nm)	242	332	369	395	408
Max. output rotational speed(RPM)	60	37.5	30	25	18.75
Motor power(W)	600				
Strain wave gear output inertia(kg-mm²)	-				
Strain wave gear output mass(KG)	-				
Outer diameter*length	110*115.2mm				

(a) 110mm Actuator Stats

Model	eRobot8000			
Strain wave gear-ratio	17-50	17-80	17-100	17-120
Peak torque for start and stop(Nm)	44	56	70	70
Permissible max.value at average load torque(Nm)	34	35	51	51
Rated torque(Nm)	21	29	31	31
Permissible maximum momentary torque(Nm)	91	113	143	112
Max. output rotational speed(RPM)	60	37.5	30	25
Motor power(W)	140			
Strain wave gear output inertia(kg-mm²)	150085			
Strain wave gear output mass(KG)	0.25			
Outer diameter*length	80*94.2mm			

(b) 80mm Actuator Stats

Model	eRobot7000		
Strain wave gear-ratio	14-50	14-80	14-100
Peak torque for start and stop(Nm)	12	16	19
Permissible max.value at average load torque(Nm)	4.8	7.7	7.7
Rated torque(Nm)	3.7	5.4	6.4
Permissible maximum momentary torque(Nm)	23	35	35
Max. output rotational speed(RPM)	60	37.5	30
Motor power(W)	75		
Strain wave gear output inertia(kg-mm²)	64030		
Strain wave gear output mass(KG)	0.13		
Outer diameter*length	70*90.4mm		

(c) 70mm Actuator Stats

Figure 3.61: Robotic Arm Actuators Stats

Taking into consideration the minimum required torque the motors should have and the rated torque of 110mm, 80mm, 70mm actuators, it has been decided that the 80 mm actuator will be chosen for motor 1 and 3, the 110 mm actuator will be chosen for motor 2 and the 70 mm actuator will be chosen for motor 4 and 5.

Motor electricity supply can be external applying flex cable system. The developed cabling system for the robotic arm is unique in that it spans from the rover bulkhead to the instrument turret in one piece, transmitting voltage and signals.

The five in total motors implies a sufficient energy demands. Assuming that the rotary speed is 4 RPM and their minimum torque is analyzed in 3.54 each motor wattage is calculated by the below formula:

$$W = M_m \cdot \frac{2 \cdot \pi \cdot RPM}{60} \quad (3.35)$$

This way the input needed wattage is:

Motors	Wattage (W)
$Motor_1$	8.8 Watt
$Motor_2$	21.7 Watt
$Motor_3$	8.8 Watt
$Motor_4$	1.5 Watt
$Motor_5$	1.5 Watt
Total Wattage (W)	42.3 W

Table 3.15: Total Arm's Wattage

Design Overview

The design can be seen in the following figures.

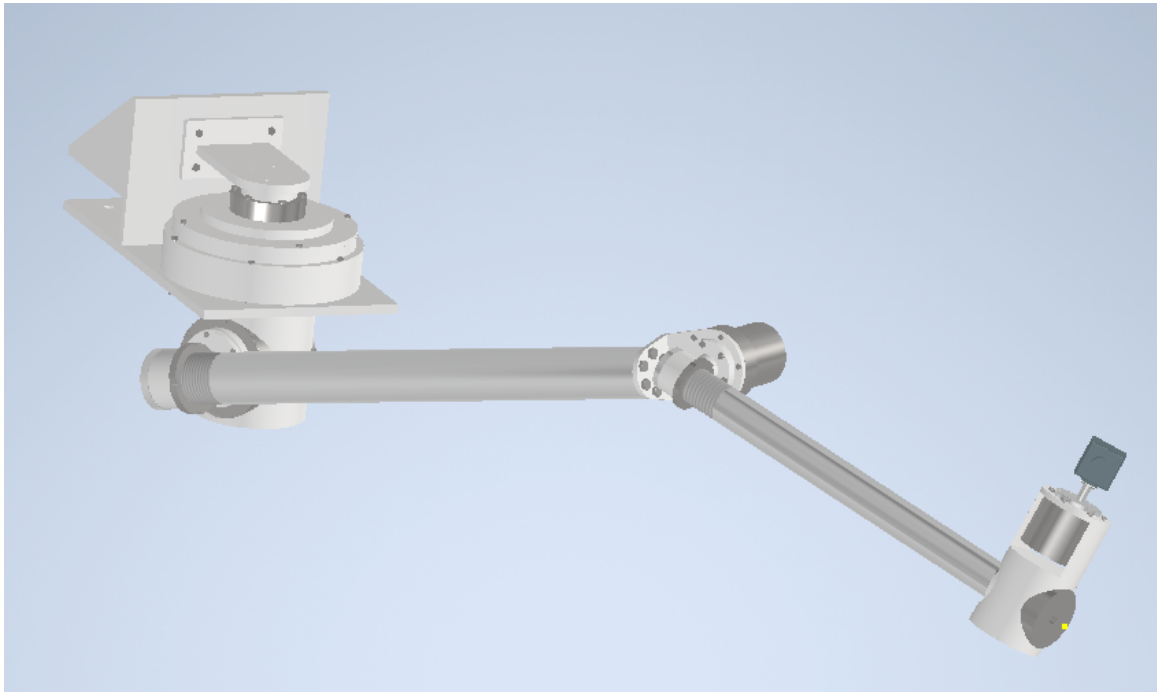


Figure 3.62: Robotic Arm Assembly

The above figure illustrates the 1.2 meter length assembled robotic arm, which weights approximately 27 kilograms. Each part will be analyzed below, from the "shoulder" to the tip.

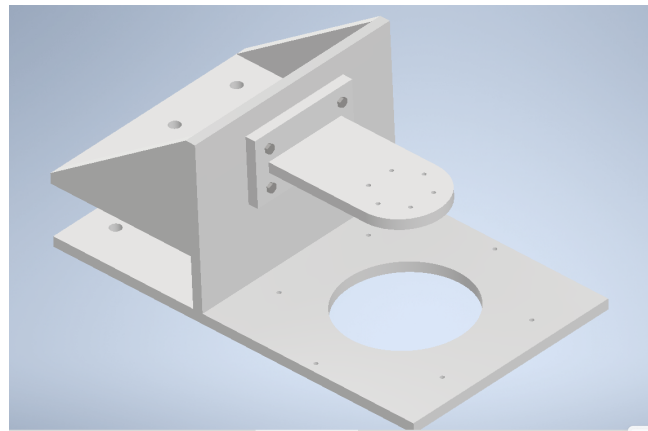
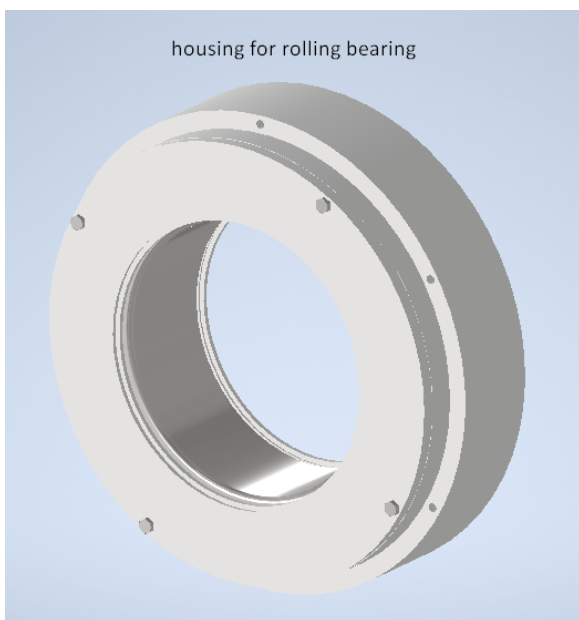
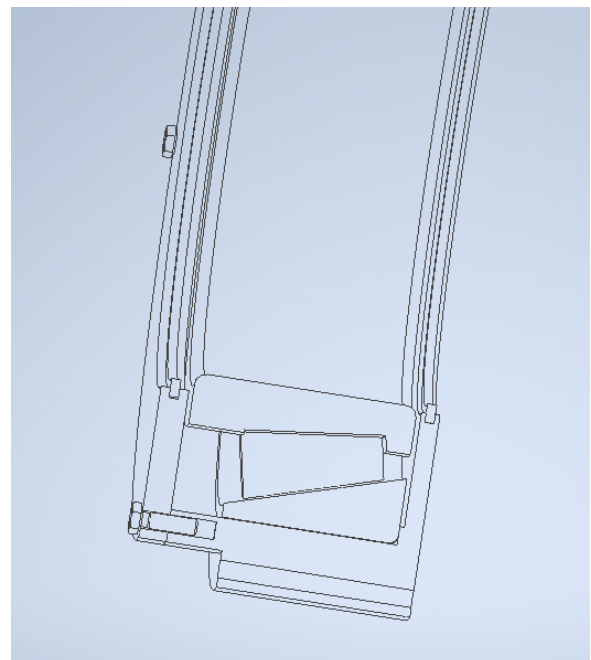


Figure 3.63: Rover Body And Arm Connecting Structure

The role of this structure is the main mounting of the arm to rover body. Moreover it enables the horizontal steering and, in collaboration with the bearing, lifts a major part of the gravitational forces. The part, which is joined with bolts, which stabilizes the motor's inner part, will be placed in its position, after the placing of the bearing housing and the rod assembly.



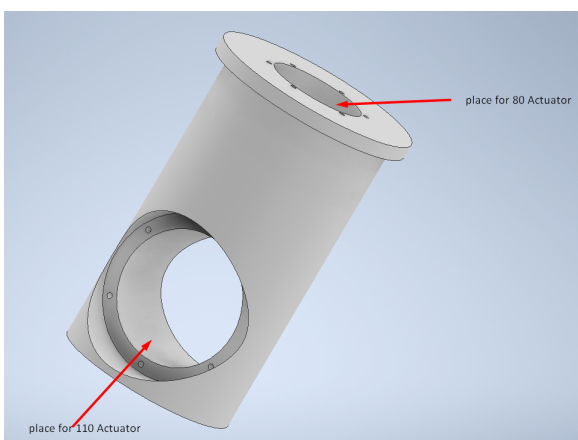
(a) Housing With Bearing Geometry



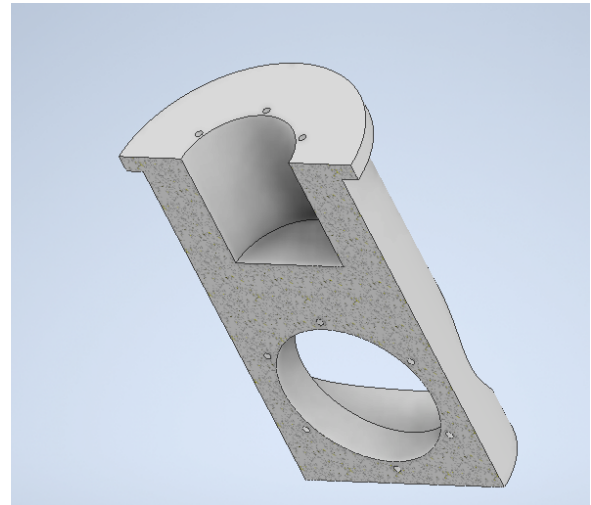
(b) Housing With Bearing On Section View

Figure 3.64: Housing With Bearing

Purpose of the housing is the sealing and the protection of the bearing. It is consisted of two shells, joined with bolts, and two sealing rings in the upper and lower bearing's outer surface. A 2D sketch shows more details and information about this assembly.



(a) Connecting Rod of Actuators 80 mm and 110 mm



(b) Rod's Section View

Figure 3.66: Actuators Housing 1

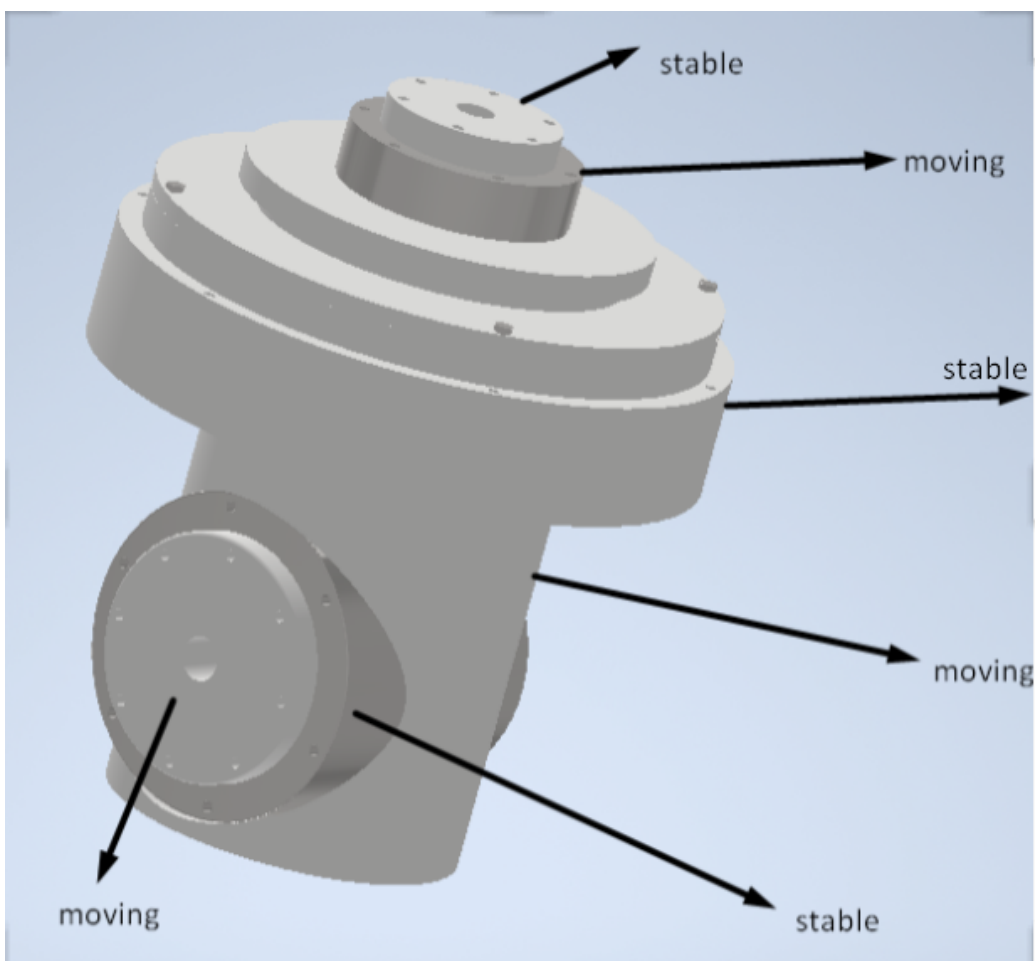


Figure 3.65: Sub-Assembly Of Part 1

This rod connects the two actuators, which are mounted in the holes, combining their perpendicular axes and the movement in two planes, playing the role of a alt azimuth steering mechanism. The lower surface of the flat extruded "ring" of the rod is in contact with a spacer. The spacer, in the other side, is in contact with the inner ring of the bearing.

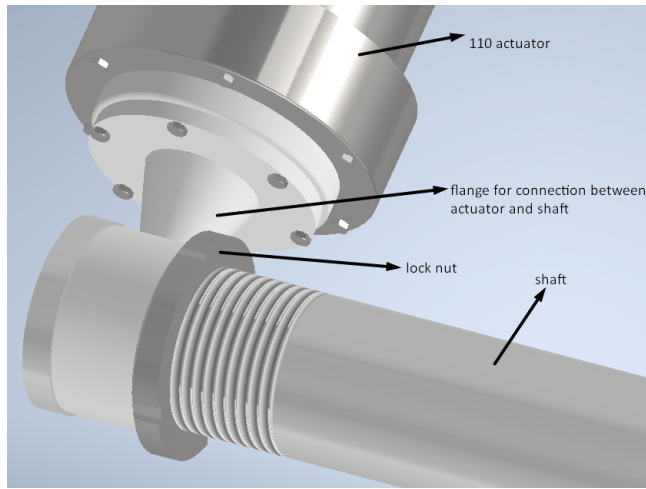


Figure 3.67: Linkage Between 110 Actuator and Upper Arm

The upper arm is being reliably stabilized, inside a joint, which is between a graduation and a lock nut, tightened with the help of the tread.

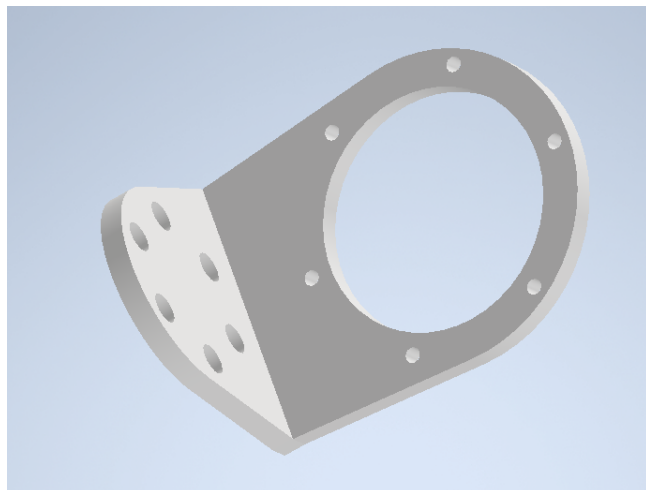


Figure 3.68: flanged connection between part 2 and stable part of the 80 actuator

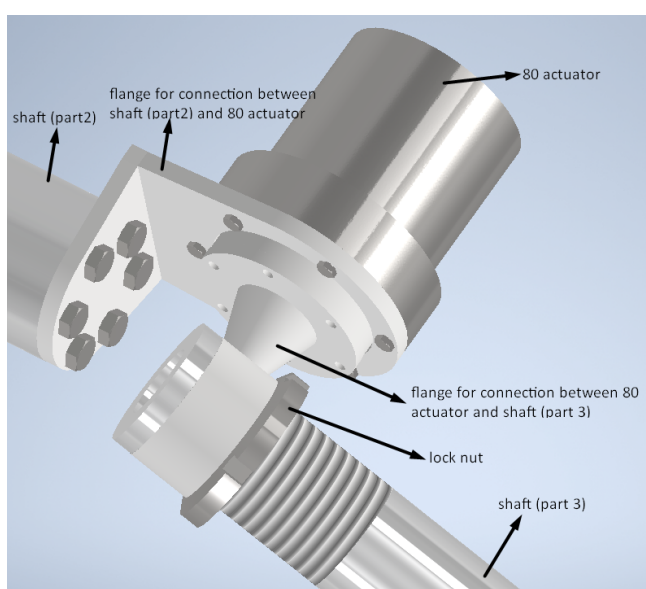


Figure 3.69: Connection Between Upper-Lower Arm and 80 Actuator

As is shown in the above figure a flange links the upper arm with the outer actuator's part, which remains stable. The inner part is connected with a joint, where the lower arm is being stabilized, as the design that has been analyzed above.

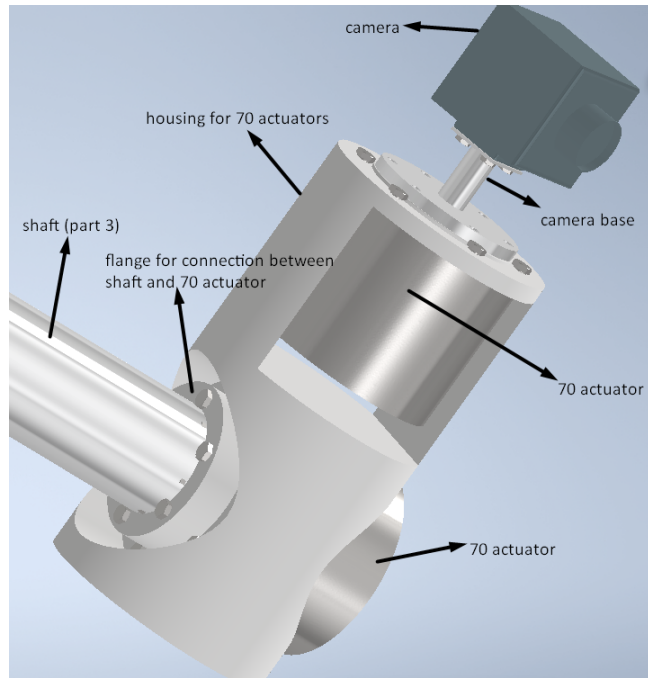


Figure 3.70: Connection of 70 Actuators and Payload

The tip of the lower arm accommodates a rod, where it encompasses the two actuators, similar to the design above?? which re orientate with precision the payload.

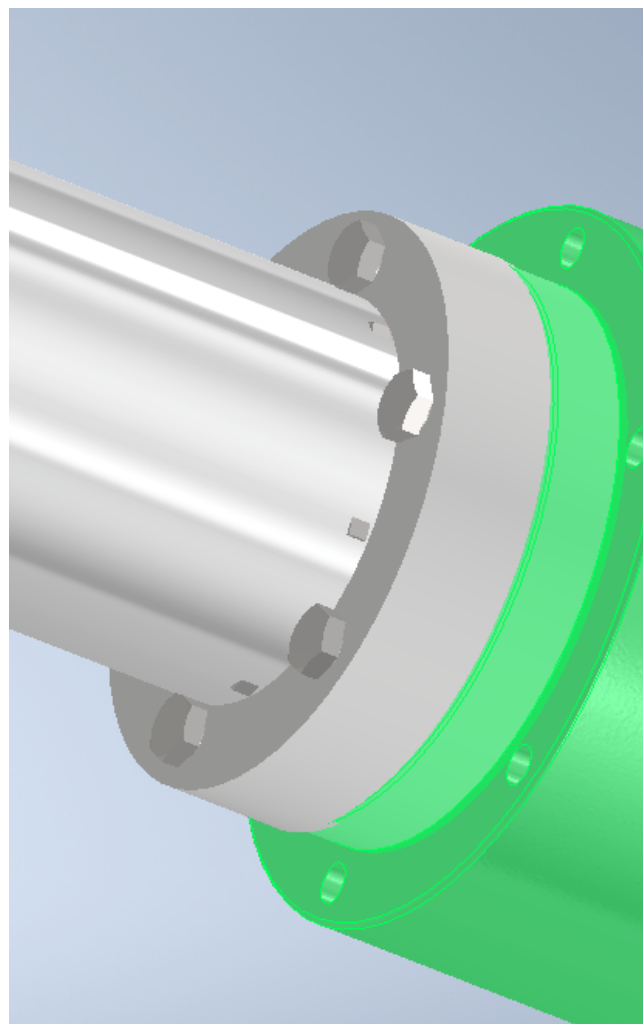


Figure 3.71: Connection of Lower Arm and 70 Actuator

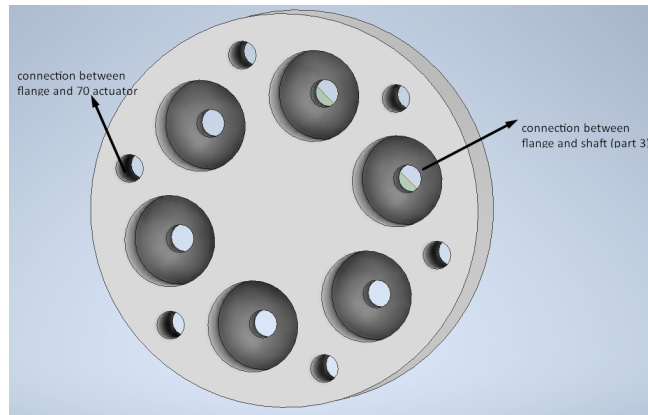


Figure 3.72: Connecting Flange of Lower Arm

The flange role is to attach the Lower arm with the actuator. The upper surface has holes with changing diameter along the depth, to house the head of the bolt in a lower plane, guaranteeing a flat surface. The bolted joint between the actuator and the flange uses the remaining holes.

Calculation of Subsystem's Parts

Bolt connections

Assuming that the preferred safety factor for shear forces is $S = 1.5$ and friction coefficient is 0.12 and taking into consideration the torques that each actuator should overcome the required tightening force and tightening torque can be calculated as [4] and can be shown in the following equations:

$$\bullet \quad F_{tightening} = \frac{F \cdot S}{\mu}$$

(Tightening force applied in bolt connection)

$$\bullet \quad F = \frac{M}{\frac{d}{2}}$$

(Shear force applied in bolt connection)

Combining the previous equations the outcome is:

$$\bullet \quad T_{tightening} = F_{tightening} \cdot (\mu(0.577d_2 + 0.5d_A) + 0.159P) \quad \text{(Tightening torque required)}$$

The bolt calculations can be shown in the following table:

Motors	Motor 1	Motor 2	Motor 3	Motor 4	Motor 5
S	1.5	1.5	1.5	1.5	1.5
μ	0.12	0.12	0.12	0.12	0.12
$F(kp)$	70.8	140	15.35	16	16
$F_{each\ bolt}(kp)$	11.8	23.3	17.55	2.66	2.66
$F_{tightening}(kp)$	91.27	291.67	135.82	20.62	20.62
$T_{tightening}(kp)$	147.5	180	219.49	33.33	33.33

Table 3.16: Bolt Checking Calculations

The strength of some other parts has to be examined. Firstly, bending stresses in parts 2 and 3(Arms) can be calculated.

To calculate the shear stresses on sections in the middle of the arms the following equation can be used:

$$\sigma_b = \frac{M_b}{\frac{\pi(d^4 - d_i^4)}{32d}}$$

Arms	$\sigma_b(MPa)$
Upper Arm	4.8
Lower Arm	5

Table 3.17: Arms Bending Stresses

The bending stresses applied in the middle of part 2 and 3 are about $5\ MPa$ (without taking into consideration the graduation) and the yield strength of Aluminum is $276\ MPa$.

After the creation of the CAD model of robotic arm subsystem and weight calculation of each part of the robotic arm, a check for torque calculation can be done. In a similar way with the initial calculations, the check calculations for the motor torques can be seen in the following chart:

Calculation check for roller bearing

The force applied on DIN 720 33024 bearing is due the weight of the robotic arm and it can be calculated as [4] by the following equation:

$$P = X \cdot F_r + Y \cdot F_a = 177N$$

That force is really smaller than Basic dynamic (356kN) and static (540kN) load rating.

3.3.5 References

During the theoretical design evaluation and understanding, various informative tools were used, providing evidence and support for the project. Architecture, joints link, dynamic behavior, kinematics and much more information and realistic data was derived by [2], [8],[16] case studies. The books of Dr. Vouhouinis, [12] and its application[13] have provided useful perspectives on static analysis, expanding knowledge of and impacting certain design considerations. Furthermore, Mr. Grekousis' studies on Machine Elements and Machine Design in[4] were useful in calculating the mechanical connections of numerous parts. Finally, the structural analysis principles established in [17] have been critical in guaranteeing the rigidity and resilience of the rover's Mobility Subsystem.

References contribution was undoubtedly precious through out the research. Overall, the references played a crucial role in contributing to the quality and integrity of this piece of work.

3.4 Panel Deployment Mechanism and Energy Management Subsystem

3.4.1 Overview

The P.D.M.E.M.S is the subsystem responsible for initially calculating the total energy requirements of the rover as to determine the surface area of solar panels needed to complete the mission, as well as designing the full panel assembly including the mechanism that would allow them to fold and unfold according to the need of the moment. The decision to include such a mechanism was made because it would allow the rover to have a bigger total panel area without hindering its ability to be transported to mars and also because this mechanism would enable it to protect the panels when it is facing the worse of the martian elements.

3.4.2 Team dependencies

P.D.M.E.M. - Robotic arm

It is of course crucial that an amount of energy allocated for the movement of the robotic arm, as without power it is useless. Although probably the most important issue that required the attention of both systems was the space allocation. Considering the fact that the body of the rover possesses a finite surface area and the importance of the panels and the robotic not running into each other, a plan had to be devised dictating the limits between both systems.

P.D.M.E.M. - Mobility

The mobility system drains the highest amount of energy of all systems on the rover, meaning that the primary purpose of the P.D.M.E.M. is to provide a sufficient amount of energy for it. Thus it was of the utmost importance that the energy demand and supply align. Additionally, the way the mobility system's mechanism was conceptualized means that it had the potential to reach up towards the panels and potentially damage them. For that reason it was necessary that both systems take this into consideration and act accordingly.

P.D.M.E.M. - Body

Arguably the most important and demanding relationship was between the P.D.M.E.M. system and the body system. The whole mechanism had to be designed with respect to the dimensions of the chassis, if those were not compatible then the whole system would not be able to be connected to the rest of the rover and thus, useless. Also the base of the mechanism had to have a feature that would enable it to be fastened to the rest of the body.

3.4.3 Subsystem management

The two goals of this subsystem are the calculations and the resolution of all energy related issues, as well as the design of a functional, dependable yet simple mechanism that would allow the deployment and retraction of the solar panels. This means that the P.D.M.E.M. subsystem dictates the allocation of the energy generated.

After the deployment mechanism's design is complete, it will undergo static analysis to determine its viability. Those calculations can be seen in detail across the following pages. The complete assembly with the mechanism can be seen in Fig. 3.81

3.4.4 Energy calculations and budgeting

One of the first issues that needed addressing was the fact that mars does not receive the same amount of solar energy as earth. Due to him being further the sun than earth the solar irradiance is, on average, 43.1% of the amount seen on earth, that translates to an average irradiance of 590 Watts/m^2 .

The second problem encountered was the lack of information surrounding the panels used on NASA's rovers opportunity and spirit, which were the inspiration for our rover, and generally in space applications. It is known that the higher end solar panels currently used on satellites have efficiencies around 30% and a maximum output power of 400 W/m^2 according to [this](#) paper by NASA. The cells used for reference were the Ultra Triple Junction (UTJ) Leone cells currently produced by Spectrolab, a subsidiary of Boeing and current supplier of NASA, which have similar characteristics as mentioned above while also being already used on similar applications.

After roughly considering the rover's geometry, it was decided that around $4m^2$ of solar panels would be more than enough to fulfill the energy needs. The way this was calculated was by taking the known data from NASA's opportunity rover to determine how many hours per martian day the panel's produce their maximum power output (pmp). This is a common way to express the average energy intake of solar parks, it is done by dividing the daily intake of each panel by their pmp, opportunity had a pmp of 140 Watts and at the start of the mission produced a total of 900 Wh/sol , that is the equivalent of its panels producing their pmp for around 6.5 hours. **The final design has a total panel surface area of $4.6m^2$** , knowing that their pmp is 400 watts we can now calculate the average daily energy intake as $(\text{pmp}) * (\text{area}) * (\text{hours of pmp/sol})$, giving us a total of 11.8 KWh/sol . This is a far cry from opportunity's 0.9 KWh/sol , this difference derives from the greater surface ($4.6m^2$ as opposed to $1.33m^2$ on opportunity) as well as the advancements made on solar cells in the more than 20 years since then. It is also known that, as time passes during the mission, the panels get damaged and dirty from the elements, reducing their power. In the case of opportunity, its power intake was reduced by 30% after a

few days, and it reached an all-time low of 50% during its final days. For reasons of safety all calculations and budgeting were made with the assumptions that the average intake is half of what is mentioned above at **5.9 KWh/sol**.

Energy management

The energy required for the rover to be able to perform its basic tasks was calculated with the assumption that the rover would, at any given point, be able to enter a hibernation mode, giving it the ability to close off any non-critical systems as to conserve energy when the situation demands it. That means that it is not required for all systems to be working, and thus consuming power, at the same time. Also the rover will include a **battery pack**, giving it the ability to store excess energy when the conditions are favorable and use it when in need. That is the reason why **all calculations are based on the average energy intake**. The general overview for the rover's energy budget is the following:

Description	percentage	average amount (KWh)
Mobility	60%	3.54
Robotic arm	5%	0.295
Panel deployment actuators	5%	0.295
Other electronics	30%	1.77

Table 3.18: Total rover energy allocation

With that allocation in mind the rover will definitely not have any problem with the panel deployment or the robotic arm, as for it's mobility, the wattage for each of the transmission and steering motors has been calculated here. Considering we have a total of 8 transmission and 8 steering motors that means that the maximum movement wattage is:

$$8 \times 24 + 8 \times 2 = 208 \text{ Watts}$$

This means that, on average, the rover will be able to move for:

$$3.54 / 0.208 = 17 \text{ Hours/sol}$$

Of course there is no need for the rover to be moving for that many hours per sol, considering that NASA's Mars rovers move at pace of around **100 meters per sol**. This means that we have even more energy leftover to be allocated for other purposes or to be saved for later usage. With all these things in mind it is obvious that the rovers energy needs are met in full and even surpassed.

3.4.5 Panel mechanism design

Panel design

As was mentioned above, the panels themselves are made from Spectrolabs Leone cells. Based on the dimensions of those cells we have designed two different types of panels to be used on the rover, the **side panels** with dimensions $907 \times 637.5 \text{ mm}$ and the **main panels** with dimensions $1870 \times 637.5 \text{ mm}$, both panels will have a width of 5 mm . The panels are basically thin plates of aluminum on which the Leone cells are attached, they also contain a tiny layer of protective transparent ceramic on top. The assembly was not designed in detail due to the lack of expertise in the field, so the panels are treated as a **black box** to be used in the full assembly. In total there are 4 side panels in the assembly and 2 main ones. Their mass is assumed as 5 Kg/m^2 , meaning that the side panels have a mass of **2.9 Kg's** each and the main ones **6 kg's**.



Figure 3.73: Main panel dimensions

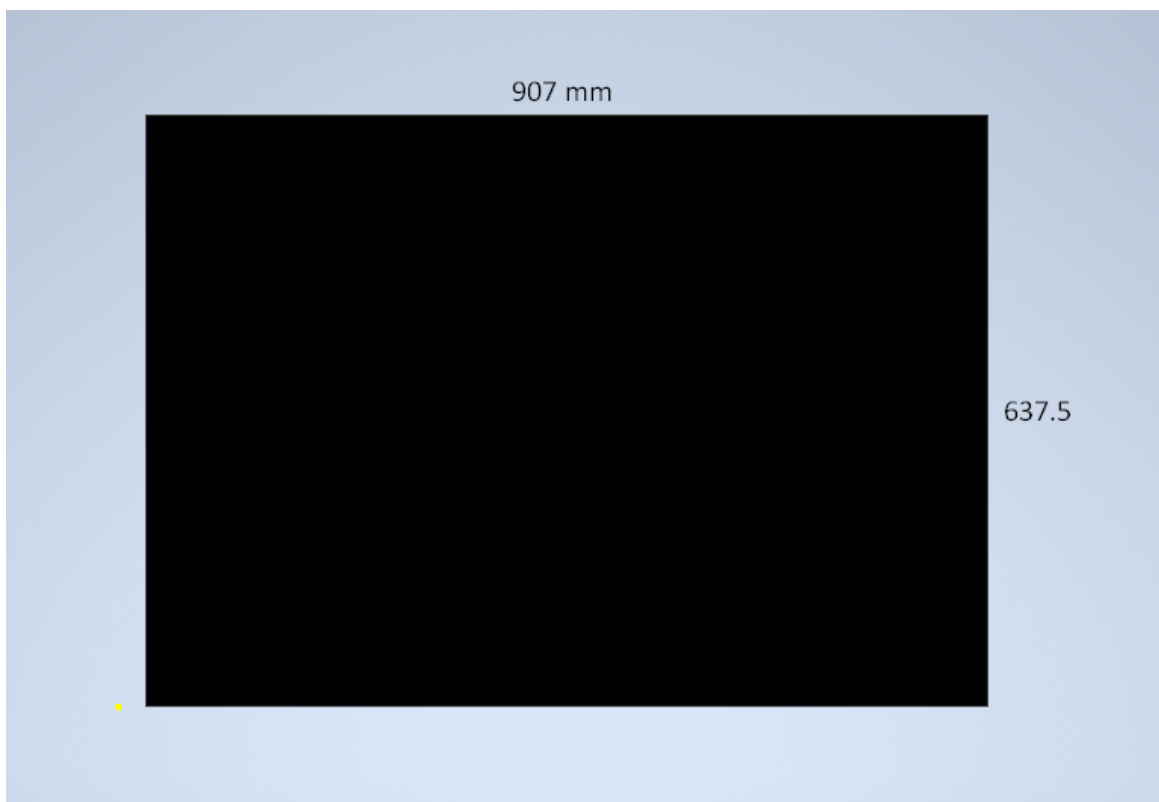


Figure 3.74: Side panel dimensions

The panels then are placed on two different types of custom framing, which is made up of multiple hollow **aluminum 6061-T6** parts. The frame includes railings in which the panels fit into. The fully assembled frame also includes the male hinges (Left and right), the female hinges, the axle (including the shaft collars) and the Lever in which the axle is fastened. The female hinges are assemblies of their own, including **cylindrical bearings** to reduce friction. Furthermore some parts of the frame include two simple extrusions, those act as stoppers when the panels are closed, essentially spreading the weight of the side panels more evenly along the main frame.

The complete side panel and main panel assemblies have masses of 6 and 12 Kg's each respectively, giving us a total of 24 Kg's just for the side panels and 24 Kg's for the main ones. The solid aluminum bases have a mass of 750 grams each for a total of all 6 Kg's for all eight. Adding the assumed weight of the actuators (15 Kg's each) gives us a **total of 84 Kg's for the whole panel deployment mechanism**.

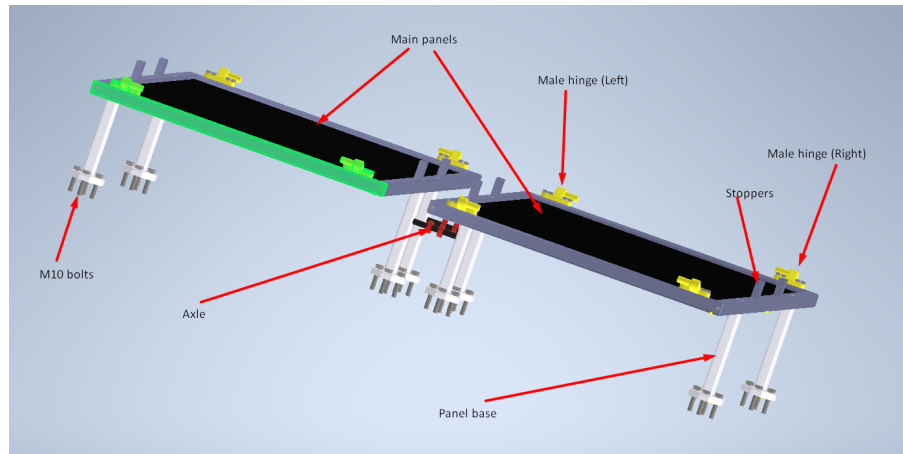


Figure 3.75: Main panel assembly

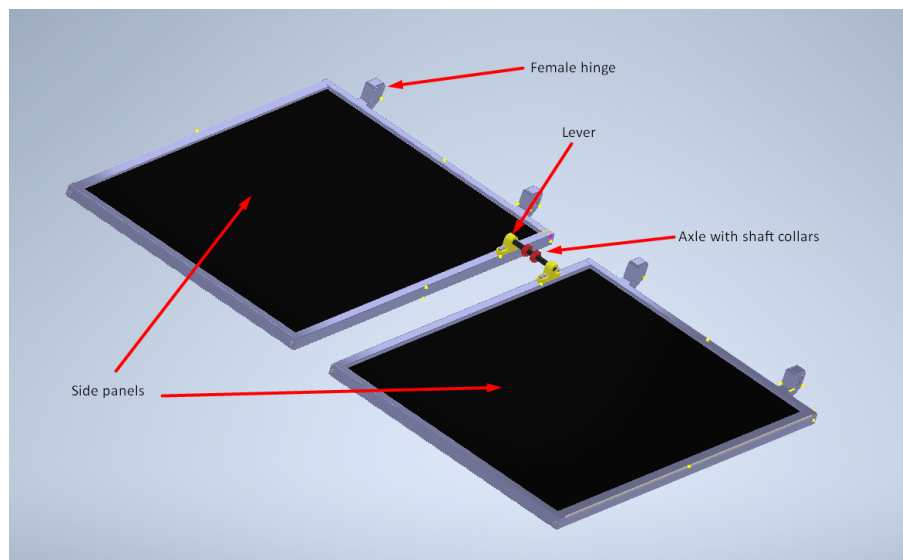


Figure 3.76: Side panel assembly

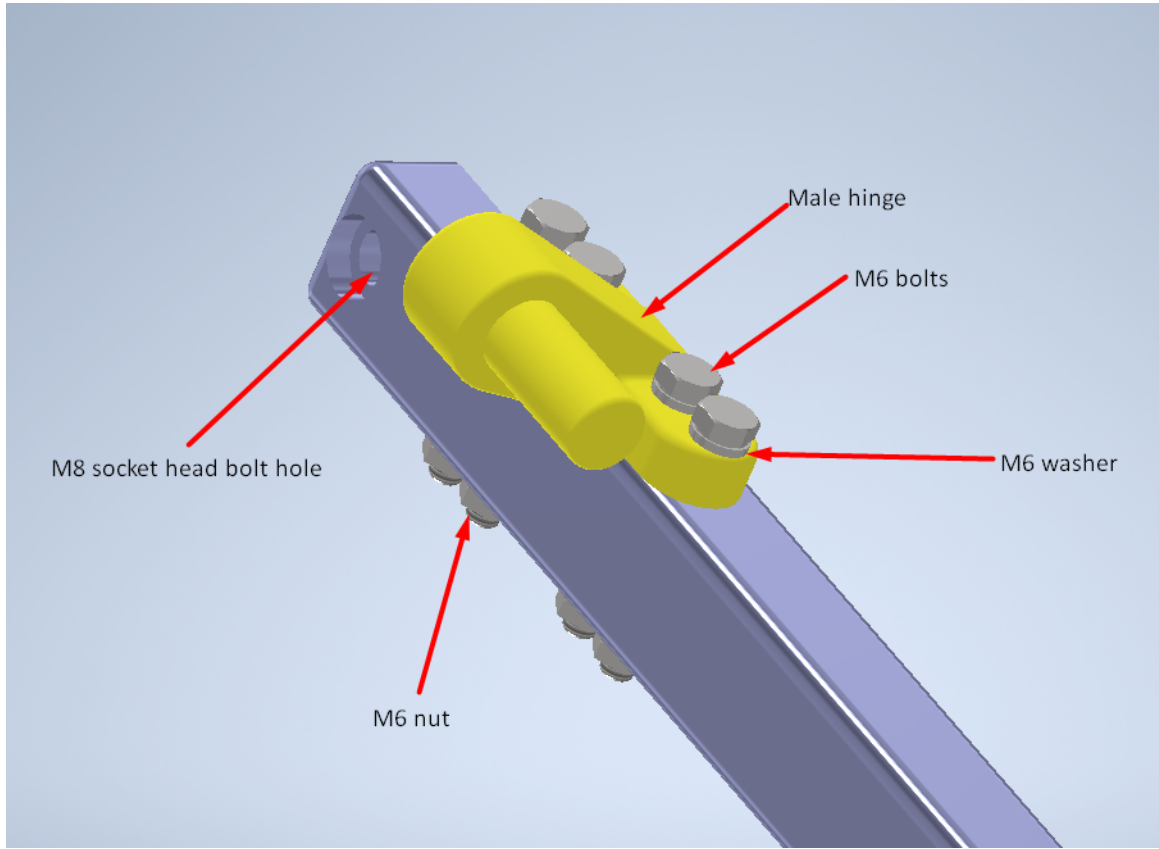


Figure 3.77: Male hinge assembly

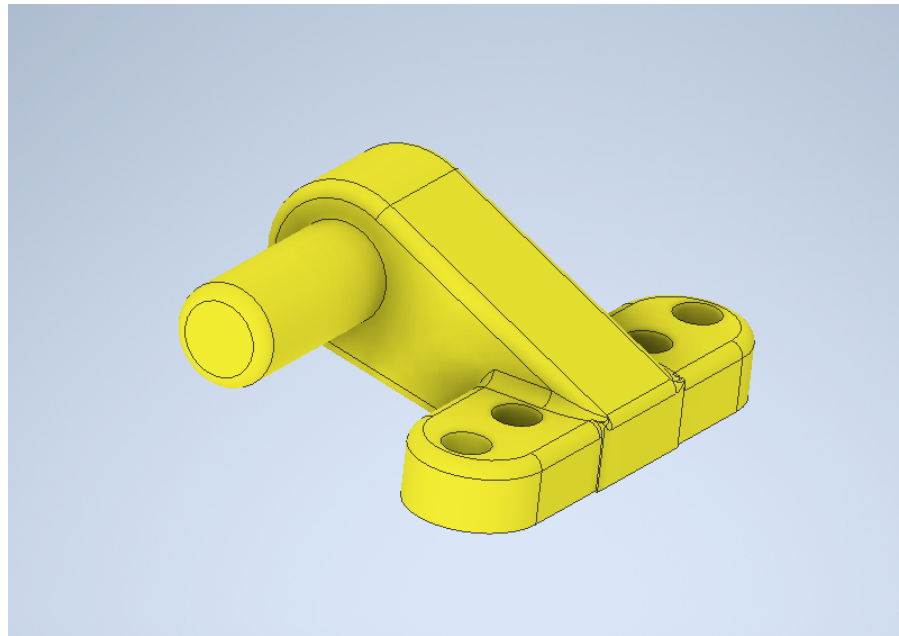


Figure 3.78: Male hinge

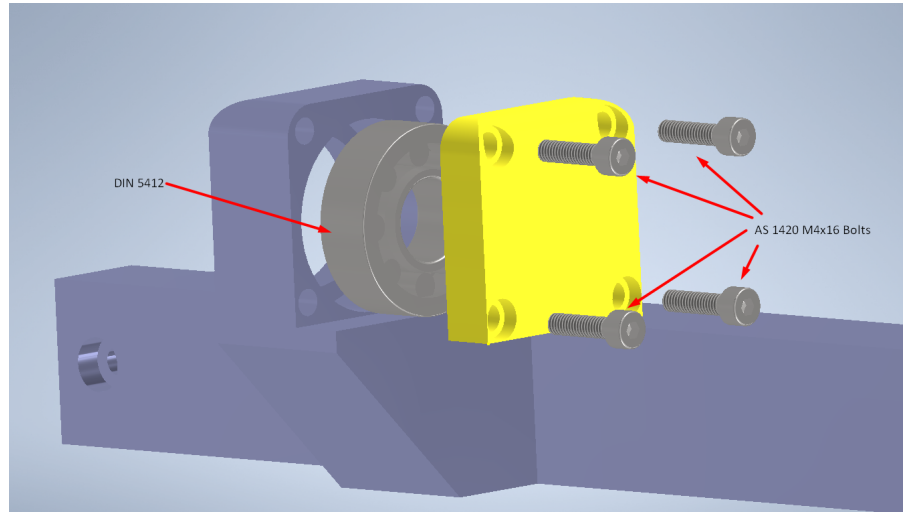


Figure 3.79: Detailed Female hinge assembly

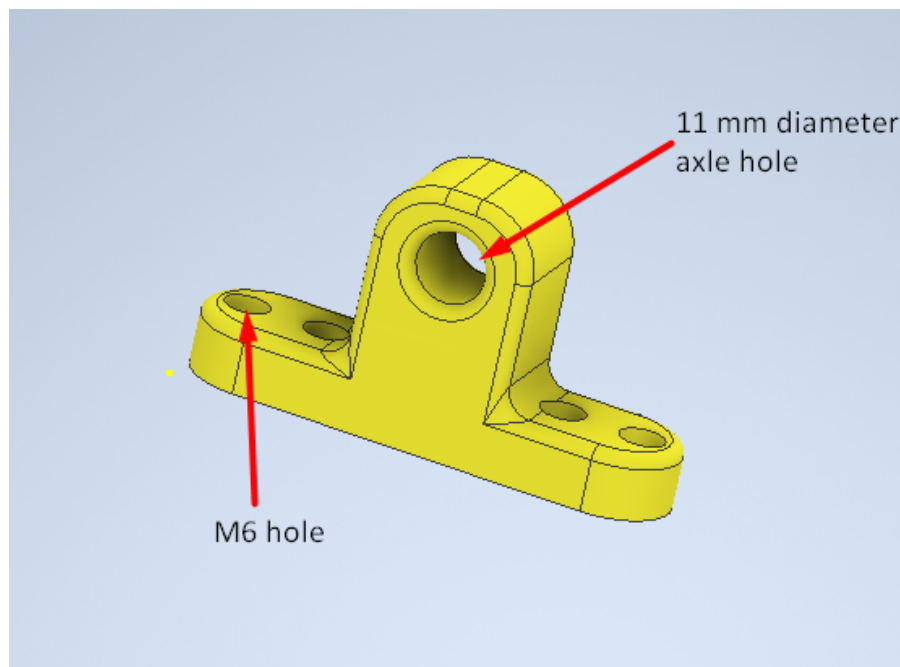


Figure 3.80: Lever

Mechanism design

The full assembly of the system seen below:

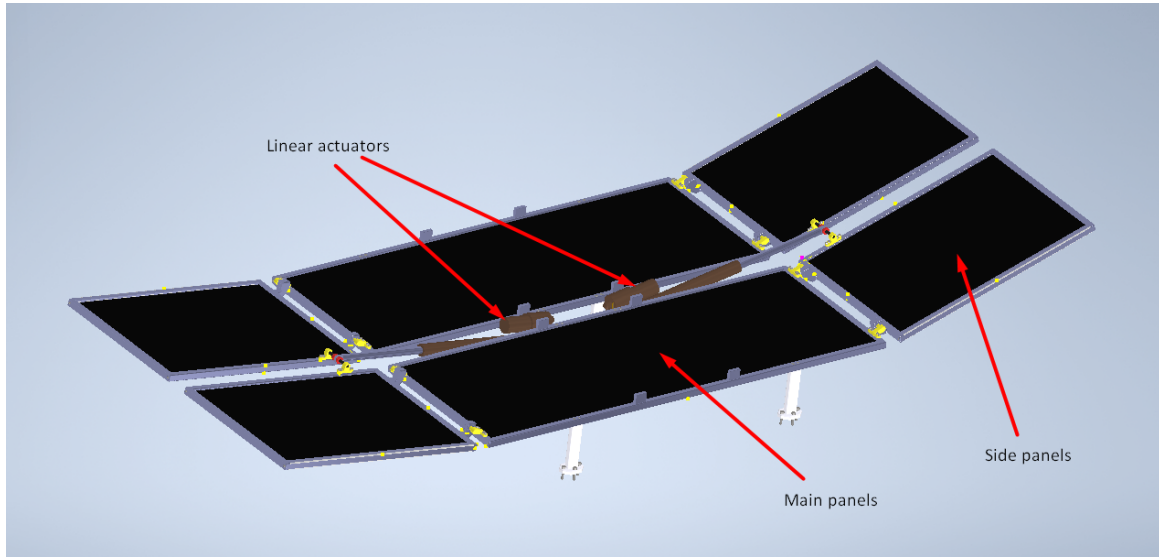


Figure 3.81: full panel assembly

Firstly, it's worth mentioning that no calculations considering the wind forces were made. This was done because **the martian atmosphere is 1 % as dense as earth's**, this means that the force caused by the winds on Mars is equivalent to the force caused by winds with speeds ten times slower on Earth. Adding to that the fact that the maximum wind speeds observed are around 100 Kph (which translates to around 10 Kph on Earth, as was mentioned before) means that the wind forces can be neglected. It should be noted that the primary problem caused by winds on Mars is the **corrosion** by the sand particles they move, but, as this cannot be realistically calculated with the tools and knowledge available, it is not taken into consideration as well.

The full assembly includes a simple deployment system with two linear actuators with a **400 mm stroke**, each actuator essentially moves 2 side panels. One of the first things that was calculated was the force necessary to open and close the panels. It is obvious that the moment caused by the force exerted by the actuators on the side panels with respect to the axis of rotation (hinges) needs to be higher than the moment caused by their weight. The friction at the hinges is considered negligible due to inclusion of bearings, and thus it is not included in the calculations. To reduce the maximum force required by the actuators, **the panels, when fully opened, do not extend fully horizontally, but stop at an angle of 10 degrees from the ground facing up**. The actuators seen in the above design are depicted in higher detail below:



Figure 3.82: Linear actuator picture

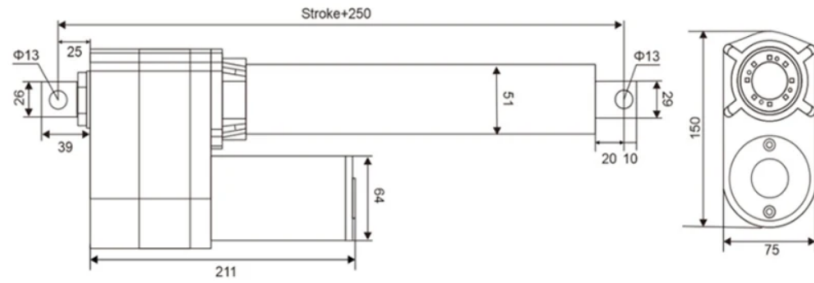


Figure 3.83: Technical drawing of the linear actuators

Actuator force calculations

It is also obvious that when the panels are **opened fully** the the force required by the actuator is at its **maximum** due to the distance of the point in which the're acting being at its lowest distance from the rotation axis, thus causing less torque.

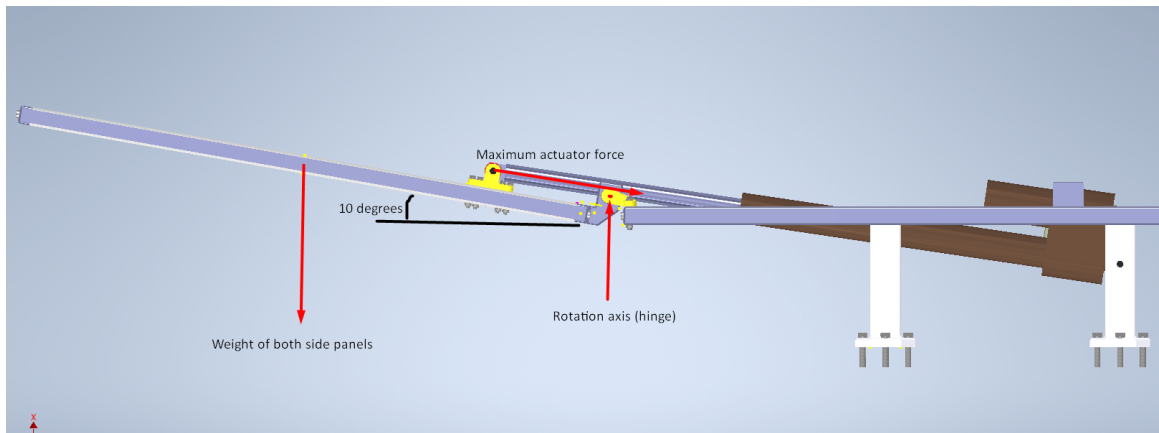


Figure 3.84: side view of the assembly with the forces acting on the side panel assebly

The problem above is presented bellow in a simplified way (all dimensions are in milimeters):

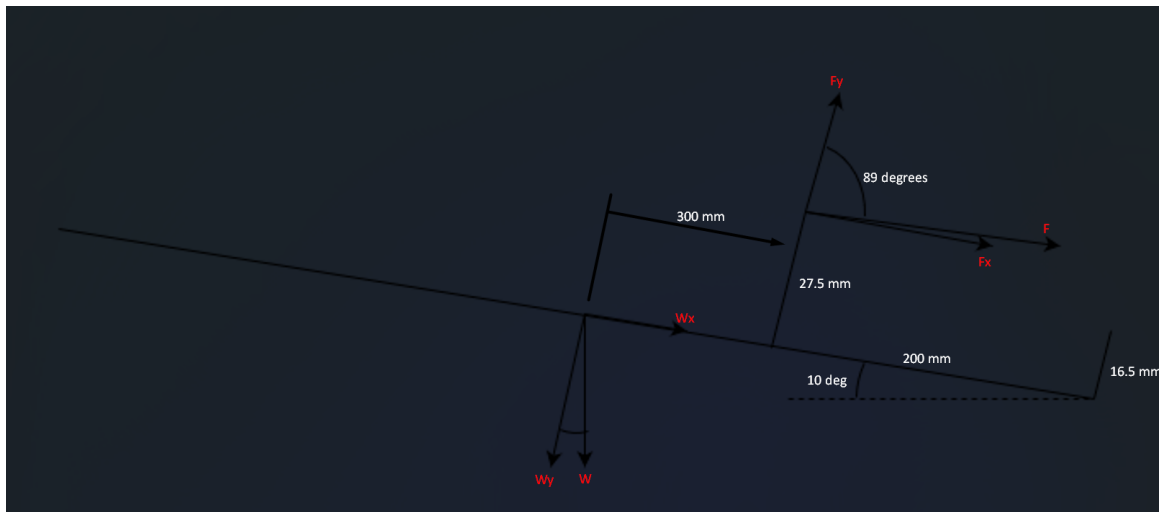


Figure 3.85: Simplified problem

We firstly calculate the actuator force with which the system ballances ($\Sigma M = 0$). The calculations for the forces causing a momment on the axis of rotation are the following :

$$\Sigma M = Fy * 200 + Fx * (27.5 - 16.5) - Wy * 500 - Wx * 16.5$$

With: $W = 2 * 6 * 9.81/3$ (due to Mars's gravity being one third as strong as earth's), $Wy = W * \cos(10)$, $Wx = W * \sin(10)$, $Fy = F * \sin(1)$, $Fx = F * \cos(1)$ we get the following equation:

$$F * \sin(1) * 200 + F * \cos(1) * (27.5 - 16.5) - W * \cos(10) * 500 - W * \sin(10) * 16.5 = 0$$

$$\rightarrow F = 1340 \text{ Newtons}$$

The actuators selected have a maximum push/pull force of **10 KN each**, which is around 8 times more than the force needed to open and close the panels, thus making them an excellent choice for this application, considering that they will probably lose some of their power after some time due to wear and tear and will collect dust and other particles, hindering their movement.

Hinge calculations

It is also important to make sure that the bearings on the female hinges and the pin in the male ones both have the ability to withstand the loads acting upon them.

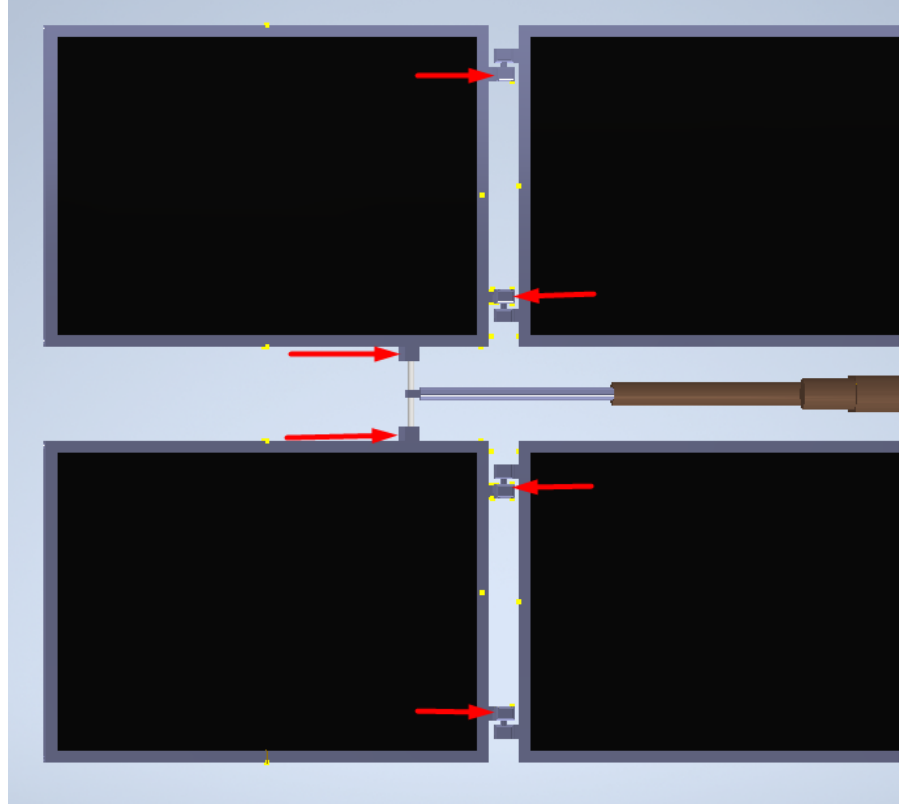


Figure 3.86: Forces acting on the hinges as seen from a plane parallel to the opened side panel(10 deg from the ground)

Each lever receives half of the force exerted by the actuator, the maximum amount of which is equal to half of the one calculated previously, because after that point the side panel assembly will rotate and the forces will be reduced. Also, it would be better if the force caused by the side panels weight was included in those calculations, but it is **negligible** compared to the other forces involved and thus ignored.

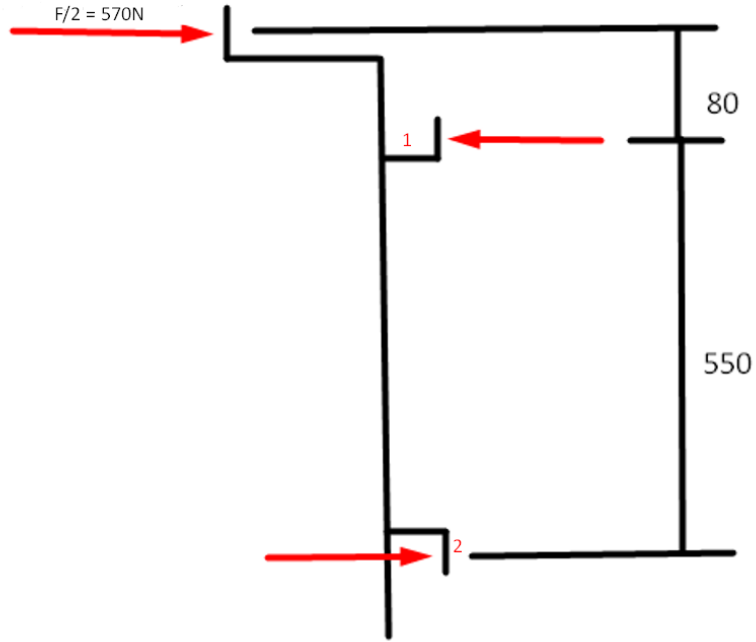


Figure 3.87: Simplified problem

$$\Sigma F = 1340/2 + N2 - N1 \rightarrow 570 + N2 - N1 = 0$$

$$\Sigma M1 = 570 * 80 - N2 * 550 = 0$$

Thus we can calculate that $N_1 = 487N$ and $N_2 = 83N$

As there is no need for the mechanism to close particularly fast or to perform many cycles during the missions life, **only static load is considered**. The bearings currently chosen are **DIN 5412 15x35x11**, which pose a static load rating of 10.4 Kn and are thus appropriate for this use.

The male hinges receive the same forces as calculated above but in the reverse direction. That means that the inner hinge receives the higher load, which in turn means that, because the hinges are mirrored, if it can handle this load then the outer one is fine as well. The pins length is 30 mm and it has a diameter of 15mm, for reasons of simplicity its assumed that the load is acting on its end.

$$M = N_1 * 0.03 = 14.61Nm$$

$$I = \pi * \frac{d^4}{64} = 2485mm^4$$

$$\sigma = M * \frac{y}{I} = 44.1Mpa$$

The male hinges will be made of maraging steel **ICO-2800**, which possesses a yield strength of 2600-2800 MPa, this means that the inner hinges have a safety factor of 59. Repeating the same calculations for the outer male hinges gives us a safety factor of 346. For our applications those safety factors are deemed satisfactory.

Lever analysis

The lever is a crucial piece of the system. A lever failure means that the panels will not be able to be closed and opened. For that reason they will also be made of maraging steel due to its exceptional strength and they will be fastened to the frame with four **AS 1110 M6X35** bolts each. Due to the complexity of the analysis required, the calculations were not made, but the Lever with its current dimensions and its mounting should be structurally sound.

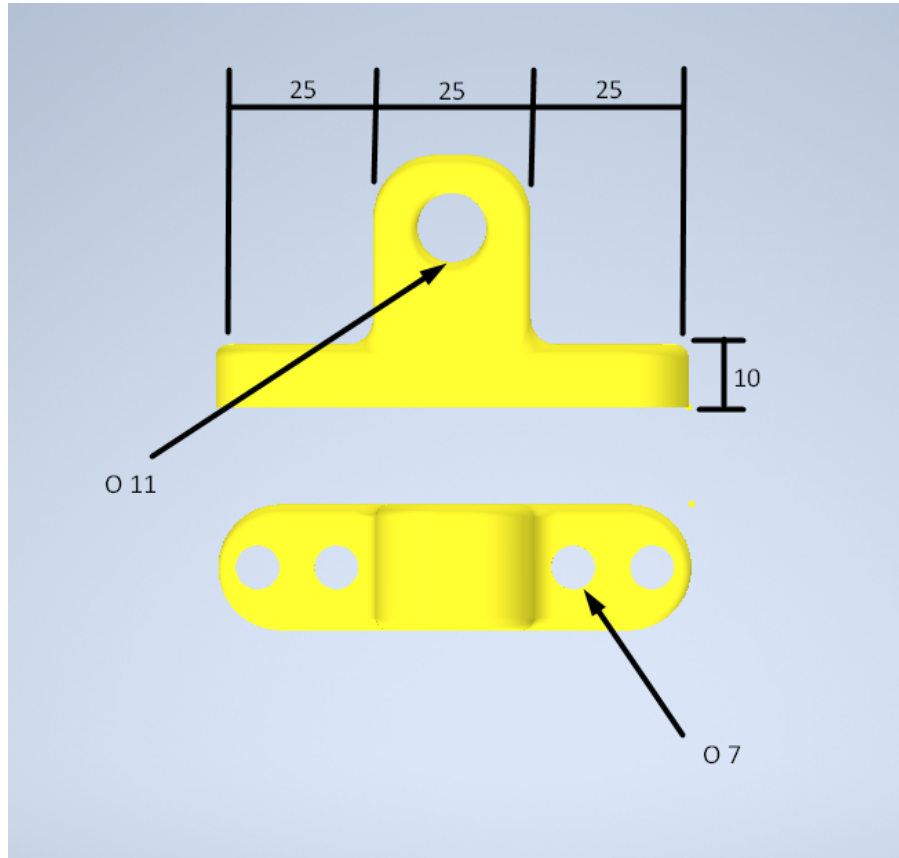


Figure 3.88: Analytic Lever dimensions

Axle calculations

The assembly includes four identical axles, two are attached to the side panels and two on the base. The actuators will be fastened on those axles with shaft collars so they will not be able to move freely along their length. The shaft collars chosen are **these**. Due to the loads received by them, a stronger material had to be chosen, in this case **ICO-2800 maraging steel**, which poses exceptional yield strength at **2600-2800 MPa**. The axles have a long middle part with a diameter of **13mm**, in the middle of which the actuator will be fastened, and on the sides an area with a smaller diameter of **11mm** so they can be fitted into the bases ad the levers.

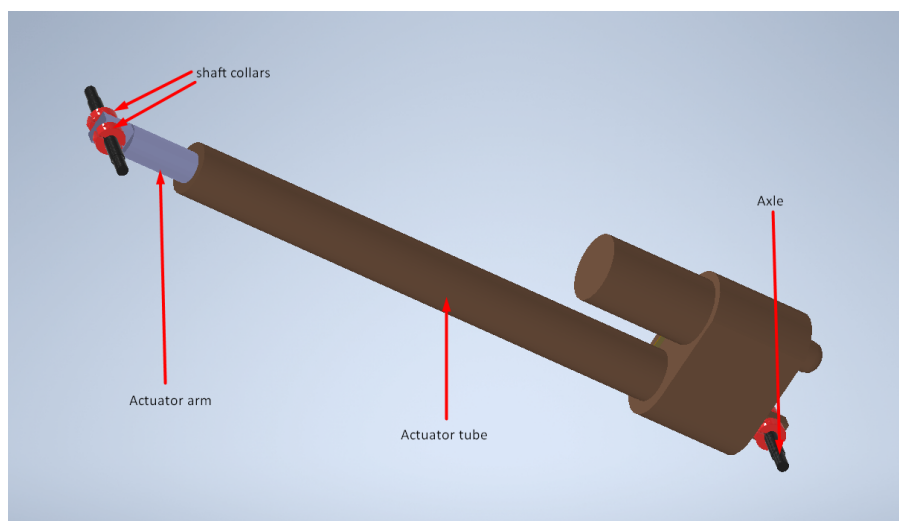


Figure 3.89: Actuator assembly with axles and shaft collars

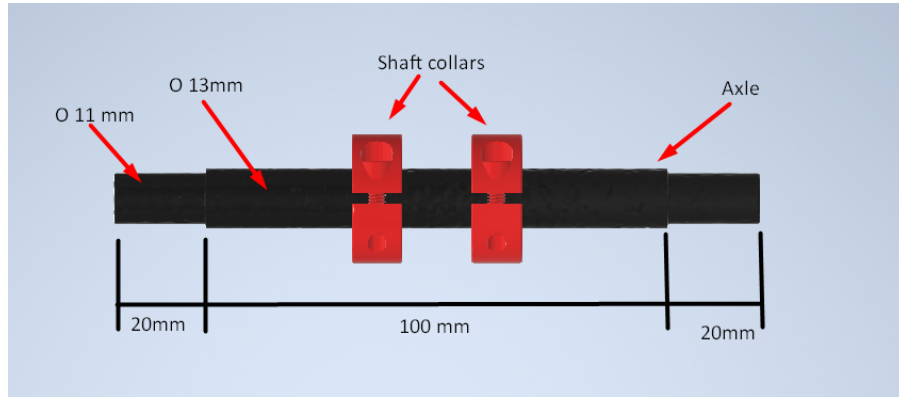


Figure 3.90: Dimensions of the base axle

The forces received by both axles in each pair are the same due to their action-reaction status, the maximum force once again being 1340 N and appearing once the panels are fully opened. Due to the axles being identically and receiving the same forces, we can calculate the safety factor for one of them and it will be true for all. Below is the free body diagram of the axle with the above-mentioned actuator force and its reactions from the sides:

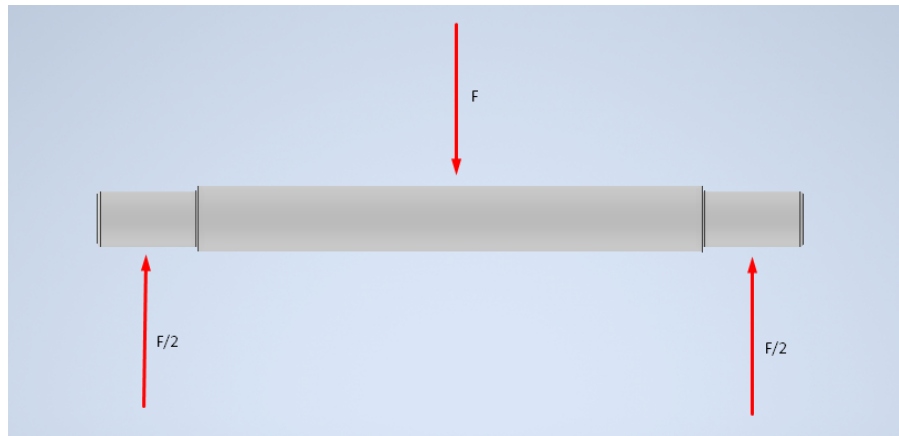


Figure 3.91: Forces acting on the base axle

The maximum stress is either at the middle or at the point in which the diameter changes, for that we need to calculate the stresses at both points. For that we need the following relations:

$$\sigma = \frac{M \cdot y}{I}$$

$$y = \frac{d}{2}$$

$$I = \pi \frac{d^4}{64}$$

Where in the middle we have $d=13\text{mm}$ and $M = \frac{F}{2} \cdot 0.06 = 34.2\text{Nm}$ and on the side $d=11\text{mm}$ $M = \frac{F}{2} \cdot 0.01 = 6.7\text{Nm}$. With that we can calculate that:

$$\sigma_1 = 158.6\text{MPa}$$

$$\sigma_2 = 43.6\text{MPa}$$

Meaning that the maximum stress appears at the midle of the axle. The safety factor is equal to the yield strength of the material divided by the maximum stress, in this case the **safety factor** is approximately **16**, making the axle appropriate for this use. Also, as was mentioned before, this means that all axles pocess the same safety factor, making them appropriate as well.

Chapter 4

Rover Assembly

4.1 Design Overview

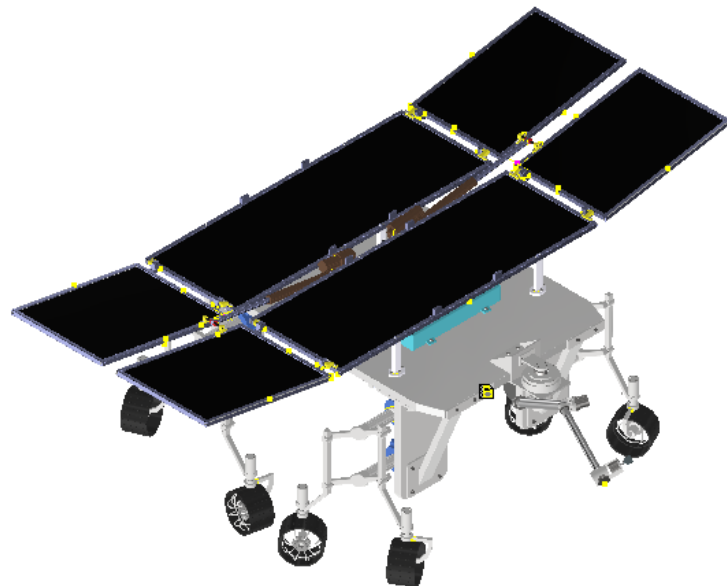


Figure 4.1: Rover Top side view

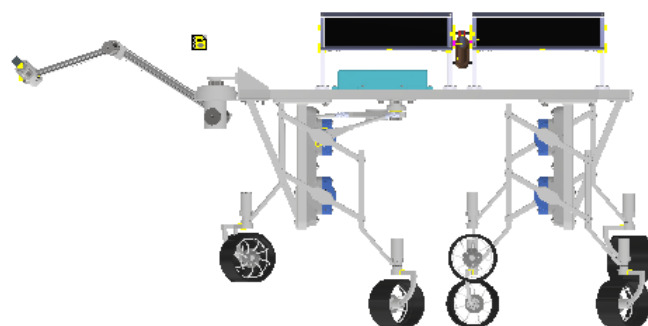


Figure 4.2: Rover side view

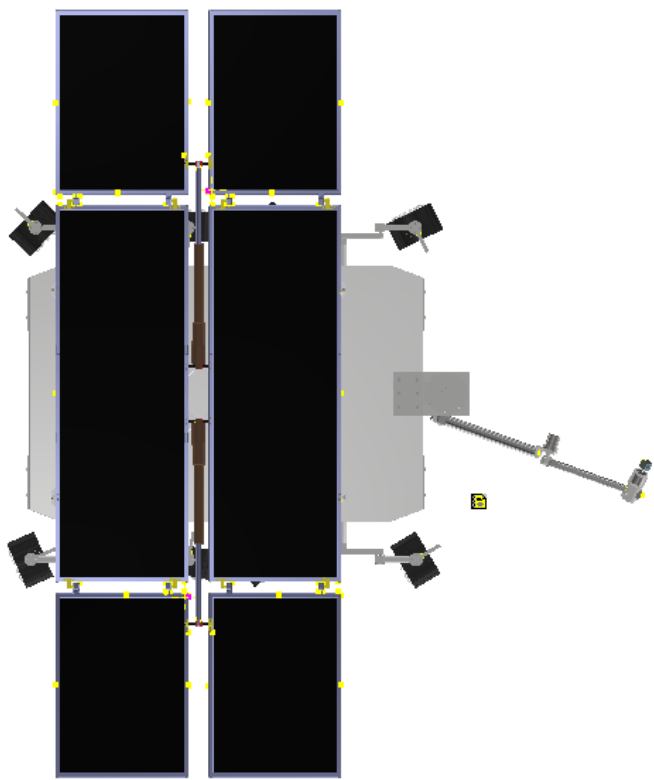


Figure 4.3: Rover top view

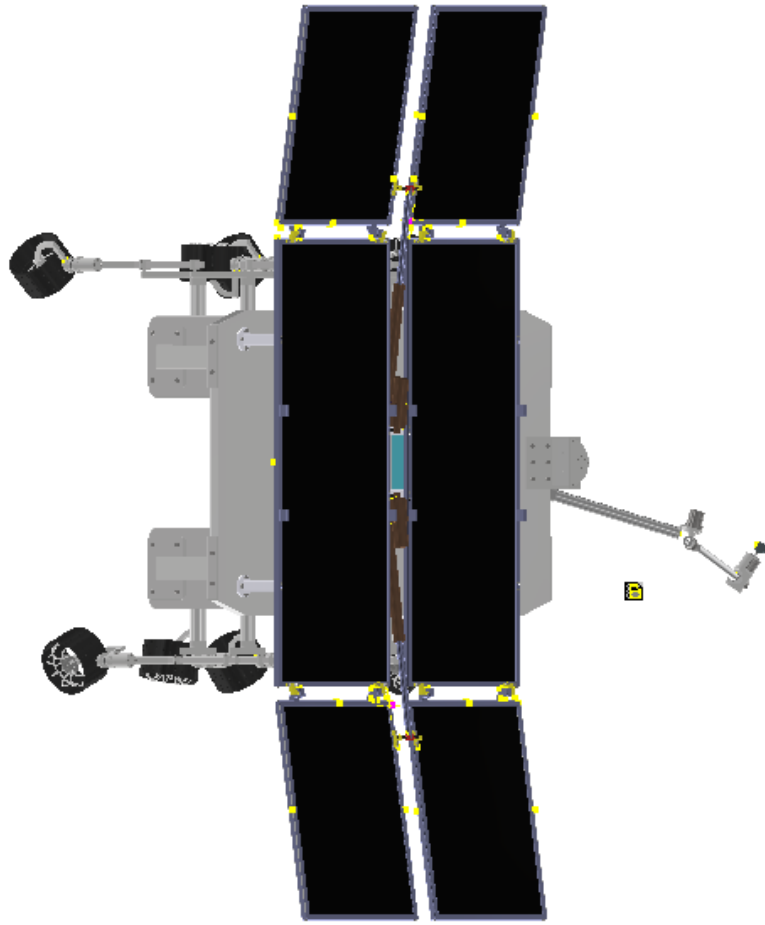


Figure 4.4: Rover back view

The rover's mobility subsystem is encased in a metal housing equipped with bearings, enabling free rotation along the axis parallel to the Y axis while restricting other degrees of freedom. Subsystem's vertical movement along the Z axis is achieved through two horizontal beams, enhancing adaptability to Mars' diverse terrains. Arced beams, fixed in all but rotational degrees along the axis parallel to the Z axis that passes through the free end of the linear part of the beam, enable wheel steering for directional control. The differential mechanism facilitates opposite rotation of the front two quarters, ensuring stability on uneven surfaces. The robotic arm, detailed in Section 3.3.4, boasts five motors providing the necessary degrees of freedom for precise scientific maneuvers. P.D.M. actuators enable solar panel deployment with a total outreach of 4.2 m, supported by an additional commercial battery pack stored in the internal structure for enhanced energy management. The comprehensive design ensures the rover's functionality and adaptability in pursuit of mission success and can be observed in the following figures.

4.2 System Functionality

This section elucidates the intricacies of the system's assembly functionality. To fulfill the mission objectives, the resolution of various logical circuits is imperative within the system's architecture. Each logical circuit is meticulously designed to contribute to the seamless operation and effectiveness of the Mars rover vehicle. Moreover, the implementation of automatic control systems is identified as a critical component for the system to function as intended.

In the forthcoming paragraphs, a detailed exploration of the system's functionality will be provided. This includes an in-depth analysis of the logical circuits responsible for diverse functionalities, underscoring their role in achieving specific mission objectives. Additionally, the design and integration of automatic control systems will be highlighted, emphasizing their pivotal role in ensuring the rover's adaptability, responsiveness, and optimal performance in the dynamic and challenging Martian environment.

In order to allow for smooth cruising on the martian surface, the rover vehicle is equipped with multiple sensors as well as various electronic tools. The sensors and the tools proposed for the mission success are:

- 7× Ultrasonic Sensors

- 1× Sunlight Sensor
- $N \times$ Temperature Sensors
- $N \times$ Heaters

The Ultrasonic Sensors will be used to let the vehicle be aware of its surroundings, ensuring seamless maneuvering across the martian surface. These sensors are proposed to be installed as follows:

- 1 on the bottom side of the vehicle's Body to measure the distance from the ground
- 2 on the sides of the vehicle's Body to measure the distance from random objects
- 1 on the front and 1 on the back of the vehicle's Body to measure the distance from upcoming or passed objects
- 2 on the panel's sides to measure the distance of random objects when the P.D.M. is activated

The outlined configuration is strategically designed to facilitate the rover's unhindered traversal of the Martian terrain, ensuring the successful accomplishment of its mission objectives. Specifically, the mobility systems have been meticulously engineered to accommodate varying topographical challenges, with the design considerations accounting for a maximum slope angle of 30° (as detailed in Section 3.1.4). The incorporation of Ultrasonic Sensors emerges as a pivotal component within this framework, playing a crucial role in detecting and assessing permitted slope angles. The Ultrasonic Sensors, known for their precision in distance measurement, will actively contribute to the rover's navigation by providing real-time feedback on the surrounding topography. By leveraging this data, the rover can dynamically adjust its mobility systems to adhere to the specified slope limitations. A proposed operational diagram of the above mentioned challenge can be seen in Fig. 4.5.

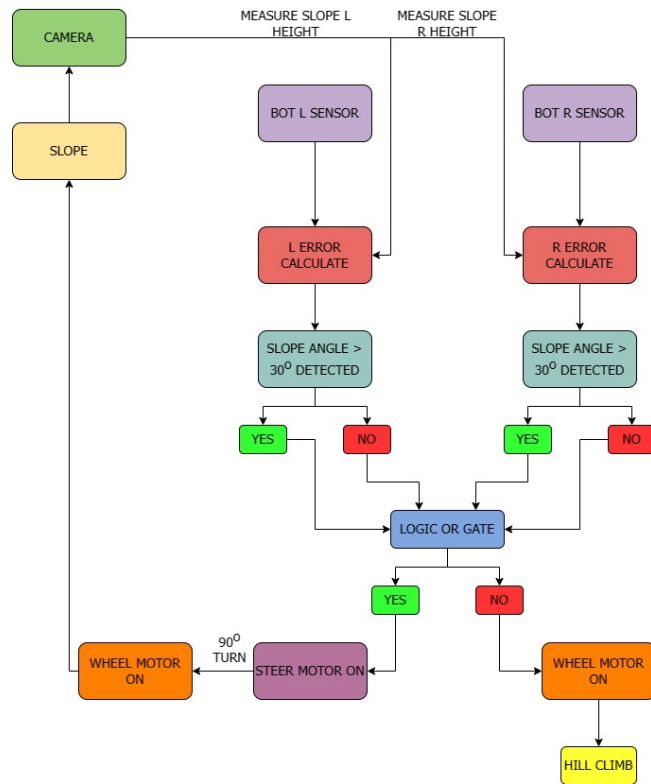


Figure 4.5: Slope Detection Operations

The Sunlight Sensor assumes a pivotal role in orchestrating the rover's energy management strategy. Upon detecting sunlight, the rover seamlessly transitions into *Mission Mode*, a critical operational phase designed for executing mission objectives. In Mission Mode, the Power Deployment Mechanism (P.D.M.) is activated, empowering the vehicle to both gather required samples as outlined in the mission objectives and harness solar energy efficiently from the panels. This strategic integration ensures that the rover optimally utilizes available sunlight to fulfill its scientific mission while simultaneously replenishing its energy reserves. Conversely, in the absence of detected sun rays, the rover enters *Rest Mode*, a discerning operational phase focused on energy conservation. During Rest Mode, the vehicle conserves energy by deactivating background and non-essential functions, relying solely on the vehicle's battery pack. This parallels the energy-saving mode commonly found in mobile phones, exemplifying a deliberate and resource-conscious approach to energy management. By dynamically shifting between Mission Mode and Rest Mode based on Sunlight Sensor inputs, the rover demonstrates a sophisticated adaptive system that maximizes its operational efficiency and longevity in the dynamic

Martian environment. A proposed logical circuit can be seen in Fig. 4.6. Please note, that these operations are draft designed in order to demonstrate the vehicle's adaptability and empower the design of the system.

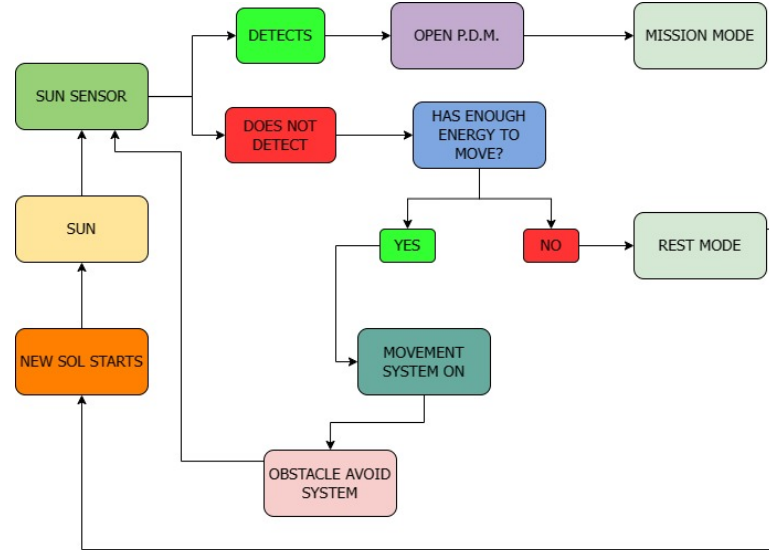


Figure 4.6: Energy Balance Operations

The integration of Temperature Sensors and Heater Elements within the rover's Thermal Control System is indispensable for ensuring the vehicle's survivability in the challenging Martian environment. The passive thermal control mechanisms play a crucial role in mitigating the impact of Mars' extreme temperature fluctuations, where the minimum temperature across the Martian atmosphere can range from -153°C to 20°C (T_{range}). These conditions pose a formidable challenge for the robot vehicle, necessitating a robust thermal control strategy to safeguard its critical components. Among others, some key components requiring meticulous thermal control are:

- Motors/Actuators
- Electronics
- Bearing Connections
- Scientific Instrumentation

A proposed thermal control system can be seen in the block diagram of Fig. 4.7.

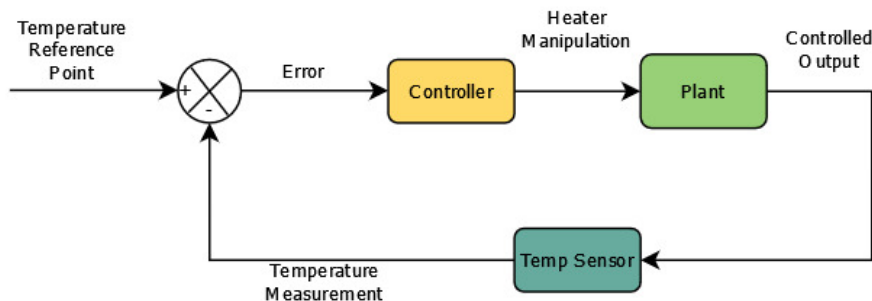


Figure 4.7: Temperature Control System

In conclusion, the success of the mission hinges significantly on the incorporation of sophisticated automation systems and operational instrumentation. In alignment with the principles governing space missions, the operations of a spacecraft constitute a paramount aspect of mission design. However, it is pertinent to note that a detailed exploration of the rover's operational procedures is intentionally omitted from this report, as it falls beyond the scope of the current course's objectives and focus.

The design choices made throughout this report, spanning from mobility and thermal control systems to energy management and scientific instrumentation, collectively contribute to the robustness and adaptability of the rover. By prioritizing automation and operational instrumentation, the mission endeavors to enhance efficiency, autonomy, and reliability, critical attributes for the successful execution of tasks on the martian surface. This approach underscores a comprehensive strategy aimed at ensuring the rover's functionality, longevity, and scientific efficacy in the challenging and dynamic environment of Mars.

Chapter 5

Conclusion

5.1 General Comments

By far the most important realization that our team made during this whole project was that the whole process of designing a complex multi-part non-conventional system with few references (from scratch) is much more challenging than initially thought. The time and effort required by all members greatly surpassed our expectations, causing countless moments of despair, while the team's morale fluctuated constantly through the semester.

The fact that most parts and systems are predominantly custom designs, made the whole process more time-consuming and the calculations more difficult. In future endeavors we should strive to avoid such a divergence from currently existing parts and systems, as this would greatly ease the workload required.

Additionally, the assumptions made at the start of the project concerning the mission deviated somewhat from start to finish. For example, at the start of the project, it was decided that the whole rover would be designed with the capability to withstand the martian temperatures, but by the end, multiple parts of those chosen did not meet that criteria. Things like these happened due to the team's lack of knowledge at the start concerning either hazardous conditions met on Mars or the capabilities of existing systems. Greater research had to be done in the initial phases so the consistency of those assumptions would be preserved.

5.2 Improvements

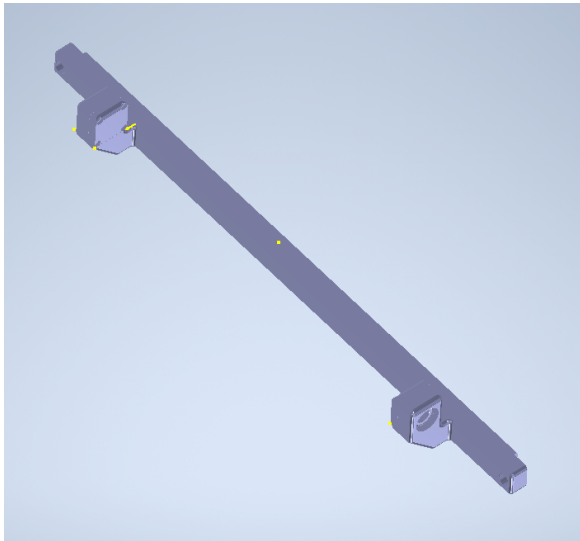
5.2.1 Mobility System

Identifying weaknesses in the Mobility system reveals an overabundance of degrees of freedom, increasing the susceptibility to failures. To mitigate this issue, a reduction in degrees of freedom and a comprehensive redesign of the mobility system are imperative. The study's lacuna in dynamic analysis further underscores the need to validate the system's functionality. Additionally, maintaining safety factors within reasonable limits is crucial to prevent over-dimensioning, requiring a careful balance between safety and efficiency. Finally, after finalizing the design of the rover all the safety factors on static analysis must be recalculated with the appropriate rover mass to further ensure the durability of the final design. Incorporating these improvements ensures a more robust and reliable design for the mobility subsystem.

5.2.2 P.D.M.E.M.

The panel deployment system as a whole includes multiple parts that, because of rushed decision-making and the lack of foresight, are not optimal for their role. Such parts should and would be redesigned if the time frame allowed it. Those parts, along with some conceptual designs of their improved versions are included below.

Hinges



(a) Female hinges



(b) Male hinges

Figure 5.1: Current side frames parts with hinges

The male hinges on the current design are bolted to the side piece of the panels frame, which is then connected to the rest of the frame. This means that most of the load is transferred **only through a few bolts** to the rest of the frame. This also means that the panels themselves are under **constant stress**, placing the whole mission in a precarious position. The female hinges on the other hand are quite complicated considering their role. They are a sub-assembly themselves, with the biggest part being a frame piece with a very complex geometry.

The design would benefit greatly if the hinges were attached to a more robust piece of the assembly. Ideally, the male hinges would have to be bolted on to the base itself, as that would decrease significantly the stress on the frame. As for the female hinges, the whole system should probably be replaced by a **simpler** one that does not include bearings, because the friction forces are not important enough to excuse the complexity of the system and the inclusion of this many parts. This hypothetical system would also be bolted on the frame, making the frame piece's geometry much simpler.

Mounts

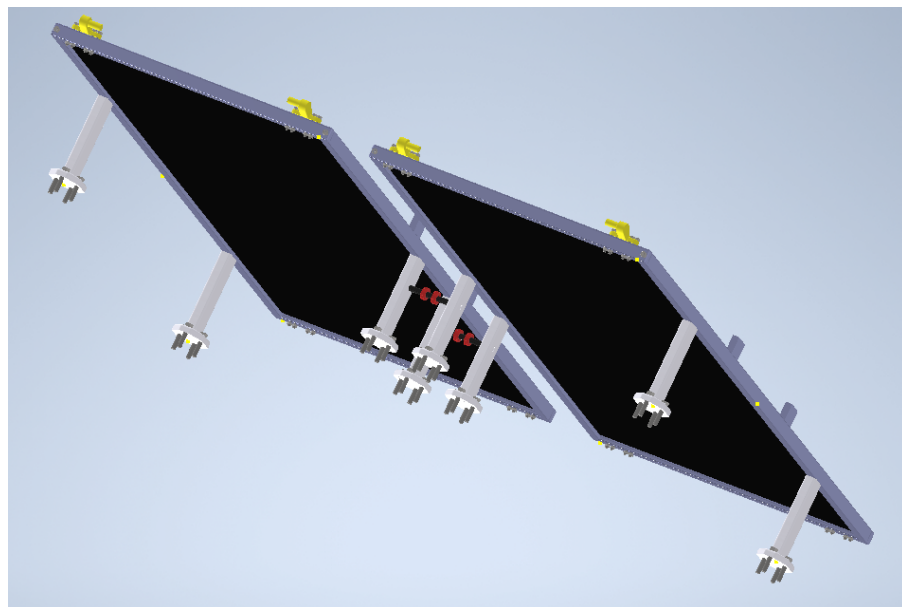


Figure 5.2: Current assembly with mounts

The current "base" of the assembly is made up of 8 unconnected mounts, those mounts are only bolted on to **some** pieces of the frame and the rover's body. This design is unstable and is not optimal, as it doesn't hold the frame pieces together. Also, because the center mounts double as bases for the axles, the whole base is asymmetrical, thus making all calculations trickier.

A much better design would be symmetrical and would need to include **supports** to distribute the panels weight more evenly across the body's surface . This would also hold the whole frame together, this way making the whole assembly more stable and robust. As was mentioned before, the ideal base should also have **extensions** for the male hinges.

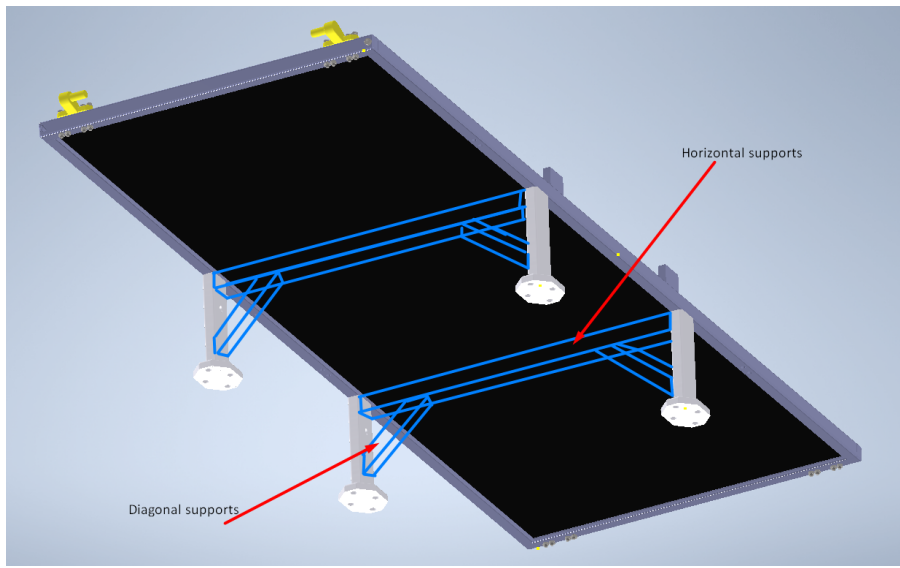


Figure 5.3: Hypothetical base design

Frame

The frame holding the panels could have been considered as being a **one-piece part** including the panels themselves. This would definitely increase it's strength, and combining that with the bolted-on hinges means that the whole assembly would be much stronger. The reason this assumption was not made was because, in such applications, solar cells are bought and assembled into panels by the interested party itself. This does not mean that the frame could not be made with less parts still.

Actuators

Finally, no linear actuators with the required force and the ability to withstand the **martian temperature range** was found. The ones currently chosen fulfill **only** the force requirement but unfortunately cant withstand the lower temperatures seen on mars. This was partially intentional, as priority was given to the clearly mechanical aspects of the assembly, leaving the thermal aspect as *optional*.

5.2.3 Robotic Arm Subsystem

The design of the robotic arm could be more weight and energy efficient, but this requires design solutions that need more complicated manufacturing processes.

Rotary Actuators

No rotary actuators with the required torque are able to withstand the martian temperature range, so passive thermal control systems have to be installed as mentioned in Fig. 4.7. Thus, thermal insulation should be addressed in the design.

Resting Mode Supporting Base

This mode is typically used to conserve energy and prevent potential damages from harsh weather conditions, of the robotic arm. Hence, the robotic arm can take breaks between tasks, reducing the risk of wear and tear on its components and prolonging its lifespan. This features can be enabled, with retracting to a docking station.

Rover Stabilization When In Danger

Due to the unpredictable nature of the environment, the Rover is equipped with emergency protocols that can be activated in case of danger. Arm's role is deploying to protect the Rover from damage.

5.3 Manufacturing

5.3.1 Cost Budget

In order to complete the design study, a cost budget is required. After draft calculations and a lot of procurement the cost budget for the proposed design can be seen in Tab. 5.1. As can someone observe, the total mission cost was procured a lot less than the budgetary constraint set in mission requirements.

The cost of the solar panels could not be calculated because they are not commercially available. But, for reference, the panels currently used on **Spacedot's Acubesat project** have dimensions of 100X300mm and cost approximately 10 thousand euros each, this means that their cost per square meter is 333 thousand euros. With that logic, a **total cost of around 1.5 to 1.6 million euros** for the present design would not be surreal.

Part	Quantity	Cost per Item (€)	Total Cost (€)
Linear actuators	2	400	800
Side panels	4	≈ 200,000	≈ 800,000
Main panels	2	≈ 400,000	≈ 800,000
Wheel Tire	8	475	3,800
Wheel Hub	8	12.23	97.84
Wheel Spokes	64	13.57	868.48
Horizontal Beams	8	167.59	1,340.72
Vertical Bars	8	375	3,000
Arched Beams	8	475	1,016
Mobility Bearings	56	Varying	344
Mobility Motors	16	100	1,600
Miscellaneous	-	Varying	1,500
Battery Pack	4	10,000	40,000
Electronics	-	-	20,000
Scientific Instrumentation	-	-	300,000
Robotic Arm Metals	3	Varying	18,000
Robotic Arm Motors	5	100	5,000
Robotic Arm Camera	1	3,000	3,000
Sensors	-	Varying	5,000
Total Cost			2,005,367.04

Table 5.1: Mission Cost Budget

5.3.2 Manufacturing processes

The manufacturing processes used for subsystem parts of the rover are:

- **3D Printing:** The utilization of 3D printing technology emerges as a strategic choice for manufacturing numerous rover components. This decision is rooted in the complexity of the parts and the unparalleled capabilities of 3D printing in crafting intricate geometries. The inherent flexibility of 3D printing allows for the creation of bespoke and intricately designed components tailored to the unique requirements of the rover. Notably, conventional manufacturing processes such as welding face challenges in the Martian/space conditions, making 3D printing a more viable and adaptable solution for this project. This approach not only enhances the efficiency of production but also aligns with the necessity for precision and customization in crafting components critical to the rover's functionality and structural integrity.
- **Molding:** The incorporation of molding processes stands as a strategic choice for manufacturing specific rover components, leveraging the versatility offered by various molding techniques. Molding proves advantageous in situations where a diversity of geometries is required for certain parts of the rover. The process enables the production of intricate shapes and designs with efficiency, contributing to the overall structural and functional requirements of the vehicle. This approach complements the 3D printing strategy, providing an alternative manufacturing method that is well-suited for specific geometrical demands. By integrating molding into the manufacturing workflow, the project aims to achieve a comprehensive and optimized production strategy, ensuring that each component is fabricated using the most fitting and efficient method for its intended purpose.
- **Lathing:** The application of lathing proves to be a judicious choice for crafting symmetrical or balanced components of the rover, particularly for parts such as shafts. Lathing, a precision machining process, excels in producing cylindrical or rotational symmetric parts with a high degree of accuracy. This method is well-suited for components where symmetry and balance are crucial to ensure optimal performance. By employing lathing for specific parts of the rover, the project aims to capitalize on the precision and efficiency offered by this machining technique, enhancing the overall functionality and

reliability of critical rotational components within the vehicle's subsystems. This targeted use of lathing underscores a nuanced manufacturing approach, where each method is strategically selected to best meet the unique requirements of the rover's diverse components.

- **Milling:** Similar to lathing, milling is a versatile machining process capable of producing a wide range of geometries. This method involves removing material from a workpiece using rotary cutters, allowing for precise shaping and detailing. Milling is well-suited for manufacturing specific rover components, especially those requiring intricate or contoured shapes. Its ability to handle various materials and accommodate diverse designs makes it a valuable addition to the manufacturing toolkit for the project.
- **Plastic Deformation Processes:** Certain stages in the manufacturing of rover components involve plastic deformation processes, particularly for elements such as threads. This approach is chosen for its efficiency, offering a cost-effective and timely means of achieving specific geometrical features. Plastic deformation processes, such as threading, provide a practical solution for creating intricate structures with relative ease.

List of Figures

1.1	Organizational Chart	4
1.2	Information Flow Diagram	5
1.3	Ideal Project Time Plan	6
1.4	Draft Project Time Plan	7
1.5	Final Project Time Plan	8
2.1	Initial Design Of The Mobility System	11
2.2	Initial Design Of The Panel Deployment Mechanism	11
2.3	Initial Design Of The Robotic Arm	12
2.4	Quality Function Deployment	12
3.1	Wheel Free Body Diagram for Flat Terrain	15
3.2	Rover Free Body Diagram On Slope	15
3.3	Mobility Subsystem Draft Iteration	16
3.4	Cross Sections of Subsystem Parts	16
3.5	Subsystem Parts	17
3.6	Free Body Diagram in slope angle f for the Mobility Subsystem	18
3.7	Vertical Bar	18
3.8	x_{max} of Eq. 3.17	19
3.9	Vertical Bar	19
3.10	Arched Beam	20
3.11	Deflection of Arched Beam	20
3.12	First Joint Desired Movement	21
3.13	2D Sketch Of The First Joint	22
3.14	Free Body Diagram Of The First Joint	22
3.15	Second Joint Desired movement	23
3.16	2D Sketch Of The Second Joint	24
3.17	Second Joint Thrust Bearing Free Body Diagram	24
3.18	Second Joint Deep Groove Bearings Free Body Diagram	25
3.19	Mobility System's Motors Degrees Of Freedom	26
3.20	2D Sketch Of Steering Motor Mounting	26
3.21	Steering Motor And Arched Beam Configuration	27
3.22	Wheel-Wheel Motor Configuration	28
3.23	Mobility Vertical Bar Final Design	29
3.24	Mobility Arched Beam Final Design	29
3.25	Mobility Horizontal Beam Final Design	30
3.26	Mobility First Joint	30
3.27	Mobility Second Joint	30
3.28	Mobility Second Joint Steering Motor Configuration	31
3.29	Wheel Motor Configuration	31
3.30	Mobility Subsystem Assembly	32
3.31	Mobility Assembly With Dummy Body	33
3.32	Wheel Parts	34
3.33	Wheel Assembly	34
3.34	Main body plate	36
3.35	SKF 30310	36
3.37	Housing design	37
3.39	Full housing assembly and connection	38
3.40	Leg	38
3.41	Leg connection	39
3.42	Leg support	39
3.44	Support connection	40
3.45	Panel connection	40
3.46	Arm connection	41

3.47	Centre piece - ball joint - rod - shaft assembly	42
3.48	Shaft assembly	43
3.49	Differential assembly	43
3.50	Full housing assembly and connection	44
3.51	Free body diagram xz	44
3.52	Free body diagram yz	45
3.53	Robotic Arm Mass Budget	47
3.54	Free Body Diagram Of Payload	47
3.55	Free Body Diagram of Lower Arm	48
3.56	Free Body Diagram of Lower Arm	48
3.57	Free Body Diagram Of Part 1	49
3.58	Free Body Diagram of Motor 3 to the Tip	49
3.59	Free Body Diagram of Assembled Payload an Lower Arm	50
3.60	Robotic Arm Actuators	50
3.61	Robotic Arm Actuators Stats	50
3.62	Robotic Arm Assembly	51
3.63	Rover Body And Arm Connecting Structure	52
3.64	Housing With Bearing	52
3.66	Actuators Housing 1	53
3.65	Sub-Assembly Of Part 1	53
3.67	Linkage Between 110 Actuator and Upper Arm	54
3.68	flanged connection between part 2 and stable part of the 80 actuator	54
3.69	Connection Between Upper-Lower Arm and 80 Actuator	54
3.70	Connection of 70 Actuators and Payload	55
3.71	Connection of Lower Arm and 70 Actuator	55
3.72	Connecting Flange of Lower Arm	56
3.73	Main panel dimensions	60
3.74	Side panel dimensions	60
3.75	Main panel assembly	61
3.76	Side panel assembly	61
3.77	Male hinge assembly	62
3.78	Male hinge	62
3.79	Detailed Female hinge assembly	63
3.80	Lever	63
3.81	full panel assembly	64
3.82	Linear actuator picture	64
3.83	Technical drawing of the linear actuators	65
3.84	side view of the assembly with the forces acting on the side panel assebly	65
3.85	Simplified problem	65
3.86	Forces acting on the hinges as seen from a plane parallel to the oppened side panel(10 deg from the ground)	66
3.87	Simplified problem	67
3.88	Analytic Lever dimensions	68
3.89	Actuator assembly with axles and shaft collars	68
3.90	Dimensions of the base axle	69
3.91	Forces acting on the base axle	69
4.1	Rover Top side view	70
4.2	Rover side view	70
4.3	Rover top view	71
4.4	Rover back view	72
4.5	Slope Detection Operations	73
4.6	Energy Balance Operations	74
4.7	Temperature Control System	74
5.1	Current side frames parts with hinges	76
5.2	Current assembly with mounts	76

List of Tables

1.1 Team Members	3
1.2 Subsystems Responsibles	5
2.1 Mission Requirements	9
2.2 Project's Toolset	10
3.1 Mass Budget	14
3.2 Motor Wattage Values	16
3.3 Mobility Subsystem Geometric Values	21
3.4 Mobility Subsystem Calculation Results	21
3.5 First Bearing Joint Calculation Results	23
3.6 Second Joint Thrust Bearing Calculation Results	25
3.7 Second Joint Deep Groove Bearing Calculation Results	25
3.8 Case-Steering Motor Bolt Connection	26
3.9 Case-Vertical Bar Bolt Connection	27
3.10 Steering System Key-Flange Configuration	27
3.11 Steering System Flange-Flange Connection	28
3.12 Steering System-Wheel Motor Bolt Connection	28
3.13 Transmission Motor-Wheel Hub Bolt Connection	29
3.14 Housing bolts connection	44
3.15 Total Arm's Wattage	51
3.16 Bolt Checking Calculations	56
3.17 Arms Bending Stresses	56
3.18 Total rover energy allocation	59
5.1 Mission Cost Budget	78

Bibliography

- [1] Prof. J.E. Akin. *Impact Load Factors for Static Analysis*. Vol. 1. Rice University, 2019.
- [2] Ravi kiran Bollineni, Sidharth S Menon, and Ganesha Udupa. “Design of Rover and Robotic arm.” In: *Materials Today: Proceedings* 24 (2020), pp. 1340–1347.
- [3] Christopher Anthony Follette. *Design and Construction of a Robotic Vehicle to Assist During Planetary Surface Operations*. The University of North Dakota, 2017.
- [4] R. Grekousis. *Machine Elements*. Vol. 1. Giahoudi-Giapouli Thessalonik, 1983.
- [5] Randel A Lindemann and Chris J Voorhees. “Mars Exploration Rover mobility assembly design, test and performance.” In: *2005 IEEE International Conference on Systems, Man and Cybernetics*. Vol. 1. IEEE. 2005, pp. 450–455.
- [6] Michael E Lisano and Pieter H Kallemeijn. “Energy management operations for the Insight solar-powered mission at Mars.” In: *2017 IEEE Aerospace Conference*. IEEE. 2017, pp. 1–11.
- [7] Xuesong Qiu et al. “Influence of joint clearance on the dynamic characteristics of the lunar rover deployable panels.” In: *2016 IEEE International Conference on Robotics and Biomimetics (ROBIO)*. IEEE. 2016, pp. 167–172.
- [8] Gurudu Rishank Reddy and Venkata Krishna Prashanth Eranki. “Design and structural analysis of a robotic arm.” In: *Blekinge Institute of Technology Karlskrona, Sweden* (2016), p. 101.
- [9] Ralph Roncoli and Jan Ludwinski. “Mission design overview for the mars exploration rover mission.” In: *AIAA/AAS Astrodynamics Specialist Conference and Exhibit*. 2002, p. 4823.
- [10] Jong-Hwi Seo et al. “Solar panel deployment analysis of a satellite system.” In: *JSME International Journal Series C Mechanical Systems, Machine Elements and Manufacturing* 46.2 (2003), pp. 508–518.
- [11] Thajid Ibna Rouf Uday et al. “Design and implementation of the next generation mars rover.” In: *2018 21st International Conference of Computer and Information Technology (ICCIT)*. IEEE. 2018, pp. 1–6.
- [12] P.A. Vouthounis. *Mechanics of Materials*. Vol. 1. Andromahi Vouthouni, 2021.
- [13] P.A. Vouthounis. *Statics*. Vol. 1. Andromahi Vouthouni, 2020.
- [14] Richard Washington et al. “Autonomous rovers for Mars exploration.” In: *1999 IEEE Aerospace Conference. Proceedings (Cat. No. 99TH8403)*. Vol. 1. IEEE. 1999, pp. 237–251.
- [15] Jinkyu Yang et al. “Interaction of highly nonlinear solitary waves with linear elastic media.” In: *Physical review. E, Statistical, nonlinear, and soft matter physics* 83 (Apr. 2011), p. 046606. DOI: 10.1103/PhysRevE. 83. 046606.
- [16] Khoo Zern Yi and Zol Bahri Razali. “Design, analysis and fabrication of robotic arm for sorting of multi-materials.” In: *Project Report, School of Mechatronic Engineering, University of Malaysia Perlis* (2013).
- [17] Warren C Young, Richard G Budynas, and Ali M Sadegh. *Roark's formulas for stress and strain*. McGraw-Hill Education, 2012.